UNESP - Universidade Estadual Paulista
"Júlio de Mesquita Filho"
Faculdade de Odontologia de Araraquara

Marcela Borsatto Queiroz

Reação tecidual e bioatividade de materiais endodônticos biocerâmicos reparadores em subcutâneo de ratos

Araraquara

2022

UNESP - Universidade Estadual Paulista

"Júlio de Mesquita Filho"

Faculdade de Odontologia de Araraquara

Marcela Borsatto Queiroz

Reação tecidual e bioatividade de materiais endodônticos biocerâmicos reparadores em subcutâneo de ratos

Tese apresentada à Universidade Estadual Paulista (Unesp), Faculdade de Odontologia, Araraquara para obtenção do título de Doutora em Odontologia, na Área de Endodontia.

Orientador: Prof. Dr. Paulo Sérgio Cerri
Coorientador: Prof. Dr. Mário Tanomaru Filho

Araraquara

2022

Q3r

Queiroz, Marcela Borsatto
Reação tecidual e bioatividade de materiais endodônticos biocerâmicos reparadores em subcutâneo de ratos / Marcela Borsatto Queiroz. -- Araraquara, 2022
139 p. : tabs., fotos

Tese (doutorado) - Universidade Estadual Paulista (Unesp), Faculdade de Odontologia, Araraquara
Orientador: Paulo Sérgio Cerri
Coorientador: Mário Tanomaru-Filho

1. Endodontia. 2. Teste de biocompatibilidade. 3. Imuno-histoquímica. 4. Interleucina-6. 5. Osteocalcina. I. Título.

Sistema de geração automática de fichas catalográficas da Unesp. Biblioteca da Faculdade de Odontologia, Araraquara. Dados fornecidos pelo autor(a).

Essa ficha não pode ser modificada.

Marcela Borsatto Queiroz

Reação tecidual e bioatividade de materiais endodônticos biocerâmicos reparadores em subcutâneo de ratos

Comissão julgadora

Para obtenção do grau de Doutora em Endodontia

1° Presidente e orientador: Prof. Dr. Paulo Sérgio Cerri

2° Examinador: Profa. Dra. Gisele Faria

3° Examinador: Profa. Dra. Raquel Assed Bezerra Segato

4° Examinador: Prof. Dr. Guilherme Ferreira da Silva

Araraquara, 29 de Março de 2022.

DADOS CURRICULARES

Marcela Borsatto Queiroz

NASCIMENTO: 31/07/1990 – Araraquara – São Paulo

FILIAÇÃO: Elaine Maria Borsatto Queiroz
Rudney da Conceição Queiroz

2010-2013: Graduação em Odontologia pela Universidade Sagrado Coração (USC, UniSagrado), Bauru-SP.

2014-2016: Especialização em Endodontia pelo Hospital de Reabilitação de Anomalias Craniofaciais (HRAC), Centrinho, USP, Bauru-SP.

2016-2018: Mestre em Odontologia, área de concentração em Endodontia, pela Universidade Estadual Paulista "Júlio de Mesquita Filho" (UNESP), Faculdade de Odontologia de Araraquara (FOAr), Araraquara-SP.

Dedico esse trabalho aos meus pais (Rudney e Elaine), por todo amor, carinho, apoio e esforço para que eu pudesse estar aqui hoje. Ao meu noivo (Vinicius) por todo amor, incentivo e compreensão nesses 17 anos juntos. E por fim, dedico também aos meus avós: Aurora, José (*in memoriam*), Hilda (*in memoriam*) e Fernando (*in memoriam*), uma parte muito importante da minha história.

AGRADECIMENTOS

Agradeço primeiramente a Faculdade de Odontologia de Araraquara-UNESP, onde eu tive a oportunidade de realizar meu mestrado e doutorado.

Agradeço principalmente e especialmente ao meu orientador Prof. Dr. Paulo Sérgio Cerri, por tem me acolhido tão bem, pela paciência e por todos os ensinamentos.

Agradeço meu coorientador Prof. Dr. Mario Tanomaru Filho pelos ensinamentos em Endodontia e pela oportunidade da pós-graduação.

Agradeço a Profa. Dra. Juliane Maria Guerreiro Tanomaru, por toda paciência, ensinamentos e contribuição.

Agradeço a Profa. Dra. Estela Sasso Cerri, pela convivência e colaboração.

Agradeço a todos os professores do departamento de Endodontia da FOAr-UNESP.

Agradeço imensamente todos os pós-graduandos da Endodontia e da Histologia pela convivência, ajuda e experiências compartilhadas.

Agradeço especialmente as minhas colegas do doutorado Rafaela e Camila, por toda ajuda e convivência nesses anos de pós-graduação.

Agradeço ao técnico do laboratório de Histologia (Pedro Sérgio Simões), pela paciência e auxílio na minha pesquisa.

À CAPES:

O presente trabalho foi realizado com o apoio da Coordenação de Aperfeiçoamento de Pessoal de Nível Superior – Brasil (CAPES) – Código de financiamento 001.

Agradeço por fim, aos meus pais (Rudney e Elaine) por todo esforço e incentivo para que eu estivesse aqui hoje. E também ao meu noivo (Vinicius) por todo amor, carinho e compreensão comigo.

“Os sonhos são como uma bússola, indicando os caminhos que seguiremos e as metas que queremos alcançar. São eles que nos impulsionam, nos fortalecem e nos permitem crescer.” Augusto Cury*

* Cury A. Nunca desista de seus sonhos. Rio de Janeiro: Sextante; 2004.

Queiroz MB. Reação tecidual e bioatividade de materiais endodônticos biocerâmicos reparadores em subcutâneo de ratos [tese de doutorado]. Araraquara: Faculdade de Odontologia da UNESP; 2022.

RESUMO

O objetivo foi avaliar a reação tecidual e o potencial bioativo causado por materiais biocerâmicos implantados no tecido conjuntivo do subcutâneo de ratos adultos. Para isso, tubos de polietileno preenchidos com um dos materiais ou vazios (grupo controle, GC) foram implantados no subcutâneo de ratos (n=8/grupo por período). Após 7, 15, 30 e 60 dias, os implantes e os tecidos circundantes foram removidos e processados para inclusão em parafina para análise dos seguintes parâmetros: número de células inflamatórias (CI) e de fibroblastos (Fb), espessura das cápsulas (EC), quantidade de colágeno birrefringente, imuno-histoquímica para detecção de interleucina-6 (IL-6) e osteocalcina (OCN), a reação de von Kossa e análise de cortes não corados sob luz polarizada. Os dados foram submetidos ao ANOVA two-way seguido pelo teste de Tukey ($p<0,05$). **Publicação 1:** Avaliar a biocompatibilidade e o potencial bioativo de um material reparador experimental à base de silicato tricálcico com 30% de tungstato de cálcio (TCS + $CaWO_4$) em comparação ao MTA Repair HP (MTA HP; Angelus, Brasil) e ao Bio-C Repair (Bio-C; Angelus, Brasil). Em todos os períodos, não houve diferenças significantes no número de CI, número de células IL-6-imunopositivas e no conteúdo de colágeno entre os materiais biocerâmicos ($p>0,05$). De 7 para 60 dias, ocorreu uma redução significante no número de CI, na imunoexpressão de IL-6 e na EC, acompanhada por um aumento significante no número de Fb e na quantidade de colágeno. Estruturas positivas ao von Kossa e birrefringentes, além de células imunopositivas à OCN foram observadas nas cápsulas ao redor de todos os materiais, exceto no GC. O TCS + $CaWO_4$ é biocompatível e apresentou potencial bioativo. **Publicação 2:** Comparar a resposta tecidual dos materiais à base de silicato tricálcico Bio-C Pulpo (Angelus, Brasil), Biodentine (Septodont, França) e MTA branco (WMTA; Angelus, Brasil). Aos 7 e 15 dias a EC dos materiais Bio-C Pulpo e Biodentine foram iguais e não houve diferença significativa ($p>0,05$), sendo maiores em comparação ao WMTA ($p<0,05$); as cápsulas ao redor de todos os materiais foram significantemente mais espessas em comparação ao GC ($p<0,05$). Aos 30 e 60 dias, a EC ao redor dos materiais não apresentou diferenças significantes em comparação à do GC. Apesar do maior número de CI observado aos 7 dias nas cápsulas do Biodentine em comparação ao Bio-C Pulpo e WMTA espécimes ($p<0,05$), diferenças significantes não foram observadas entre os grupos contendo os materiais ($p>0,05$), nos períodos de 15 e 30 e 60 dias. De 7 para 60 dias, ocorreu uma redução significante na EC, no número de CI e de células IL-6-imunopositivas que foi acompanhada por um aumento significante no número de Fb e na quantidade de colágeno nas cápsulas de todos os grupos. As cápsulas ao redor de todos os materiais apresentaram estruturas von Kossa-positivas e birrefringentes, e células OCN-imunopositivas, enquanto que estas estruturas bem como células imunopositivas à OCN não foram encontradas no GC. O Bio-C Pulpo, semelhantemente ao Biodentine e WMTA, é biocompatível e permite a reparação do tecido conjuntivo, além de induzir a imunoexpressão de osteocalcina e a deposição de calcita sugerindo que este material deve apresentar um potencial bioativo. Assim, o Bio-C Pulpo pode ser uma alternativa de material reparador em diferentes procedimentos clínicos de pulpotomia, capeamento pulpar direto e indireto, em dentes decídíduos e dentes permanentes jovens.

Palavras chave: Endodontia. Teste de biocompatibilidade. Imuno-histoquímica. Interleucina-6. Osteocalcina.

Queiroz MB. Tissue reaction and bioactivity of bioceramic endodontic repair materials in subcutaneous tissue of rats [tese de doutorado]. Araraquara: Faculdade de Odontologia da UNESP; 2022.

ABSTRACT

The aim was to evaluate the tissue reaction and the bioactive potencial caused by bioceramic materials implanted in the subcutaneous connective tissue of adult rats. For this, polyethylene tubes filled with one of the materials or empty (control group, CG) were implanted into the subcutaneous tissue of rats (n=8/group per period). After 7, 15, 30 and 60 days, the implants and surrounding tissues were removed and processed for embedding in paraffin to evaluate the following parameters: number of inflammatory cells (IC) and fibroblasts (Fb), capsule thickness (CT), amount of birefringent collagen, immunohistochemistry detection of interleukin-6 (IL-6) and osteocalcin (OCN), von Kossa reaction and analysis of unstained sections under polarized light. Data were submitted to two-way ANOVA followed by Tukey's test ($p<0.05$). **Publication 1:** To evaluate the biocompatibility and bioactive potential of an experimental repair material containing 70% tricalcium silicate and 30% calcium tungstate (TCS + $CaWO_4$) compared to MTA Repair HP (MTA HP; Angelus, Brazil) and Bio- C Repair (Bio-C; Angelus, Brazil). In all periods, there were no significant differences in the number of IC, number of IL-6-immunolabelled cells and in the collagen content among the bioceramic materials ($p>0.05$). From 7 to 60 days, there was a significant reduction in the number of IC, in the immunoexpression of IL-6 and in CT accompanied by a significant increase in the number of Fb and the amount of collagen. von Kossa-positive and birefringent structures, besides to OCN-immunolabelled cells were observed in the capsules around all materials, except in the CG. TCS + $CaWO_4$ is biocompatible and showed bioactive potencial.
Publication 2: To compare the tissue response of Bio-C Pulpo (Angelus, Brazil) with Biodentine (Septodont, France) and White MTA (WMTA; Angelus, Brazil) tricalcium silicate-based materials. At 7 and 15 days, significant difference was not found in the CT around Bio-C Pulpo and Biodentine specimens, but the CT of these groups was greater than in WMTA ($p<0.05$); the CT around materials was significantly higher than in CG specimens ($p<0.05$). At 30 and 60 days, significant difference in the CT was not detected among the groups, including the CG. Despite the higher number of IC observed at 7 days in Biodentine capsules than in Bio-C Pulpo and WMTA specimens ($p<0.05$), no significant differences were observed among bioceramic materials ($p>0.05$) at 15 and 30 and 60 days. From 7 to 60 days, there was a significant reduction in the number of IC, number of IL-6-immunopositive cells and CT, which was accompanied by a significant increase in the number of Fb and the amount of collagen in the capsules of all groups. The capsules around all materials showed von Kossa-positive and birefringent structures, and OCN-immunopositive cells, while these structures as well as OCN-immunopositive cells were not found in the CG. The Bio-C Pulpo, similarly to Biodentine and WMTA, is biocompatible and allows the connective tissue repair. Moreover, Bio-C Pulpo induces the immunoexpression of osteocalcin and the deposition of calcite suggesting that this material may have a bioactive potential. Thus, the Bio-C Pulpo can be an alternative repair material in different clinical procedures of pulpotomy, direct and indirect pulp capping, in deciduous teeth and young permanent teeth.

Keywords: Endodontics. Biocompatibility test. Immunohistochemistry. Interleukin-6. Osteocalcin.

SUMÁRIO

1 INTRODUÇÃO

Um material reparador endodôntico ideal deve tem a capacidade de selar as vias de comunicação entre o sistema de canais radiculares e seus tecidos circundantes, deve ser não tóxico, não carcinogênico, não genotóxico, biocompatível, insolúvel em fluidos teciduais e dimensionalmente estável. Os materiais reparadores são amplamente utilizados em pulpotomias, proteções pulpares, processos de regeneração pulpar, barreiras apicais, perfurações radiculares e obturação retrógrada[1,2]. Esses materiais apresentam silicato de cálcio em sua composição sendo considerados como bioativos[3].

O Mineral Trióxido Agregado (MTA) foi desenvolvido por Torabinejad, em 1993, e recomendado como material reparador, o primeiro a ser desenvolvido foi o MTA cinza[3]. Em 1998, o ProRoot MTA cinza (ProRoot MTA cinza; Denstply, Tulsa, OK, USA) foi introduzido no mercado. Este material continha na sua composição 53,1% de silicato tricálcico, 22,5% de silicato dicálcico, 21,6% de óxido de bismuto (Bi_2O_3) e vestígios de sulfato de cálcio[4-6]. Inicialmente a razão para a introdução do MTA branco como substituto do MTA cinza foi fornecer uma tonalidade mais próxima da cor dos dentes, em oposição à cor cinza contrastante[7]. Os elementos de transição tardia como por exemplo Cr, Mn, Fe, Cu têm elétrons d-livres (elétrons não envolvidos na ligação) por isso, exibem cores fortes quando em suas formas de óxido, já os óxidos de elementos que não possuem elétrons facilmente excitados como Mg, Al, Si, P, S, K, Ca e Ti tendem a ser incolores ou brancos, em contra partida o elemento mais pesado Bi tem um óxido amarelo[8]. O MTA branco da Angelus (WMTA; Angelus, Indústria de Produtos Odontológicos S/A, Londrina, PR, Brasil), começou a ser comercializado em Março de 2002, é considerado um material biocompatível e possui capacidade de selamento e bioatividade[9]. A principal diferença na composição química entre o MTA cinza (ProRoot; Denstply, Tulsa, OK, USA) e o MTA branco (MTA; Denstply, Tulsa, OK, USA), é uma diminuição significativa na quantidade de ferro e outros elementos metálicos quando comparado ao cinza[10].

O MTA (Angelus, Indústria de Produtos Odontológicos S/A, Londrina, PR, Brasil) foi denominado como material “hidráulico” à base de silicato de cálcio[11]. A denominação de cimento “hidráulico” ocorreu em 2005[12,11], pois esse cimento necessita de água para a sua reação de presa (por meio de uma reação de hidratação). Assim, este material pode ser empregado em ambientes úmidos

contendo sangue, fluido tecidual, soluções irrigadoras e materiais restauradores[12]. Há formação de carbonato de cálcio quando esses materiais estão em contato com o sangue[13], em obturações retrógradas[14], na utilização como material de barreira em procedimentos reparadores[15], e formação de apatita quando o material é utilizado como cimento endodôntico em contato com a dentina[16] e em terapias de polpa vital[17].

O MTA é fabricado a partir do Cimento Portland (CP), utilizado na fabricação de concreto para a construção civil, tanto o ProRoot MTA[4,5,12,18] quanto o MTA Angelus[18,19]. Portanto, o MTA apresenta CP como componente principal[18]. Atualmente a empresa afirma que o MTA é produzido apenas a partir de produtos sintetizados. Pois, uma desvantagem seria que no estudo realizado com cimento Portland branco, cimento Portland cinza, GMTA e MTA, mostrou que esses materiais apresentavam contaminação por metais pesados como arsênio, cromo, cádmio, cobre, ferro, manganês, níquel, bismuto, zinco e chumbo[20]. Em um estudo com duas marcas comerciais de MTA (MTA branco; Denstply, Tulsa, OK, USA e MTA branco; Angelus, Indústria de Produtos Odontológicos S/A, Londrina, PR, Brasil) mostrou que estes materiais contendo silicato de cálcio apresentaram nível de contaminação semelhante ao CP, onde levando em consideração que o MTA é constituído por 80% em peso do cimento, o nível de contaminação por íons metálicos é considerado alto em comparação ao CP[21].

Com o intuito de eliminar esta desvantagem do MTA, devido aos efeitos adversos que esses metais pesados podem causar no organismo[22], biomateriais contendo silicato tricálcico sintetizado puro têm sido pesquisados[23-28]. Sendo assim, a Angelus substituiu o CP industrial por misturas sintéticas de silicato de cálcio, por causa da preocupação com a lixiviação de íons de alumínio, detectados em vários órgãos periféricos e que também estão associados ao estresse oxidativo no cérebro[29-31]. Além disso, metais pesados tóxicos como cromo, arsênico e chumbo são encontrados nos CP comerciais, resultantes do uso de matérias-primas e resíduos naturais impuros[21]. Com isso, atualmente os cimentos à base de silicatos de cálcio sintéticos são produzidos em laboratórios com a utilização de matérias-primas mais puras e com processos de fabricação apropriado a fim de evitar essas contaminações[18].

Além da possibilidade de contaminação pelos metais pesados, a presença do óxido de bismuto (Bi_2O_3) como radiopacificador no MTA provocava aumento na porosidade[32] e na solubilidade[33], diminuição na sua resistência à compressão[5,32], além

da possível redução na liberação de hidróxido de cálcio, prejudicando a estabilidade dimensional do material[33]. Além disso, diversos estudos demonstraram a citotoxicidade[34,35] e a reação inflamatória mais intensa provocada pelo óxido de bismuto em comparação à outros radiopacificadores, dentre eles o óxido de zircônio[36-39], óxido de nióbio[38,40] e tungstato de cálcio[41,42].

A presença do óxido de bismuto no MTA da Angelus também foi associada com a alteração de cor das estruturas dentais[43]. A alteração de cor é atribuída a interação entre o óxido de bismuto com estruturas dentárias duras[43] e o hipoclorito de sódio utilizado como solução irrigadora durante o tratamento[44,45]. O radiopacificador óxido de bismuto interage com a dentina e outros componentes, resultando na migração de íons para a dentina, causando assim uma alteração da coloração do dente[43,44,46]. O óxido de bismuto é um bom agente radiopacificante devido ao seu alto peso molecular (465,96 g/mol), pois requer pequenas quantidades para um nível ideal de radiopacidade (ou seja, 3 mm de Al – norma ISO 6876/2012) em comparação com radiopacificadores alternativos, como o tungstato de cálcio com 287,92 g/mol e o óxido de zircônio com 123,21 g/mol de peso molecular[47].

Os cimentos à base de silicato tricálcico têm sido amplamente utilizados para terapia endodôntica desde a década de 90, quando o MTA foi introduzido[48]. Há evidências de que o uso de silicato tricálcico fornece propriedades adequadas de manipulação, tempo de presa, solubilidade, pH alcalino ao microambiente e liberação de íons cálcio, escoamento e porosidade, além de boas propriedades biológicas[23-29,49,50].

Os cimentos à base de silicato tricálcico apresentam biocompatiblidade e estes materiais tem demostrado também potencial bioativo[27,51,52]. A hidratação do silicato tricálcico após reação com água forma silicato de cálcio hidráulico hidratado e hidróxido de cálcio[53]. Viola et al.[54] (2012) avaliaram a resposta tecidual por meio de tubos de polietileno implantados no subcutâneo de ratos e preenchidos com os materiais MTAS (material experimental MTA Sealer), MTA Angelus e CP. Os autores encontraram que ocorreu um processo inflamatório moderado nas cápsulas que foi observado em todos os grupos nos períodos de 7 e 14 dias. Após 60 dias, verificaram a redução significativa do número de células inflamatórias em relação aos períodos iniciais, porém não houve diferenças significantes entre os grupos. A imunomarcação de osteopontina (OPN) foi observada no citoplasma dos fibroblastos das cápsulas próximas aos implantes. Estruturas positivas para o de von Kossa foram também

observadas nas cápsulas adjacentes a todos os materiais implantados. Os resultados indicaram fortemente que o MTAS, MTA e o CP apresentaram biocompatibilidade e podem ser empregados como materiais reparadores endodônticos.

A Angelus, em virtude dos diversos estudos que apontavam a citotoxicidade do óxido de bismuto[34,35], em 2018, alterou sua formulação substituindo este radiopacificador pelo tungstato de cálcio ($CaWO_4$). O $CaWO_4$ associado ao CP, promoveu maiores valores de pH e de liberação de íons cálcio quando comparado ao MTA da Angelus[55], aumento da resistência à compressão e diminuição da solubilidade do CP[55,56]. Além disso, não alterou as propriedades mecânicas e o tempo de presa final do cimento CP puro[56]. Quando o $CaWO_4$ foi associado ao CP, o material manteve a sua propriedade antimicrobiana[57], além de não ser citotóxico[58].

A associação ao CP na proporção de 20% de $CaWO_4$, proporcionou ao material a radiopacidade equivalente a 3,11 mm Al[47]. A associação de 20% de $CaWO_4$ ao cimento de silicato de cálcio apresenta potencial bioativo semelhante ao do WMTA Angelus, contendo ainda o óxido de bismuto como agente radiopacificador[59], além de baixa solubilidade e fornecer um pH alcalino ao meio[26]. A associação de 30% de $CaWO_4$ ao cimento de silicato de cálcio também resultou num cimento com adequadas propriedade físico-químicas tais como radiopacidade, tempo de presa, solubilidade, além de manter a liberação de hidroxila (OH^-), proporcionando uma alcalinização do meio e também apresentou viabilidade celular nos ensaios em cultura de células SAOS-2 de MTT (Metiltetrazólio), NR (vermelho neutro) e potencial bioativo devido à indução de formação de nódulos de mineralização e aumento da expressão de fosfatase alcalina[28,60].

O MTA Repair HP (MTA HP; MTA Repair High Plasticity; Angelus, Indústria de Produtos Odontológicos S/A, Londrina, PR, Brasil) é um material à base de silicato tricálcico que apresenta as mesmas indicações e o mesmo radiopacificador quando comparado ao WMTA Angelus (com o tungstato de cálcio), de acordo com o fabricante. Porém, uma diferença encontrada, é a sua consistência na manipulação. Uma das principais desvantagens do MTA Angelus e do ProRoot MTA (Dentsply, Tulsa Dental, Tulsa) é a sua consistência de manipulação e sua dificuldade de inserção e condensação clínica[2,61]. Com isso o MTA HP foi desenvolvido a fim de melhorar essa característica. MTA HP é composto por silicato tricálcico, silicato dicálcico, aluminato tricálcico, óxido de cálcio e tungstato de cálcio ($CaWO_4$) em seu

pó enquanto o líquido contém água e plastificantes, de acordo com o fabricante (Angelus, MTA Repair HP). A presença de plastificantes em seu líquido melhorou a capacidade de manipulação desse material, já que o WMTA Angelus apresenta uma consistência arenosa e de difícil inserção[3,62]. Há evidência de que a cultura de células de fibroblastos L929 na presença de MTA Angelus contendo óxido de bismuto mostrou-se mais citotóxica em comparação ao MTA HP[62]. Além disso, o MTA HP implantado no tecido conjuntivo do subcutâneo de ratos apresentou biocompatibilidade, além de resultados que apontam para uma possível bioatividade deste material[52,62].

Outro radiopacificador utilizado em materiais reparadores à base de silicato de cálcio é o óxido de zircônio (ZrO_2) que mostrou ser "inerte"[33], desde que não alterou as propriedades do material à base de silicato de cálcio[36,63,64]. A associação de ZrO_2 ao material à base de silicato de cálcio não interferiu na liberação do íons cálcio[24,36], e na capacidade de alcalinizar o meio, além de manter o potencial bioativo do material[22,36]. Além disso, este radiopacificante não sofre lixiviação quando imerso em água ou HBSS[24]. Quando o silicato de cálcio hidráulico está associado ao radiopacificador ZrO_2, apresenta um tempo de presa semelhante ao do MTA Angelus (contendo o óxido de bismuto), baixa solubilidade, radiopacidade superior a 3 mm Al, além de proporcionar um pH alcalino ao meio[26,36]. O ZrO_2 microparticulado ou nanoparticulado associado aos cimentos à base de silicato de cálcio, proporcionou adequadas propriedades físico-químicas de radiopacidade, tempo de presa, pH alcalino ao meio e resistência a compressão, além de promover uma menor reação inflamatória em comparação ao óxido de bismuto[36].

Um material que apresenta ZrO_2 em sua composição é o Biodentine (Septodont, Saint Maur des Fossés, França), que é um biomaterial à base de silicato de cálcio com indicações como material reparador semelhantes às do MTA[66-70], porém este material apresenta melhor consistência em comparação ao WMTA[71]. Biodentine consiste em um pó que contém silicato tricálcico e dicálcico, carbonato de cálcio, além do ZrO_2 como agente radiopacificante. O líquido é composto por cloreto de cálcio e redutor de água em solução aquosa com mistura de um superplastificante à base de policarboxilato[67,69]. A hidratação do MTA é mais lenta que a do Biodentine e do silicato tricálcico associado a 20% de ZrO_2, devido à menor quantidade de silicato tricálcico presente no material[23]. O Biodentine possui um tempo de presa inicial de aproximadamente 16,2 minutos e final de aproximadamente 35,4 minutos, menor que

o do MTA Angelus que possui tempo de presa inicial de aproximadamente 24 minutos e final de aproximadamente 209 minutos. O Biodentine possui radiopacidade de aproximadamente 2,79 mm de Al, sendo considerada abaixo do valor da norma ISO 6876/2002[72]. Células Saos-2 cultivadas com extratos de Biodentine e de MTA apresentaram índices de viabilidade celular dentro de padrões que permitiram sugerir que estes materiais são citocompatíveis. Biodentine e de MTA adicionados a cultura de células Saos-2 transfectadas com o gene que codifica a proteína morfogenética óssea-2 (BMP-2) mostraram resultados sugestivos de que estes materiais devem apresentar bioatividade[73]. Perfurações de furca em molares de ratos selados com Biodentine ou MTA (com óxido de bismuto) promoveram uma redução significante no infiltrado inflamatório, na imunoexpressão de interleucina-6 (IL-6) e de osteoclastos, além de favorecerem o aumento significante de fibroblastos, osteoblastos e colágeno no ligamento periodontal, indicando que os materiais favoreceram a reparação dos tecidos periodontais[74]. O Biodentine também induziu a formação de tecido mineralizado pelas células do periodonto em dentes de cães com perfuração de furca[38]. Implantes de Biodentine no tecido conjuntivo do subcutâneo também apresentou cápsulas com estruturas positivas ao von Kossa nos períodos de 1, 4 e 8 semanas, além da detecção de precipitados superficiais nos implantes contendo cálcio e fósforo após a realização de microscopia eletrônica de varredura e espectroscopia de raios X por dispersão de energia (SEM/EDX), sugerindo o potencial bioativo deste material[75]. A presença de calcificação distrófica foi observada após 15 dias em cápsulas formadas em resposta ao MTA e ao Biodentine, bem como impregnação de prata pelo método de von Kossa nas estruturas, indicando o início do processo de mineralização. Na análise de luz polarizada, as cápsulas ao redor do WMTA e Biodentine, após 30 e 60 dias, apresentaram estruturas birrefringentes próximas à abertura dos tubos, indicando a formação de estruturas mineralizadas[76].

O Bio-C Repair (Angelus, Indústria de Produtos Odontológicos S/A, Londrina, PR, Brasil) é composto por silicatos de cálcio, aluminato de cálcio, óxido de cálcio, óxido de zircônio, óxido de ferro, dióxido de silício e agente de dispersão, que se apresenta pronto para uso e com indicações semelhantes ao MTA. Benetti et al.[77] (2019) avaliaram a citotoxicidade, a biocompatibilidade e a biomineralização dos materiais MTA, MTA HP e Bio-C Repair, por meio da exposição de células de fibroblastos L929 aos extratos dos materiais, bem como por meio de implantes em subcutâneo de ratos por 7 e 30 dias. A análise das culturas das células L929 revelaram

que todos os materiais apresentaram citocompatibilidade após 48 horas de exposição aos extratos em todas as diluições. Após 7 e 30 dias aos implantes no subcutâneo, os materiais causaram uma resposta inflamatória moderada e leve, respectivamente, e todos apresentaram cápsulas contendo estruturas positivas ao von Kossa e birrefringentes, sugerindo potencial para induzir biomineralização.

Lopés-Garcia et al.[78] (2019) demonstraram as propriedades biológicas do cimento Bio-C Repair, onde apresentou valor de pH alcalino e maior viabilidade celular, adesão celular e maiores taxas de migração celular em células da polpa dentária humana (hDPCS), quando comparado ao Bio-C Sealer. Ghilotti et al.[79] (2020) avaliaram a citoxicidade do Bio-C Repair e o Biodentine em hDPCS, por meio da análise da viabilidade celular (ensaio MTT), morfologia celular (ensaio de imunofluorescência) e fixação celular (ensaio de citometria de fluxo), e a caracterização dos elementos químicos dos materiais foi realizada por microscopia eletrônica de varredura (MEV) e análise de energia dispersiva de raios X (SEM-EDX); os autores observaram que o Biodentine era composto principalmente por cálcio, carbono e oxigênio (entre outros elementos), enquanto que o Bio-C Repair evidenciou uma baixa concentração de cálcio e a maior concentração de zircônio, na análise de MEV houve uma adesão adequeda das células da polpa aos materiais sem alterações no citoesqueleto nos eluatos dos materiais; o Bio-C Repair apresentou excelente citocompatibilidade semelhante ao Biodentine. Oliveira et al.[80] (2020) analisaram a descoloração, radiopacidade, pH e liberação de íons cálcio de Biodentine, Bio-C Repair e Bio-C temp e seus efeitos biológicos nas células da polpa dental humana (hDPCs); os autores concluiram que o Bio-C Repair apresentou maior radiopacidade e menor alteração de cor do que os demais materiais avaliados e viabilidade celular maior que 80%, porém todos os materiais proporcionaram valores de pH alcalino ao meio de imersão.

O Bio-C Pulpo (Angelus, Brasil) é um material biocerâmico que contém o radiopacificador ZrO_2 em sua composição. Ele é composto por silicato tricálcico, silicato dicálcico, cálcio aluminato, hidróxido de cálcio, óxido de zircônio, fluoreto de cálcio, dióxido de silicone e óxido de ferro e seu líquido apresenta água destilada, plastificante, cloreto de cálcio e metilparabeno. Este material possui propriedades físico-químicas adequadas no que se refere a radiopacidade, tempo de presa, escoamento, alteração dimensional, além de proporcianar uma alcalinização ao meio[81]. O Bio-C Pulpo é um material biocompatível e induz a imunoexpressão de osteocalcina (OCN), osteopontina (OPN) e sialoproteína óssea (BSP) no tecido

conjuntivo do subcutâneo de ratos, semelhantemente ao MTA (Angelus) com o óxido de bismuto como radiopacificador[82]. Bio-C Pulpo, MTA HP e MTA (com tungstato de cálcio) quando implantados no subcutâneo de ratos induziram inicialmente uma reação inflamatória moderada que reduziu gradativamente com o decorrer do tempo. Além disso, o Bio-C Pulpo, semelhantemente ao MTA HP e ao WMTA, promoveu a deposição de estruturas positivas ao von Kossa, além de estruturas birrefringentes sugerindo que estes materiais biocerâmicos possam ter um papel indutor na biomineralização. Esta hipótese foi reforçada pela presença da fosfatase alcalina em células adjacentes às estruturas von Kossa-positivas. Além disso, a análise histológica de cortes do fígado e análises bioquímicas das enzimas hepáticas glutâmico-oxaloacético transaminase (GOT) e glutâmico-pirúvico transaminase (GPT) também indicaram que estes materiais não induzem alterações no fígado[52].

Estudos prévios avaliando as propriedades físico-químicas, biológicas e antimicrobianas de materiais à base de silicato tricálcico puro (Mineral Research Processing, Meyzieu, França) associado aos radiopacificadores ZrO_2, $CaWO_4$ e o MTA HP demonstraram que esses materiais apresentaram adequadas propriedades físico-químicas no que se refere ao tempo de presa, solubilidade, pH e radiopacidade. Os materiais apresentaram citocompatibilidade quando expostos às células Saos-2, além de estimular a expressão gênica para fosfatase alcalina e deposição de estruturas positivas ao vermelho de alizarina, sugerindo um potencial bioativo destes materiais. Os cimentos de TCS associados ao ZrO_2 ou $CaWO_4$ bem como o MTA HP apresentaram efetividade contra as bactérias *E. faecalis*. Esses dados sugerem que o cimento de TCS puro associado aos radiopacificadores ZrO_2, $CaWO_4$ são semelhantes ao MTA HP e apresentam boas propriedades para serem utilizados como biomateriais reparadores na Endodontia[28,50]. O TCS + $CaWO_4$ apresentou os maiores valores de radiopacidade (4.61 mm Al), a menor solubilidade (0,81%) e pH alcalino em todos os períodos avaliados (3 horas, 12 horas, 24 horas, 7 dias, 14 dias e 21 dias). Os resultados obtidos com células Saos-2 cultivadas com extrato do TCS + $CaWO_4$ sugeriram que este material é citocompatível; no ensaio de qPCR (PCR real time) ocorreu a estimulação da maior expressão gênica para fosfatase alcalina (ALP), além disso houve a deposição de estruturas positivas ao vermelho de alizarina (ARS), sugerindo um potencial bioativo deste material. No teste de contato direto com células planctônicas do *E. faecalis* não foram detectas unidades formadoras de colônias (CFU), sugerindo o potencial anti-microbiano deste material. Diante desses resultados

promissores do material TCS associado à 30% de $CaWO_4$ obtidos no estudo *in vitro*[28] e diante da norma ISO 10993-6/2006 que preconiza que os materiais sejam avaliados *in vivo*, particularmente a sua biocompatibilidade, foi idealizado o modelo experimental do presente estudo. As avaliações de biocompatibilidade e bioatividade são importantes, desde que os materiais reparadores endodônticos entram em íntimo contato com os tecidos periapicais[38,83]. Dentre os diferentes métodos para avaliar a bicompatibilidade de materiais, a análise da reação inflamatória assoaciada a espessura da cápsula são parâmetros indicativos da intensidade bem como da extensão do processo inflamatório induzido pelos materiais endodônticos[52,84-86]. A detecção imuno-histoquímica de interleucinas (IL) pró-inflamatórias, dentre elas a IL-1 e IL-6, constitui-se em parâmetros que fornecem maior suporte aos resultados quantitativos da reação inflamtória[52,84-87]. A IL-6 é produzida por uma variedade de células que incluem macrófagos, linfócitos, plasmócitos, células endoteliais, fibroblastos e mastócitos[83,88]. Há indícios de que essa citocina seja responsável pela manutenção da reação inflamatória, maturação dos plasmócitos e ativação e diferenciação das células T[88,89]. A redução significante na imunoexpressão da IL-6 que ocorre concomitante à regressão do processo inflamatório, aponta para uma importante participação desta interleucina na cascata de eventos induzidos pelos materiais dentários implantados no tecido conjuntivo do subcutâneo de ratos, contituindo-se numa metodologia indicada para a avaliação do processo inflamatório[52,83,86,87,90].

O potencial bioativo dos materiais endodônticos implantados no tecido conjuntivo do subcutâneo tem sido avaliado por diferentes metodologias, dentre elas a detecção de osteocalcina (OCN)[51,52,77], osteopontina[54,91,92] e sialoproteína óssea[92,82], proteínas da matriz óssea que são secretadas pelos osteoblastos. A detecção de fosfatase alcalina, enzima envovlida com o processo de mineralização dos tecidos, também tem sido utilizada como uma das ferramentas sugestivas do potencial bioativo dos materiais endodônticos[52,85]. O método de von Kossa para detectar a deposição de cálcio/fosfato[93] nas cápsulas ao redor dos implantes tem sido amplamente utilizado como um método sugestivo do potencial bioativo dos materiais. Frequentemente, à este método associa-se a análise sob luz polarizada de cortes sem coloração para avaliar a presença de estruturas birrefrigentes, que são indicativas de calcita amorfa[52,62,77,86,94,95].

Diante dos resultados *in vitro* favoráveis obtidos com o cimento experimental à base de silicato tricálcico (TCS) contendo 30% de $CaWO_4$[28], no presente estudo foi avaliado *in vivo* a reação tecidual e a bioatividade deste material experimental (70% de TCS + 30% do $CaWO_4$) em comparação ao Bio-C Repair e MTA HP. No segundo artigo, nosso propósito foi comparar a resposta tecidual dos materiais biocerâmicos reparadores que também podem ser indicados para pulpotomia, Bio-C Pulpo em comparação ao Biodentine e WMTA.

2 PROPOSIÇÃO

2.1 Objetivo Geral

No presente estudo, foi avaliado a reação tecidual causada por materiais biocerâmicos implantados no tecido conjuntivo do subcutâneo dorsal de ratos adultos. A biocompatibilidade dos materiais foi avaliada por meio da descrição morfológica e morfométrica da reação inflamatória, espessura das cápsulas, imunoexpressão de interleucina-6, presença de fibroblastos e colágeno nas cápsulas. A bioatividade dos materiais foi investigada a partir do von Kossa, presença de calcita birrefringente e imunoreatividade à osteocalcina. A pesquisa foi dividida em duas partes, com os seguintes objetivos específicos de cada artigo:

2.2 Objetivos Específicos

Artigo 1- Avaliar a biocompatibilidade e o potencial bioativo de um material reparador experimental contendo silicato tricálcico puro (TCS) associado ao radiopacificador tungstato de cálcio ($CaWO_4$), em comparação ao MTA Repair HP (Angelus, Indústria de Produtos Odontológicos S/A, Londrina, PR, Brasil) e ao Bio-C Repair (Angelus, Indústria de Produtos Odontológicos S/A, Londrina, PR, Brasil).

Artigo 2- Comparar a reação tecidual induzida pelos materiais à base de silicato tricálcico Bio-C Pulpo (Angelus, Indústria de Produtos Odontológicos S/A, Londrina, PR, Brasil), Biodentine (Septodont, Saint Maur des Fossés, França) e MTA branco (Angelus, Indústria de Produtos Odontológicos S/A, Londrina, PR, Brasil).

3 PUBLICAÇÕES

3.1 Publicação 1*

Abstract

Aim To evaluate the tissue reaction of a tricalcium silicate-based repair material associated with 30% calcium tungstate (TCS + $CaWO_4$) in comparison to Bio-C Repair (Bio-C; Angelus, Brazil) and to MTA Repair HP (MTA HP; Angelus, Brazil).

Methodology Polyethylene tubes filled with one of the materials or empty (control group, CG) were implanted into the subcutaneous tissues of rats for 7, 15, 30 and 60 days (n=8/group per period). The implants with surrounding connective tissue were removed and prepared for paraffin-embedding. The capsule thickness, number of inflammatory cells and the amount of collagen were measured. Interleukin-6 (IL-6) and osteocalcin (OCN) immunohistochemistry reactions were performed and the number of immunolabelled cells was computed. von Kossa reaction and analysis of unstained sections under polarized light were also carried out. Data were submitted to two-way ANOVA analysis followed by Tukey *post-hoc* test ($p<0.05$).

Results In the periods of 7, 15 and 30 days, no significant differences in the number of inflammatory cells, number of IL-6-immunopositive cells and in the collagen, content were observed among TCS + $CaWO_4$, Bio-C and MTA HP materials ($p>0.05$). At 60 days, no significant difference was observed in the number of inflammatory cells and in the immunoexpression of IL-6 among bioceramic materials and CG specimens ($p>0.05$). From 7 to 60 days, a significant reduction in the number of inflammatory cells, number of IL-6-immunopositive cells and in the capsule, thickness was accompanied by a significant increase in the collagen in the capsules of all groups. OCN-immunolabelled cells, von Kossa-positive structures and amorphous calcite deposits were observed in the capsules around all materials. In contrast, these structures and immunoexpression of OCN were not seen in the CG specimens.

* O artigo segue as normas do periódico *International Endodontic Journal*, ao qual foi submetido e está em revisão.

Conclusions These findings indicate that the experimental material (TCS + $CaWO_4$) is biocompatible and has a bioactive potential, similarly to the MTA HP and Bio-C Repair, and suggest its use as a root repair material.

INTRODUCTION

White mineral trioxide aggregate (WMTA, Angelus, Londrina, Brazil) is indicated for several clinical procedures including pulp capping, root repair, retrograde filling, and apexification due its physicochemical and biological properties (Cintra *et al.* 2017, Tanomaru-Filho *et al.* 2017, Lee *et al.* 2018, Benetti *et al.* 2019, ElReash *et al.* 2019, Ferreira *et al.* 2019). However, the composition and manufacture of MTA has undergone modifications over time in an attempt to reduce its drawbacks such as granular consistency, long setting-time, difficulty in handling, and change in tooth colour (Marciano *et al.* 2017, De Souza *et al.* 2018, Ferreira *et al.* 2019, ElReash *et al.* 2019). Although the tooth discoloration seems to be solved by replacing bismuth oxide (radioapacifier) by calcium tungstate ($CaWO_4$), the WMTA-Angelus is a material manufactured from Portland Cement (PC) and contains tricalcium aluminate, besides di- and tricalcium silicate (Camilleri 2020). On hydration reaction, in addition to the calcium silicate hydrate and calcium hydroxide, WMTA gives also rise to a calcium aluminate phase associated with un-reacted powder (Camilleri 2011).

Tricalcium silicate (TCS) is manufactured by the sol-gel method using calcium oxide and silicon oxide as pure raw materials (Din *et al.* 2009, Camilleri 2011). The X-ray diffraction analysis showed that TCS was 99% pure while the Portland cement contained only 68% of tricalcium silicate. In addition, the pure TCS provided a greater deposition of hydroxyapatite after immersion in physiological solution than the PC (Camilleri 2011). Thus, experimental TCS materials have been proposed as alternative materials to the WMTA-Angelus (Camilleri *et al.* 2013, Grech *et al*. 2013, Camilleri *et al.* 2014a, Barbosa *et al.* 2021, Queiroz *et al.* 2021a and 2021b, Taha *et al.* 2021). Several agents, such as niobium oxide, zirconium oxide and calcium tungstate, have provided adequate radiopacity to the calcium silicate-based materials for use as endodontic repair filling material (Silva *et al.* 2014 and 2015, Bosso-Martelo *et al.* 2016, Barbosa *et al.* 2021, Queiroz *et al.* 2021b).

Calcium tungstate ($CaWO_4$) associated with TCS-based cements has shown, in accordance with the ISO standard 6876/2012, adequate physical-chemical properties including the solubility, radiopacity, setting time, alkaline pH (Bosso-Martelo *et al.* 2016, Queiroz *et al.* 2021b), flowability, film thickness and porosity (Marciano *et al.* 2016). In a previous study, an experimental TCS-based cement (70% TCS with 30% $CaWO_4$) exhibited low cytotoxicity to the human osteoblastic cells (Saos-2). Alkaline phosphatase (ALP) activity was greater in Saos cells exposed to cement extracts of 70% TCS with 30% $CaWO_4$ than those containing TCS + niobium oxide and MTA Repair HP. Exposure of Saos-2 to the 70% TCS + 30% $CaWO_4$ cement extracts showed an overexpression of ALP mRNA and an accentuated amount of mineralized nodules. Moreover, this experimental material (70% TCS+30% $CaWO_4$), in direct contact with planktonic *E. faecalis,* exhibited antibacterial effectivity (Queiroz *et al.* 2021b).

Currently, MTA Repair HP (MTA HP; Angelus Indústria de Produtos Odontológicas S/A), a tricalcium silicate-based material containing $CaWO_4$ as radiopacifier, is available on the market. MTA HP has setting time, solubility and radiopacity according to ISO standard 6876/2012 (Guimarães *et al.* 2018, Queiroz *et al.* 2021b), 14,96 % of water sorption (Guimarães *et al.* 2018), provides an alkaline pH (around 10) to the microenvironment (Queiroz *et al*. 2021b), releases calcium ions (Guimarães *et al.* 2018) and presents antibacterial activity against *E. faecalis* (Queiroz *et al.* 2021b). MTA HP was not cytotoxic to Saos-2 cells and induced the formation of mineralized nodules similar to white MTA Angelus (Cintra *et al.* 2017, Tomás-Catalá *et al.* 2017). Morphological and immunohistochemistry findings revealed that MTA HP implanted into subcutaneous tissues is biocompatible and has a bioactive potential (Delfino *et al.* 2021), suggesting that this material may be an alternative for clinical use.

Bio-C Repair (Bio-C; Angelus) is a new ready to use bioceramic repair material. Bio-C has indications similar to MTA Angelus and is composed of calcium silicates [tricalcium silicate (Ca_3SiO_5), besides dicalcium silicate (Ca_2SiO_4)], calcium aluminate, calcium oxide, zirconium oxide (ZrO_2), iron oxide, silicon dioxide and dispersing agent. Bio-C Repair co-cultured with L929 fibroblasts presented cytotoxicity similar to the MTA HP and white MTA Angelus (Benetti *et al.* 2019). An *in vitro* study comparing the cytocompatibility of Bio-C Repair, Biodentine and ProRoot MTA revealed a high viability index of human dental pulp cells (hDPCS) exposed to these cements. Moreover, no

cytoskeleton change was observed in hDPCS, which were adhered to repair cements (Ghilotti *et al.* 2020).

However, dispersing agents and plasticizers added to Bio-C Repair and MTA HP can alter the biological response of materials (Lima *et al.* 2020) since these plasticizers may contain resins that inhibit cell viability and proliferation, and could promote possible systemic damage (Bakopoulou *et al.* 2009, Delfino *et al.* 2021).

In the present study, we evaluated the inflammatory reaction and the presence of osteocalcin and structures indicative of calcite deposits induced by an experimental pure TCS associated with 30% $CaWO_4$, used as radiopacifier agent, in comparison with Bio-C Repair and MTA Repair HP. The null hypothesis would be that the tissue response induced by the experimental bioceramic material would not be different from that Bio-C Repair and MTA Repair HP materials when implanted in the subcutaneous tissue of rats.

MATERIALS AND METHODS

Animals

This study was approved (protocol # 03/2019) by the Ethical Committee for Animal Research of XXXXXX (XXXXXXX) in compliance with XXXX national law on animal use. Animal care was described according to Preferred Reporting Items for Animal Studies in Endodontology (PRIASE) 2021 guidelines (Nagendrababu *et al.* 2021).

Thirty-two adults male Holtzman rats (*Rattus norvegicus albinus*), weighing an average of 220 gr were used in this study. The animals were kept in the room under a light-dark 12:12 cycle at controlled temperature (23 ± 2ºC) and humidity (55 ± 10%) and with food and water provided *ad libitum*. The animals were housed in polyethylene cages (40x30x15 cm) with white pine shavings bedding. The animals were randomly distributed in according to the sacrifice period, as followed: 7, 15, 30 and 60 days after implantation into subcutaneous tissues (8 animals in each period). In each animal, four polyethylene tubes (one from each group) were implanted into the subcutaneous tissues. The groups were named as follows: TCS + $CaWO_4$ (Tricalcium silicate cement + 30% Calcium Tungstate), Bio-C Repair (Bio-C; Angelus, Londrina, Brazil), MTA HP (MTA Repair HP; Angelus, Londrina, Brazil) and

Control Group (CG, empty polyethylene tubes). The chemical composition and trade were described in Table 1. In each animal, the four polyethylene tubes (one of each group) were randomly positioned in the subcutaneous tissues.

The sample size estimation was based in previous study, which has also evaluated the biocompatibility of bioceramic materials implanted into the subcutaneous tissues (Delfino *et al.* 2021). In the present study, the sample size (n=7) was calculated for detection of a 30% difference among materials considering a 15% variability using 90% test power and an alpha error of 0.05 to recognize significant differences. Considering the possible animal loss during experiment or sample loss during histological procedures, 8 animal per material were used in each period (Figure 1). However, the morphological, morphometrical and immunohistochemical analyses were conducted with 7 samples of each group per period.

Materials handling

The experimental material (TCS + $CaWO_4$) was previously prepared using a ratio of 70% TCS (Mineral Research Processing, Meyzieu, France) and 30% calcium tungstate ($CaWO_4$; Sigma Aldrich, St Louis, MO, USA) by weight. This experimental material was mixed at a ratio of 1g of powder and 330 µl of distilled water during 60 seconds when the material exhibited a putty consistency. The Bio-C Repair is provided by manufacturer in a syringe ready to use; this material exhibits a creamy consistency. MTA HP was prepared using a powder/liquid mixing ratio of 1g : 340 µl of vehicle (water and plasticizer) for 40 seconds, obtaining a cement similar a modeling clay. All materials were prepared for used as retrograde filling. The materials were manipulated inside a laminar flow chamber under aseptic conditions, with sterile glass plate and spatula, and inserted into the sterile polyethylene tubes with the aid of an amalgam presser. After that, the tubes containing the materials were immediately inserted into the animals subcutaneous.

Surgical procedures

The animals were anesthetized with a solution containing 0.08mL of 10% ketamine hydrochloride (Virbac do Brasil Indústria e Comércio Ltda, São Paulo, São Paulo, Brazil) and 0.04mL of 2% xylazine hydrochloride (União Química Farmacêutica Nacional S / A, São Paulo, São Paulo, Brazil) per 100 g of body weight administered with a syringe and insulin needle by intraperitoneal route.

After sedation, the animals had the dorsal region shaved and the antisepsis was made with a 5% iodine solution; subsequently, a 2 cm incision was made in the cranio-caudal plane with the aid of a n° 15 scalpel blade (Fibra Cirúrgica, Joinville, Santa Catarina, Brazil). The skin was divulsed with blunt-ended scissors and, subsequently, the polyethylene tubes (Embramed Indústria e Comércio Ltda., São Paulo, São Paulo, Brazil) measuring 10 mm length x 1.5 mm diameter were inserted into subcutaneous connective tissue. In each animal, four polyethylene tubes (one tube per group) were placed in the dorsal subcutaneous tissue. One hundred and twenty-eight polyethylene tubes were implanted in thirty-two animals (four implants in each animal). The incised skin site was sutured with simple stitches using 4-0 silk thread (Ethicon Inc., São José dos Campos, São Paulo, Brazil). After 7, 15, 30 and 60 days of implantation, eight animals (in each time point) were euthanized with anesthetic overdose and the implants were removed with the surrounding tissues.

Histological processing

The tissues surrounding the implanted polyethylene tubes were removed and immediately immersed in a 4% formaldehyde solution (prepared from paraformaldehyde) buffered with 0.1 M sodium phosphate with pH 7.2 at room temperature. After 48 hours, the samples were dehydrated, treated with xylene and immersed in liquid paraffin at 60ºC during 4 hours. The samples were embedded in paraffin for obtaining longitudinal sections of implants. Using a rotating microtome (Leica, model RM2125 RST, Heidelberg, Germany) and disposable stainless-steel knives (Leica, model 818, Heidelberg, Germany), forty 6-µm-thick sections were adhered onto glass slides. Five slides containing two non-serial sections were stained with haematoxylin and eosin (HE) for morphological analysis and estimation of the number of inflammatory cells in the capsules. In sections adhered to silanized slides with 4% 3-aminopropyltriethoxysilane (Sigma-Aldrich Co., Saint Louis, Missouri, USA), immunohistochemistry reactions for detection of interleukin-6 (IL-6) and osteocalcin (OCN) were carried out.

Biocompatibility assays

- *Morphological and quantitative analyses in HE-stained sections*

The main constituents of capsules such as cell types (inflammatory cells and fibroblasts), presence of collagen fibers, blood vessels, and extension of inflammatory reaction were analyzed.

To estimate whether the adjacent tissues were damaged and the extent of inflammatory reaction, the capsule thickness was measured. In each specimen, the thickness of capsule was measured from three HE-stained non-serial sections (distance between the sections around 100 μm). In each section, the image was captured at 65x magnification and the measuring was made from the capsule surface to the adjacent tissues (Saraiva *et al.* 2018, Delfino *et al.* 2021) using an image analysis system (Image-Pro Express 6.0, Olympus). Thus, the capsule thickness was obtained from the average value of the three measurements made in each specimen. According to Yaltirik *et al.* (2004), the capsules measuring until 150 μm were categorized as thin, while those with thickness greater than 150 μm were considered thick.

The degree of the inflammatory infiltrate was also estimated in three non-serial sections (with minimum interval between sections of 100 μm) per specimen. In each section, a standardized field (0.09 mm^2) of the capsule adjacent to the opening of the implanted tubes was captured at x695 magnification. In each specimen, the number of inflammatory cells and fibroblasts was computed in a total field of 0.27 mm^2. The number of inflammatory cells (neutrophils, lymphocytes, plasma cells and macrophages) was computed using an image analysis system (Olympus Image-Pro Express 6.0 program, Tokyo, Japan). Morphological features such as: multilobed nucleus (neutrophils), rounded cell with round and basophilic nucleus (lymphocytes), elliptical cells with nucleus eccentrically located in the basophilic cytoplasm (plasma cells), irregularly shaped cells with indented nucleus (macrophages) were used to identify the inflammatory cells (Silva *et al.* 2014, da Fonseca *et al.* 2016, Delfino *et al.* 2020). The fibroblasts were identified by elliptical/fusiform shape. Thus, the number of inflammatory cells and fibroblasts per mm^2 was estimated in each specimen. This analysis was performed in all specimens of all groups and periods.

- *Immunohistochemistry for detection of IL-6*

For detection of IL-6, the mouse monoclonal anti-IL-6 antibody (Abcam Inc., Cambridge, MA, USA; code: ab9324) was used. The immunohistochemistry for IL-6 detection was performed in all specimens (n = 7 samples per group/period). After dewaxed and hydration, the slides were immersed in 0.001 M sodium citrate buffer with pH 6.0 and the sections were heated in a microwave for 30 min at 94-98 ºC for antigen recovery. After cooling-off, the sections were washed in 0.05 M Tris-HCl buffer with pH 7.4 and, then, immersed in 5% aqueous hydrogen peroxide solution for 20 min to block

endogenous peroxidase. After washings, the sections were incubated in 2% bovine serum albumin (BSA; Sigma-Aldrich Co., Saint Louis, Missouri, USA) for 30 minutes at room temperature. Then, the sections were incubated overnight (16 to 18 hours) in a humid chamber at 4°C with mouse anti-IL-6 primary antibody at 1:100 dilution. Afterwards, the sections were incubated for 1 hour at room temperature with labelled polymer-HRP (EnVision + Dual Link System-HRP, Dako Inc., Carpinteria, CA, USA; code: K4061). Subsequently, the sections were washed in TRIS buffer, and peroxidase activity was revealed by the 3,3'-diaminobenzidine chromogen (DAB; Dako Inc., Carpinteria, California, USA; code: K3468) for 3 min. The sections were counterstained with Carazzi's hematoxylin. As negative controls, sections were submitted to all steps, except the incubation with primary antibody, which was replace by non-immune serum.

The number of immunostained cells (brown/yellow colour) was computed in the capsules of all specimens. Using a digital camera (DP-71, Olympus, Tokyo, Japan) coupled to a light microscope (BX-51, Olympus, Tokyo, Japan), a standard area of 0.09 mm^2 of the capsule adjacent to the opening of the tube was captured, at x695 magnification. The number of IL-6-immunolabelled cells was computed with the aid of an image analysis system (Image Pro-Express 6.0, Olympus). Thus, the number of immunolabelled cells per mm^2 of capsule was calculated in each specimen, and the average per group in each time point was calculated.

- *Amount of collagen in the capsules*

The collagen in the capsules was quantified in sections subjected to the 0.1% picrosirius-red solution and analyzed under polarized light microscope (BX-51, Olympus). In each specimen, three non-serial sections (minimal distance between sections of 100 μm) were used. Using a digital camera attached to the light microscope equipped with polarized filters, a field of the capsule was captured at x695 magnification with rigorously standardized parameters (light intensity, diaphragm aperture, condenser position and exposure time).

The ImageJ® image analysis software (http://rsbweb.nih.gov/ij) was used to estimate the birefringent collagen content in the capsules. The hue definition considered in the birefringence was as follows: red/orange, 2–38 and 230–256; yellow, 39–51; and green, 52–128 (Koshimizu *et al.* 2013, de Pizzol-Júnior *et al.* 2018). Thus, the amount of collagen was represented by the percentage of

birefringent areas (from hue choice) of the total area (expressed in pixels) calculated by image analysis program (Silva *et al.* 2017).

Immunoexpression of osteocalcin (OCN), presence of von Kossa-positive and birefringent structures

- *Immunohistochemistry for detection of OCN*

After dewaxing, the antigen recovery was obtained by immersion of sections in 0.001 M sodium citrate buffer at pH 6.0 heated in microwave at 94 ºC for 10 min. After cooling, the sections were washed in sodium phosphate buffer (50mM PBS + 200mM NaCl, pH 7.3), and the endogenous peroxidase was inactivated by treatment in 5% aqueous hydrogen peroxide solution for 30 min. After washings, the sections were incubated with 2% BSA, for 30min at room temperature and, subsequently, the sections were incubated overnight at 4 °C with rabbit anti-osteocalcin primary antibody diluted 1:500 (Sigma-Aldrich Co., Saint Louis, Missouri, USA; code: SAB 1306277 -40TST). The sections were washed and incubated for 1 hour with labelled polymer-HRP (EnVision + Dual Link System-HRP, Dako Inc., Carpinteria, CA, USA; code: K4061) at room temperature. After washing in buffer, the reaction was reveled with DAB (Dako Inc., Carpinteria, California, USA; code: K3468) and the sections were counterstained with Carazzi's haematoxylin. As negative control, sections were incubated with non-immune serum instead of primary antibody.

The immunohistochemistry for osteocalcin detection was performed in all specimens. A standardized field was captured at x40 magnification (final magnification: x695) in the middle portion of the capsule in juxtaposition to the tube opening. Using an image analysis system, the cells exhibiting immunolabelling in their cytoplasm (in brown/yellow colour) were computed in a standardized area (in the middle portion). Thus, the number of OCN-immunolabelled cells per mm^2 was calculated in each specimen.

von Kossa reaction and birefringent structures

In each specimen, three non-serial sections were subjected to the von Kossa reaction for detection of calcium/phosphate deposits (Meloan & Putcher 1985) in the capsules. After hydration, the sections were immersed in the cold 5% silver nitrate solution for 1 hour under an incandescent lamp

(100 Watts). The slides were quickly washed in distilled water and, then, immersed in 5% sodium hyposulfite solution for 5 min. After washing in distilled water for 5 min, the sections were stained with picrosirius-red (Viola *et al.* 2012, Delfino *et al.* 2020) and mounted in resinous medium (Permount®, Fisher Scientific, New Jersey, USA).

To confirm the presence of calcium deposits, unstained sections were dewaxed, mounted in resinous medium and analyzed under polarized illumination (BX-51, Olympus, Tokyo, Japan) to verify if birefringent structures were present in the capsules.

Statistical analysis

The data were evaluated by two-way ANOVA analysis followed by the Tukey *post-hoc* test (Prism 6.0 software; GraphPad, San Diego, CA, USA) at significance level of $p<0.05$.

RESULTS

Biocompatibility assays

-Morphological findings and thickness of capsules

The general view of HE-stained sections (Figure 2a-2p) revealed that the inflammatory reaction induced by materials was located in the connective tissue in close juxtaposition to the opening of polyethylene tubes. None inflammatory infiltrate was observed in the adjacent loose connective and muscle tissues. Moreover, after 60 days, the capsules were apparently thinner than those of the initial time point.

As shown in Figure 2q, at 7 and 15 days, the capsules thickness of TCS + $CaWO_4$ specimens was significantly higher than those of the other groups ($p<0.05$) whereas no significant difference was detected between Bio-C and MTA HP. In these periods, the lowest values were observed in the CG specimens ($p<0.05$). After 30 days, no significant difference was detected between TCS + $CaWO_4$ and CG, TCS + $CaWO_4$ and MTA HP as well as between Bio-C and MTA HP specimens. However, the capsules of TCS + $CaWO_4$ was thinner than those of Bio-C ($p=0.0481$) whereas the thickness of capsules in Bio-C ($p=0.0017$) and MTA HP ($p=0.0025$) was significantly greater than CG specimens. At 60 days, no significant difference was observed among groups; all groups exhibited thin capsules (from 70 to

149 μm). In all groups, a significant reduction in the thickness of capsules was observed from 7 to 60 days.

-Inflammatory reaction and number of fibroblasts

At 7 days, the specimens of all groups were invariably surrounded by capsules containing numerous inflammatory cells, mainly macrophages, plasma cells and lymphocytes (Figure 3a-3d). Despite the marked presence of inflammatory infiltrate in the capsules after 15 days, fibroblasts dispersed among blood vessels, macrophages and thin collagen fibers were observed (Figure 3e-3h). At 30 (Figure 3i-3l) and 60 (Figure 3m-3p) days, the capsules of all groups exhibited connective tissue with fibroblasts between bundles of collagen fibres; few inflammatory cells were observed.

Concerning numerical density of inflammatory cells (Figure 3q), the highest values were observed in all groups at 7 days. At 7 and 15 days, no significant difference was detected ($p>0.05$) in the number of inflammatory cells among TCS + $CaWO_4$, Bio-C and MTA HP specimens ($p>0.05$); in these groups, the number of inflammatory cells were significantly higher than in CG group ($p<0.05$). After 30 and 60 days, significant differences in the number of inflammatory cells were not observed among the TCS + $CaWO_4$, Bio-C, MTA HP and CG groups ($p>0.05$). In all groups, a significant decrease in the number of inflammatory cells was observed in the capsules from 7 to 60 days ($p<0.05$).

Regarding the number of fibroblasts (Figure 3r), significant differences were not observed among the groups, except at 30 days. In this period, the capsules of Bio-C contained a greater number of fibroblasts than the capsules of CG ($p=0.0076$) and TCS + $CaWO_4$ ($p=0.0208$). From 7 to 60 days, a significant increase in the number of fibroblasts was detected in the capsules of all groups.

-Immunohistochemistry for detection of IL-6

Sections subjected to the immunohistochemistry for detection of IL-6, a pro-inflammatory cytokine, exhibited immunoreactivity (brown-yellow colour) in the cytoplasm of inflammatory cells, fibroblasts and vascular cells in the capsules of all groups and in all periods (Figure 4a-4p). At 7 days, an enhanced IL-6 immunoexpression was observed in all groups (Figure 4a-4d). A gradual reduction in the immunoexpression was also observed in the capsules of all groups over time (Figure 4a-4p). At 60

days, the immunoexpression was seen mainly in the fibroblasts and vascular cells (Figure 4m-4p). In the sections of negative control, no IL-6-immunolabelled cell was observed (data not shown).

The quantitative analysis of IL-6-immunolabeled cells (Figure 4q) showed no significant difference among TCS + $CaWO_4$, Bio-C and MTA HP specimens at 7, 15 and 30 days. In these periods, the capsules around the bioceramic materials contained a greater number of IL-6-immunolabelled cells than in CG capsules ($p<0.05$). However, at 60 days significant differences in the number of IL-6-immunolabelled cells were not observed among TCS + $CaWO_4$, Bio-C, MTA HP and CG groups. From 7 to 60 days, a significant reduction in the number of IL-6-positive cells was observed in all groups ($p<0.05$).

- *Amount of collagen in the capsules*

At 7 days, the capsules of all groups showed few birefringence (Figure 4a-d) in comparison with 60 days (Figure 5e-5h). After 60 days, thick bundles of birefringent collagen irregularly arranged were seen in the capsules (Figure 5e-5h).

The quantitative analysis (Figure 5i) revealed that the lowest values of birefringent collagen content were observed in all groups at 7 days. A gradual and significant increase of collagen content was observed in the capsules of all groups over time. Significant differences among the groups were not observed at any period, except at 7 days. In this period, the collagen content in the TCS + $CaWO_4$ group was greater than in MTA HP ($p=0.0096$).

Immunoexpression of osteocalcin (OCN), presence of von Kossa-positive and birefringent structures

-Immunohistochemistry for detection of OCN

At 7 and 15 days, few OCN-immunolabelled cells were observed in the capsules around TCS + $CaWO_4$ (Figure 6a and 6e), Bio-C (Figure 6b and 6f) and MTA HP (Figure 6c and 6g). An apparent increase in the immunoexpression was seen in the capsules adjacent to the bioceramic materials at 30 (Figure 6i-6k) and 60 (Figure 6m-6o) days. No immunolabelled cell was observed in the capsules of CG specimens (Figure 6d, 6h, 6l and 6p). OCN-immunolabelled cells were not observed in the sections used as negative controls (data not shown).

As shown in Figure 6q, the number of OCN-immunolabelled cells was significantly greater in the capsules around TCS + $CaWO_4$, Bio-C and MTA HP specimens than in CG, in all periods. Moreover, no significant difference in the immunoexpression of OCN was found among the bioceramic materials in all time points. From 7 to 60 days, significant increase in the number of OCN-immunolabelled cells was detected around the TCS + $CaWO_4$, Bio-C and MTA HP specimens, while in CG no significant difference was detected from 7 to 60 days.

-*von Kossa-positive and birefringent structures*

Sections subjected to the von Kossa histochemical method showed black/brown structures, i.e. von Kossa-positivity, in capsules around TCS + $CaWO_4$ (Figure 7a and 7e), Bio-C (Figure 7b and 7f) and MTA HP specimens (Figure 7c and 7g). No von Kossa-positive structure was observed around CG specimens (Figure 7d and 7h). The careful analysis under polarized illumination of unstained sections revealed birefringent and irregular structures in the capsules around TCS + $CaWO_4$ (Figure 7i and 7l), Bio-C (Figure 7j and 7m) and MTA HP (Figure 7k and 7n). Birefringent structures were not found in the capsules of CG specimens (data not shown).

DISCUSSION

Biomaterials containing synthesized tricalcium silicate (TCS) have been proposed as repair materials due to their good biological properties (Camilleri *et al.* 2013, Camilleri *et al.* 2014a, Taha *et al.* 2021). Here, no significant differences were observed in the tissue response induced by experimental TCS, Bio-C and MTA HP, either in the biocompatibility or in the ability to stimulate osteocalcin synthesis and deposition of calcite structures in the connective tissue of rat subcutaneous.

In the present study, the morphological and quantitative analyses revealed that TCS + $CaWO_4$, Bio-C and MTA HP caused initially a moderate inflammatory reaction in the connective tissue of subcutaneous. At 7 and 15 days, the inflammatory infiltrate, observed in the capsules around the repair materials, was significantly greater than in CG specimens, indicating that substances released by these materials may be responsible, at least in part, for tissue damage. Here, the materials were placed in the subcutaneous tissue immediately after insertion into the polyethylene tubes. Considering that initial

setting time of materials is approximately 17 minutes (Ferreira *et al.* 2019) to 32.5 minutes for MTA HP (Queiroz *et al.* 2021b), 61.78 minutes for TSC + $CaWO_4$ (Queiroz *et al.* 2021b) and 7 minutes (Koutroulis *et al.* 2019) to 12 minutes for Bio-C Repair (Lima *et al.* 2020), it is reasonable to suggest that substances released during setting time were harmful to host tissue. Furthermore, one reaction product of calcium silicate-based is the hydroxyl (OH), which provides an alkaline pH to the microenvironment. At first hours, the pH in the medium containing the TCS + $CaWO_4$ is around 9.5 (Queiroz *et al.* 2021b), in Bio-C Repair is around 7 (Oliveira *et al.* 2021) and MTA HP is around 9.3 (Queiroz *et al.* 2021b). It is known that alkaline pH stimulates the recruitment of leukocytes (Scheller *et al.* 2011, Silva *et al.* 2015, Ferreira *et al.* 2019, Hoshino *et al.* 2021) that migrate from blood vessels towards the materials surface, causing capsule thickening as observed at initial time points. However, a significant reduction in the number of inflammatory cells around the calcium silicate-based materials observed over time indicates a suppression in the tissue injury caused by these materials. In fact, no significant difference was found in the number of inflammatory cells between the capsules around calcium silicate-based materials and CG specimens at 30 and 60 days, reinforcing the concept that, after final setting time, the recruitment of inflammatory cells decreases significantly culminating with the formation of thin collagenous capsules.

Immunohistochemistry for detection of IL-6, an interleukin that acts as a proinflammatory cytokine, revealed also a significant reduction in the number of IL-6-immunolabelled cells in capsules around all groups over time. IL-6 is a cytokine produced by a variety of cells including macrophages, lymphocytes, plasma cells, endothelial cells, fibroblasts and mast cells (Scheller *et al.* 2011, da Fonseca *et al.* 2016, de Oliveira *et al.* 2017). There is evidence that this cytokine is responsible for the maintenance of inflammatory reaction since IL-6 plays a role in the maturation of plasma cells as well as in the T cell activation and differentiation (Scheller *et al.* 2011, Tanaka *et al.* 2014). Elevated levels of IL-6 have been detected in chronic inflammatory disorders such as rheumatoid arthritis (Tanaka *et al.* 2014), periodontal disease (de Oliveira *et al.* 2017) and apical periodontitis (Schweitzer *et al.* 2021). The number of IL-6-immunolabelled cells in the capsules seems to be directly associated with degree of inflammatory reaction induced by endodontic materials (da Fonseca *et al.* 2016, Saraiva *et al.* 2018, Delfino *et al.* 2020 and 2021, Hoshino *et al.* 2021). In the present study, no significant difference in the

immunoexpression of IL-6 among the calcium silicate-based materials was observed in all periods, similarly to the results regarding the numerical density of inflammatory cells, indicating that connective tissue injury caused by TCS + $CaWO_4$, Bio-C and MTA HP is transient.

It is important to emphasize that the reduction in the inflammatory reaction was accompanied by a significant increase in the number of fibroblasts and amount of collagen fibers in the capsules around all specimens over time. In all periods, significant differences in the number of fibroblasts in the capsules were not seen among the groups, except at 30 days, when the number of fibroblasts was significantly greater in Bio-C than in TCS + $CaWO_4$ and CG specimens. Significant differences in the collagen content were only found between TCS + $CaWO_4$ and MTA HP at 7 days. In this period, the capsules around TCS + $CaWO_4$ contained a greater content of collagen than in MTA HP specimens. In general, several inflammatory cells and few fibroblasts were seen in the capsules at 7 days while, in the period of 60 days, the fibroblasts were the main cell type observed in the collagen-rich capsules. Moreover, thin capsules measuring approximately 150 μm were found around all specimens at 60 days, reinforcing the idea that there was a regression of inflammatory reaction over time (Saraiva *et al.* 2018, Delfino *et al.* 2020). It has been suggested that ionic dissolution products of dicalcium silicate material may stimulate proliferation and differentiation of MG63 osteoblast-like cells since these cells exhibited a marked increase in alkaline phosphatase (ALP) and type I collagen (COLI) mRNA expression (Sun *et al.* 2009). Here, it is conceivable to suggest that ionic dissociation from calcium silicate materials may induce fibroblast proliferation, culminating with connective tissue repair as observed in the capsules around the TCS + $CaWO_4$, Bio-C and MTA HP specimens after 60 days. Therefore, our findings showed clearly that fibroblasts and collagen fibers, typical components of healthy connective tissue, replaced the inflammatory reaction initially induced by calcium silicate materials. These results taken together indicate that the TCS + $CaWO_4$, Bio-C Repair and MTA HP materials are biocompatible.

The TCS + $CaWO_4$ experimental material was manipulated with distilled water and has handling consistency similar to MTA Angelus, while MTA HP has an organic plasticizer in its liquid, which seems to increase its push-out bond strength when compared to white MTA Angelus (Ferreira *et al.* 2019). MTA HP liquid contains polymers, which improve the plasticity of the repair material (Silva *et al.* 2016, Guimarães *et al.* 2018, Tomás-Catalá *et al.* 2018, Benetti *et al.* 2019, ElReash *et al.* 2019,

Ferreira *et al.* 2019) and promote greater flow than white MTA Angelus (Ferreira *et al.* 2019). Bio-C Repair is a bioceramic repair material "ready to use" with similar indications to MTA and composed of calcium silicates [tricalcium silicate (Ca_3SiO_5) and dicalcium silicate (Ca_2SiO_4)], calcium aluminate, calcium oxide, zirconium oxide (ZrO_2), iron oxide, silicon dioxide. The liquid of Bio-C Repair contains methylparaben and plasticizer with distilled water and calcium chloride (Lima *et al.* 2020). The addition of plasticizer improves the material handling.

Besides biocompatibility, our findings suggest that the TCS + $CaWO_4$, Bio-C Repair and MTA HP materials may express a bioactive potential in the connective tissue of rat subcutaneous. In the present study, von Kossa-positive structures were seen around TCS + $CaWO_4$, Bio-C and MTA HP specimens suggesting the presence of calcium deposits in the capsules (Viola *et al.* 2012, Silva *et al.* 2015, Hoshino *et al.* 2021). Although von Kossa histochemical method reacts with phosphates in calcium deposits, it has been demonstrated that phosphate can be also associated with cations other than calcium (Meloan & Puchtler 1985). However, there are several studies showing that high amount of calcium ions are released by calcium silicate-based materials (Niu *et al.* 2014, Silva *et al.* 2014 and 2015, Bosso-Martelo *et al.* 2016). Calcium ions released in the microenvironment may be responsible, at least in part, for the bioactive behaviour of these materials (Gandolfi *et al.* 2010 and 2011, Bosso-Martelo *et al.* 2016). Calcium peaks in prismatic-cubic crystals, likely calcite, were detected by scanning electron microscope connected with energy dispersive X-ray analysis (SEM-EDX) of MTA discs immersed in phosphate-buffered saline (Gandolfi *et al.* 2010). Calcium supersaturation in the extracellular fluid may result in precipitation of calcium phosphate that could culminate in the nucleation of apatite and, together with other factors and molecules (osteocalcin, osteopontin, ALP), promotes an increase in the amount of apatite as well as in the growth of these crystals (Anderson 1995, Bonewald *et al.* 2003, Ding *et al.* 2009). In fact, it is expected that a bioactive material should stimulate the formation of hydroxyapatite (Gandolfi *et al.* 2011), whose identification requires further analyses such as Fourier transform infrared (FTIR) microspectroscopy and dark field electron microscopy (Katchburian *et al.* 2001, Bonewald *et al.* 2003, Gandolfi *et al.* 2011). Here, the examination of unstained sections of capsules around the calcium silicate materials revealed birefringent structures, which are suggestive of amorphous calcite (Holland *et al.* 1999, Cintra *et al.* 2017, Benetti *et al.* 2019,

Bueno *et al.* 2019, Delfino *et al.* 2020 and 2021). It is known that when calcium silicate materials are hydrated, calcium ions are released (Camilleri *et al.* 2014b, Gandolfi *et al.* 2014, Niu *et al.* 2014, Silva *et al.* 2014 and 2015, Bosso-Martelo *et al.* 2016) and react with carbonate dioxide from the interstitial liquid giving rise to calcium carbonate (Seux *et al.* 1991, Camilleri *et al.* 2014b), a birefringent structure (Holland *et al.* 1999, Cintra *et al.* 2013, Delfino *et al.* 2020 and 2021, Silva *et al.* 2021).

Among the mineralization markers, the ALP, osteocalcin (OCN), osteopontin (OPN) and bone sialoprotein appear to have important participation in different phases of biomineralization (Bonewald *et al.* 2003, Ding *et al.* 2009). In the present study, the OCN was immunohistochemically evaluated in the capsules around the implants. The capsules of TCS + $CaWO_4$, Bio-C and MTA HP were immunoreactive to OCN, a glycoprotein synthetized by cells of mineralized tissues such as osteogenic cells lineage (Benetti *et al.* 2019). Although OCN-immunolabelled cells were observed in the capsules in all periods, a significant increase in the immunoexpression was observed in the capsules around calcium silicate materials over time. These findings indicate that TCS + $CaWO_4$, Bio-C and MTA HP may promote the precipitation of "calcified" structures stimulating the OCN production by mesenchymal-derived cells of subcutaneous connective tissue. It has been suggested that extracellular calcium promotes an increase in the OPN mRNA levels in pulp cells (Rashid *et al.* 2003). OPN is a non-collagen protein found in the mineralized tissues that, similarly to OCN, plays a role in the mineralization process (Sodek & McKee 2000, Bonewald *et al.* 2003). Human dental pulp cells (hDPCs) cultured with elevated calcium ions concentration expressed high levels of OPN and OCN mRNA, indicating that the calcium ions concentration interferes in the expression of ossification related genes (An *et al.* 2012). Therefore, it is conceivable to suggest that calcium released by silicate calcium-based materials could stimulate the connective tissue cells to produce OCN. This hypothesis is supported by the fact that von Kossa-positive and birefringent structures as well as OCN-immunolabelled cells were not observed in the capsules of CG.

Thus, our findings revealed that plasticizers and other substances present in the Bio-C Repair and MTA Repair HP did not promote significant injuries to the connective tissue when compared with TCS + $CaWO_4$. During the choice of a repair material, it is important to have in mind that the products of reaction of the material will be in direct contact with the tissues (Peters 2013, Collado-González *et*

al. 2019). Thus, the recruitment of inflammatory cells induced by materials may be transient, and the repair material may stimulate the proliferation of resident cells as well as induce the secretion of structural components of healthy tissues. Here, our findings, taken together, indicate that the experimental material is biocompatible, induces the repair of connective tissue and probably may exhibit bioactivity. Further studies are needed to evaluate the biointeraction of the TCS + $CaWO_4$ and confirm whether this experimental material is able to stimulate the differentiation and activity of mineralized tissue producing cells.

CONCLUSION

The TCS + 30% $CaWO_4$ constitutes an alternative as repair material since this bioceramic material allows the fibroblasts proliferation and collagen formation over time. Moreover, this experimental bioceramic material allow the precipitation of calcite crystals and stimulate the production of osteocalcin, suggesting that this material has bioactive potential.

CONFLICT OF INTEREST

The authors deny any conflict of interests to this study.

REFERENCES

An S, Gao Y, Ling J, Wei X, Xiao Y (2012) Calcium ions promote osteogenic differentiation and mineralization of human dental pulp cells: implications for pulp capping materials. *Journal of Materials Science: Materials in Medicine* **23,**789-95.

Anderson, HC (1995) Molecular biology of matrix vesicles. *Clinical Orthopaedics and Related Research* **314,** 266-80.

Bakopoulou A, Papadopoulos T, Garefis P (2009) Molecular toxicology of substances released from resin-based dental restorative materials. *International Journal of Molecular Sciences* **10,** 3861-99.

Barbosa DD, Delfino MM, Guerreiro-Tanomaru JM *et al.* (2021) Histomorphometric and immunohistochemical study shows that tricalcium silicate cement associated with zirconium oxide or niobium oxide is a promising material in the periodontal tissue repair of rat molars with perforated pulp chamber floors. *International Endodontic Journal* **54,** 736-52.

Benetti F, Queiroz ÍOA, Cosme-Silva L, Conti LC, de Oliveira SHP, Cintra LTA (2019) Cytotoxicty, biocompatibility of a new ready-for-use bioceramic repair material. *Brazilian Dental Journal* **30,** 325-32.

Bonewald LF, Harris SE, Rosser J *et al.* (2003) von Kossa staining alone is not sufficient to confirm that mineralization in vitro represents bone formation. *Calcified Tissue International* **72,** 537-47.

Bosso-Martelo R, Guerreiro-Tanomaru JM, Viapiana R, Berbert FL, Duarte MA, Tanomaru-Filho M (2016) Physicochemical properties of calcium silicate cements associated with microparticulate and nanoparticulate radiopacifiers. *Clinical Oral Investigations* **20,** 83-90.

Bueno C, Vasques A, Cury M *et al.* (2019) Biocompatibility and biomineralization assessment of mineral trioxide aggregate flow. *Clinical Oral Investigations* **23,** 169-77.

Camilleri J (2011) Characterization and hydration kinetics of tricalcium silicate cement for use as a dental biomaterial. *Dental Materials* **27,** 836-44.

Camilleri J, Sorrentino F, Damidot D (2013) Investigation of the hydration and bioactivity of radiopacified tricalcium silicate cement, Biodentine and MTA Angelus. *Dental Materials* **29,** 580-93.

Camilleri J, Grech L, Galea K *et al.* (2014a) Porosity and root dentine to material interface assessment of calcium silicate-based root-end filling materials. *Clinical Oral Investigations* **18,** 1437-1446.

Camilleri J, Laurent P, About I (2014b) Hydration of Biodentine, Theracal LC, and a prototype tricalcium silicate-based dentin replacement material after pulp capping in entire tooth cultures. *Journal of Endodontics* **40,** 1846-54.

Camilleri J (2020) Classification of hydraulic cements used in dentistry. *Frontiers in Dental Medicine* **1:** 9. doi: 10.3389/fdmed.2020.00009.

Cintra L, Benetti F, de Azevedo Queiroz ÍO *et al.* (2017) Cytotoxicity, biocompatibility, and biomineralization of the new high-plasticity MTA material. *Journal of Endodontics 43*, 774-778.

Cintra LT, Ribeiro TA, Gomes-Filho JE et al. (2013) Biocompatibility and biomineralization assessment of a new root canal sealer and root-end filling material. *Dental Traumatology: Official Publication of International Association for Dental Traumatology* **29,** 145-50.

Collado-González M, López-García S, García-Bernal D *et al.* (2019) Biological effects of acid-eroded MTA Repair HP and ProRoot MTA on human periodontal ligament stem cells. *Clinical Oral Investigations* ***23*****,** 3915-24.

da Fonseca TS, da Silva GF, Tanomaru-Filho M, Sasso-Cerri E, Guerreiro-Tanomaru JM, Cerri PS (2016) In vivo evaluation of the inflammatory response and IL-6 immunoexpression promoted by Biodentine and MTA Angelus. *International Endodontic Journal* **49,** 145-53.

de Oliveira PA, de Pizzol-Júnior JP, Longhini R, Sasso-Cerri E, Cerri PS (2017) Cimetidine reduces interleukin-6, matrix metalloproteinases-1 and -9 immunoexpression in the gingival mucosa of rat molars with induced periodontal disease. *Journal of Periodontology* **88,** 100-11.

de Pizzol Júnior JP, Sasso-Cerri E, Cerri PS (2018) Matrix metalloproteinase-1 and acid phosphatase in the degradation of the lamina propria of eruptive pathway of rat molars. *Cells* **7**, 206.

De Souza LC, Yadlapati M, Lopez HP, Silva R, Letra A, Elias CN (2018) Physico-chemical and biological properties of a new Portland Cement-based root repair material. *European Endodontic Journal* **3,** 38-47.

Delfino MM, Guerreiro-Tanomaru J, Tanomaru-Filho M, Sasso-Cerri E, Cerri PS (2020) Immunoinflammatory response and bioactive potential of GuttaFlow bioseal and MTA Fillapex in the rat subcutaneous tissue. *Scientific Reports* **10,** 7173.

Delfino MM, de Abreu Jampani JL, Lopes CS *et al.* (2021) Comparison of Bio-C Pulpo and MTA Repair HP with White MTA: effect on liver parameters and evaluation of biocompatibility and bioactivity in rats. *International Endodontic Journal* **54,** 1597-13.

Ding S-J, Shie M-Y, Wang C-Y (2009) Novel fast-setting calcium silicate bone cements with high bioactivity and enhanced osteogenesis in vitro. *Journal of Materials Chemistry,* **19,** 1183-90.

ElReash AA, Hamama H, Abdo W, Wu Q, El-Din AZ, Xiaoli X (2019) Biocompatibility of new bioactive resin composite versus calcium silicate cements: an animal study. *BMC Oral Health* **19,** 194.

Ferreira C, Sassone LM, Gonçalves AS *et al.* (2019) Physicochemical, cytotoxicity and in vivo biocompatibility of a high-plasticity calcium-silicate based material. *Scientific Reports* ***9,*** 3933.

Gandolfi MG, Taddei P, Tinti A *et al.* (2010) Kinetics of apatite formation on a calcium-silicate cement for root-end filling during ageing in physiological-like phosphate solutions. *Clinical Oral Investigations,* **14,** 659-68.

Gandolfi MG, Taddei P, Siboni F, Modena E, De Stefano ED, Prati C (2011) Biomimetic remineralization of human dentin using promising innovative calcium-silicate hybrid "smart" materials. *Dental Materials* **27,** 1055-69.

Gandolfi MG, Siboni F, Primus CM, Prati C (2014) Ion release, porosity, solubility, and bioactivity of MTA Plus tricalcium silicate. *Journal of Endodontics* **40,** 1632-37.

Ghilotti J, Sanz JL, López-García S *et al.* (2020) Comparative Surface Morphology, Chemical Composition, and Cytocompatibility of Bio-C Repair, Biodentine, and ProRoot MTA on hDPCs. *Materials* **13,** 2189.

Grech L, Mallia B, Camilleri J (2013) Investigation of the physical properties of tricalcium silicate cement-based root-end filling materials. *Dental Materials* **29,** e20-8.

Guimarães BM, Prati C, Duarte M, Bramante CM, Gandolfi MG (2018) Physicochemical properties of calcium silicate-based formulations MTA Repair HP and MTA Vitalcem. *Journal of Applied Oral Science* **26,** e2017115.

Holland R, de Souza V, Nery MJ, Otoboni-Filho JA, Bernabé PF, Dezan-Júnior E (1999) Reaction of rat connective tissue to implanted dentin tubes filled with mineral trioxide aggregate or calcium hydroxide. *Journal of Endodontics* **25,** 161-66.

Hoshino RA, Delfino MM, da Silva, GF *et al.* (2021) Biocompatibility and bioactive potential of the NeoMTA Plus endodontic bioceramic-based sealer. *Restorative Dentistry & Endodontics* **46,** e4.

Katchburian E, Antoniazzi MM, Jared C *et al.* (2001) Mineralized dermal layer of the Brazilian tree-frog *Corythomantis* greening. *Journal of Morphology* **248,** 56-63

Koshimizu JY, Beltrame FL, de Pizzol Jr JP, Cerri PS, Caneguim BH, Sasso-Cerri E (2013) NF-kB overexpression and decreased immunoexpression of AR in the muscular layer is related to structural damages and apoptosis in cimetidine-treated rat vas deferens. *Reproductive Biology and Endocrinology* **11**.

Koutroulis A, Kuehne SA, Cooper PR, Camilleri J (2019) The role of calcium ion release on biocompatibility and antimicrobial properties of hydraulic cements. *Scientific Reports* **9,** 19019.

Lee BS, Lin HP, Chan JC *et al.* (2018) A novel sol-gel-derived calcium silicate cement with short setting time for application in endodontic repair of perforations. *International Journal of Nanomedicine* **13,** 261-71.

Lima SPR, Santos GLD, Ferelle A, Ramos SP, Pessan JP, Dezan-Garbelini CC (2020) Clinical and radiographic evaluation of a new stain-free tricalcium silicate cement in pulpotomies. *Brazilian Oral Research* **34,** e102.

Marciano MA, Duarte MA, Camilleri J (2016) Calcium silicate-based sealers: assessment of physicochemical properties, porosity and hydration. *Dental Materials **32***, e30–e40.

Marciano MA, Camilleri J, Costa RM, Matsumoto MA, Guimarães BM, Duarte MAH (2017) Zinc oxide inhibits dental discoloration caused by white mineral trioxide aggregate Angelus. *Journal of Endodontics* **43,** 1001-7.

Meloan SN & Puchtler H (1985) Chemical mechanisms of staining methods. von Kossa technique: what von Kossa really wrote and a modified reaction for selective demonstration of inorganic phosphates. *Journal of Histotechnology* **1,** 11-3.

Nagendrababu V, Kishen A, Murray PE *et al.* (2021) PRIASE 2021 guidelines for reporting animal studies in Endodontology: a consensus-based development. *International Endodontic Journal* **54,** 848-57.

Niu LN, Jiao K, Wang TD, Zhang W *et al.* (2014) A review of the bioactivity of hydraulic calcium silicate cements. *Journal of Dentistry* **42,** 517-33.

Oliveira LV, de Souza GL, da Silva GR *et al.* (2021) Biological parameters, discolouration and radiopacity of calcium silicate-based materials in a simulated model of partial pulpotomy. *International Endodontic Journal*, 10.1111/iej.13616.

Peters OA (2013) Research that matters - biocompatibility and cytotoxicity screening. *International Endodontic Journal* **46,** 195-97.

Queiroz MB, Torres FFE, Rodrigues EM *et al.* (2021a) Development and evaluation of reparative tricalcium silicate-ZrO_2 -Biosilicate composites. *Journal Biomedical Materials Research Part B Applied Biomaterials* **109,** 468-76.

Queiroz MB, Torres FFE, Rodrigues EM *et al.* (2021b) Physicochemical, biological, and antibacterial evaluation of tricalcium silicate-based reparative cements with different radiopacifiers. *Dental Materials* **37,** 311-20.

Rashid F, Shiba H, Mizuno N *et al.* (2003) The effect of extracellular calcium ion on gene expression of bone-related proteins in human pulp cells. *Journal of Endodontics*, **29:** 104-107.

Saraiva JA, da Fonseca TS, da Silva GF *et al.* (2018) Reduced interleukin-6 immunoexpression and birefringent collagen formation indicate that MTA Plus and MTA Fillapex are biocompatible. *Biomedical Materials* **13,** 035002.

Scheller J, Chalaris A, Schmidt-Arras D, Rose-John S (2011) The pro- and anti-inflammatory properties of the cytokine interleukin-6. *Biochimica et Biophysica Acta* **1813,** 878-88.

Schweitzer C, Garrido M, Paredes *et al.* (2021) Localization of interleukin-6 signaling complex in epithelialized apical lesions of endodontic origin. *Clinical Oral Investigations* **25,** 4075-83.

Seux D, Couble ML, Hartmann DJ, Gauthier JP, Magloire H (1991) Odontoblast-like cytodifferentiation of human dental pulp cells in vitro in the presence of a calcium hydroxide-containing cement. *Archives of Oral Biology* **36,** 117-28.

Silva GF, Bosso R, Ferino RV *et al.* (2014) Microparticulated and nanoparticulated zirconium oxide added to calcium silicate cement: Evaluation of physicochemical and biological properties. *Journal of Biomedical Materials Research. Part A* **102,** 4336-45.

Silva GF, Tanomaru-Filho M, Bernardi MIB, Guerreiro-Tanomaru JM, Cerri PS (2015) Niobium pentoxide as radiopacifying agent of calcium silicated-based material: evaluation of physicochemical and biological properties. *Clinical Oral Investigations* **19,** 2015-25.

Silva EJNL, Carvalho NK, Senna PM, De-Deus G, Zuolo ML, Zaia AA (2016) Push-out bond strength of MTA HP, a new high-plasticity calcium silicate-based cement. *Brazilian Oral Research* **30,** e84.

Silva GF, Guerreiro-Tanomaru JM, da Fonseca TS *et al.* (2017) Zirconium oxide and niobium oxide used as radiopacifiers in a calcium silicate-based material stimulate fibroblast proliferation and collagen formation. *International Endodontic Journal* 50, e95-e108.

Silva ECA, Tanomaru-Filho M, Silva GF, Lopes CS, Cerri PS, Guerreiro Tanomaru JM (2021) Evaluation of the biological properties of two experimental calcium silicate sealers: an in vivo study in rats. *International Endodontic Journal* **54,** 100-11.

Sodek J & McKee MD (2000) Molecular and cellular biology of alveolar bone. *Periodontology 2000* **24,** *99-126*

Sun J, Wei L, Liu X *et al.* (2009) Influences of ionic dissolution products of dicalcium silicate coating on osteoblastic proliferation, differentiation and gene expression. *Acta Biomaterialia* **5,** 1284-93.

Taha NA, Aboyounes FB, Tamimi ZZ (2021) Root-end microsurgery using a premixed tricalcium silicate putty as root-end filling material: a prospective study. *Clinical Oral Investigations* **25,** 311-17.

Tanaka T, Narazaki M, Kishimoto T (2014) IL-6 in inflammation, immunity, and disease. *Cold Spring Harbor Perspectives in Biology* **6,** a016295.

Tanomaru-Filho M, Andrade AS, Rodrigues EM *et al.* (2017) Biocompatibility and mineralized nodule formation of Neo MTA Plus and an experimental tricalcium silicate cement containing tantalum oxide. *International Endodontics Journal* **50,** e31-9.

Tomás-Catalá CJ, Collado-González M, García-Bernal D *et al.* (2017) Comparative analysis of the biological effects of the endodontic bioactive cements MTA-Angelus, MTA Repair HP and NeoMTA Plus on human dental pulp stem cells. *International Endodontic Journal* **50,** e63-e72.

Tomás-Catalá CJ, Collado-González M, García-Bernal D *et al.* (2018) Biocompatibility of new pulp-capping materials NeoMTA Plus, MTA Repair HP, and Biodentine on human dental pulp stem cells. *Journal of Endodontics* ***44*****,** 126-32.

Viola NV, Guerreiro-Tanomaru JM, da Silva GF, Sasso-Cerri E, Tanomaru-Filho M, Cerri PS (2012) Biocompatibility of an experimental MTA sealer implanted in the rat subcutaneous: quantitative and immunohistochemical evaluation. *Journal Biomedical Materials Research Part B, Applied Biomaterials* **100,** 1773-81.

Yaltirik M, Ozbas H, Bilgic B, Issever H (2004) Reactions of connective tissue to mineral trioxide aggregate and amalgam. *Journal of Endodontics* **30,** 95-9.

Table 1 – Bioceramic materials, manufacturer, chemical composition and proportions.

Materials	Composition	Ratio
TSC + 30% $CaWO_4$ (TCS, Mineral Research Processing, Meyzieu, France and $CaWO_4$, Sigma Aldrich, St Louis, MO, USA)	**Powder:** 70% pure tricalcium silicate (TCS) + 30% calcium tungstate ($CaWO_4$) **Liquid:** distilled water	**Powder:** 1g (70% TSC + 30% $CaWO_4$) **Liquid:** 330 µl of distilled water
BIO-C Repair (Angelus, Londrina, Brazil)	Calcium silicates, calcium aluminate, calcium oxide, zirconium oxide, iron oxide, silicon dioxide and dispersing agent (ready to use).	Syringe (ready to use)
MTA Repair HP (Angelus, Londrina, Brazil)	**Powder:** tricalcium silicate, dicalcium silicate, tricalcium aluminate, calcium oxide and calcium tungstate ($CaWO_4$). **Liquid:** water and plasticizer	**Powder:** 1g **Liquid:** 340 µl of vehicle

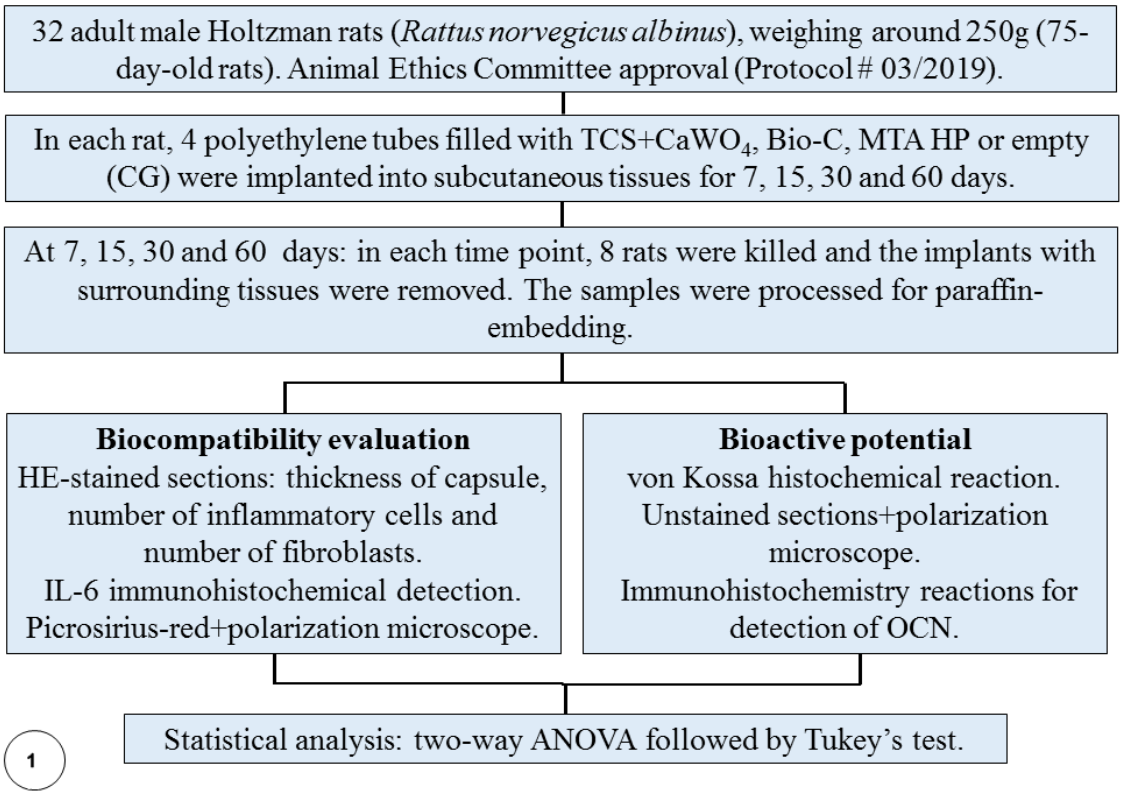

Figure 1 - Flowchart showing the experimental design and methodologies used to evaluate the biocompatibility and bioactive potential of an experimental bioceramic material.

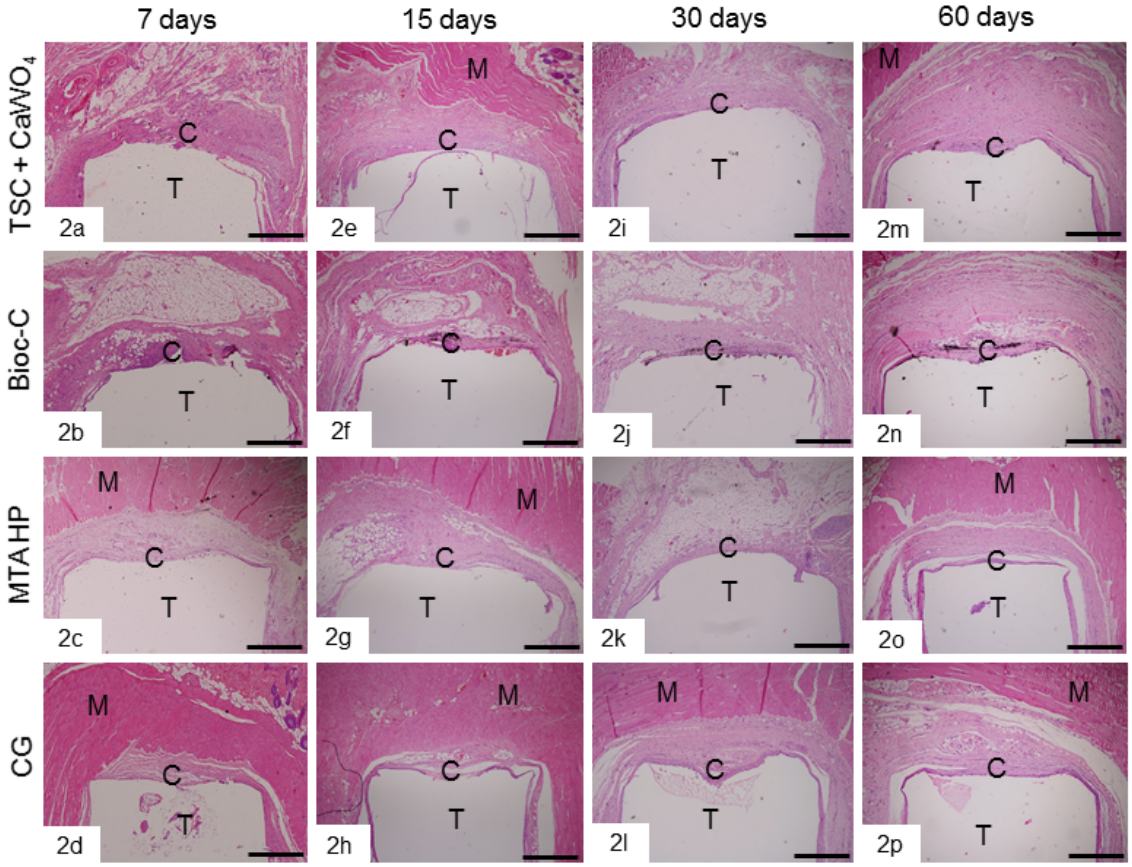
7 days
15 days
30 days
60 days
TSC + CaWO4
Bioc-C
MTA HP
CG
C
T
M
2a
2b
2c
2d
2e
2f
2g
2h
2i
2j
2k
2l
2m
2n
2o
2p

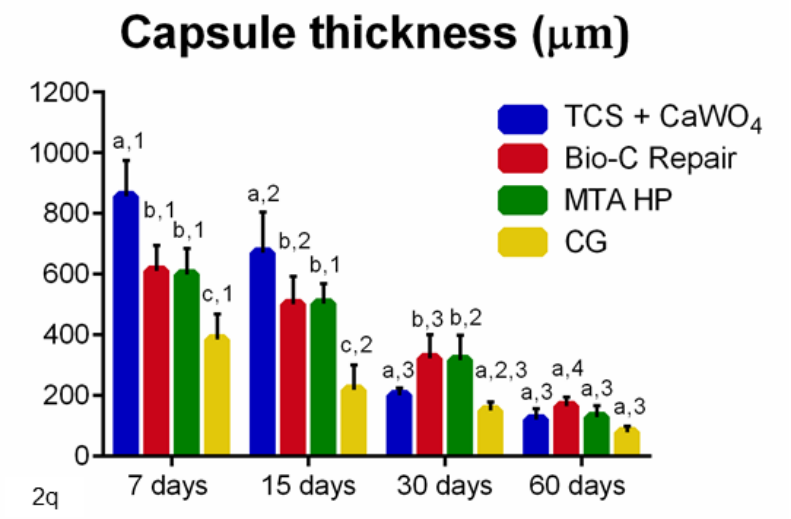
Capsule thickness (µm)
1200
1000
800
600
400
200
0
TCS + CaWO4
Bio-C Repair
MTA HP
CG
a,1
b,1
b,1
c,1
a,2
b,2
b,1
c,2
a,3
b,3 b,2
a,2,3
a,3
a,4
a,3
a,3
7 days
15 days
30 days
60 days
2q

Figures 2a-2p – Light micrographs of sections of capsules of TCS + $CaWO_4$ (2a, 2e, 2i and 2m), Bio-C Repair (2b, 2f, 2j and 2n), MTA HP (2c, 2g, 2k and 2o) and CG specimens (2d, 2h, 2l and 2p) after 7, 15, 30 and 60 days of implantation.

Light micrographs show a general view of capsules (C) around the implants (T). At 7 and 15 days, the capsules around TCS + $CaWO_4$ (2a and 2e), Bio-C Repair (2b and 2f) and MTA HP (2c and 2g) are thick in comparison to CG specimens (2d and 2h). In all groups, thin capsules are seen at 30 (2i-2l) and 60 (2m-2p) days. M, muscle tissue; T, space of implanted polyethylene tube. HE. Bars: 900 μm. **Figure 2q –** Capsule thickness (in μm) of TCS + $CaWO_4$, Bio-C Repair, MTA HP and CG groups. Superscript letters indicate the comparison among the groups; different letters = significant difference. Superscript numbers indicate the analysis of each group over time; different numbers = significant difference. Tukey's test ($p<0.05$).

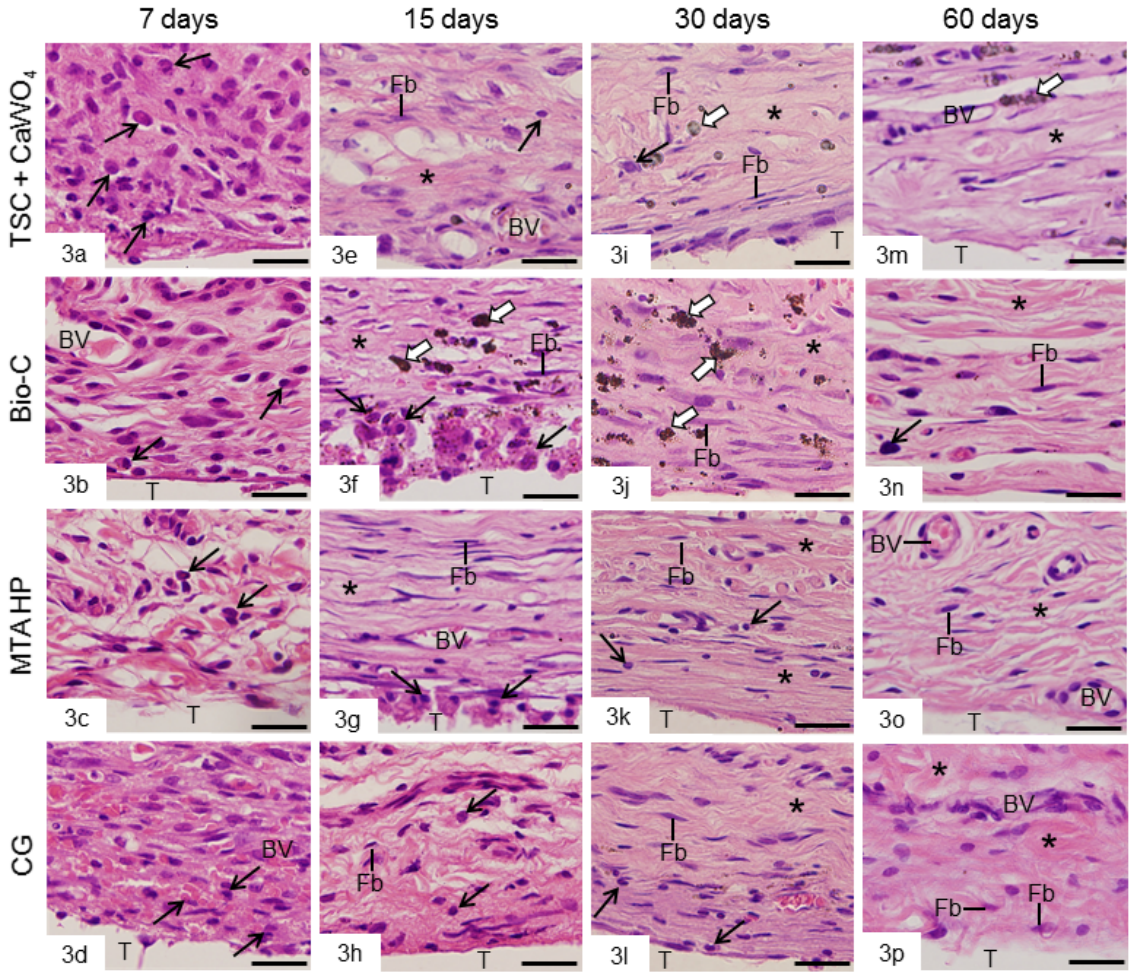
7 days
15 days
30 days
60 days
TSC + CaWO4
Bio-C
MTA HP
CG
3a
3b
3c
3d
3e
3f
3g
3h
3i
3j
3k
3l
3m
3n
3o
3p
Fb
BV
T
Number of inflammatory cells
Number of fibroblasts
3q
3r
7 days
15 days
30 days
60 days
TCS + CaWO4
Bio-C Repair
MTA HP
CG

Figures 3A-3P – Light micrographs of sections of capsules of TCS + $CaWO_4$ (3a, 3e, 3i and 3m), Bio-C Repair (3b, 3f, 3j and 3n), MTA HP (3c, 3g, 3k and 3o) and CG specimens (3d, 3h, 3l and 3p) after 7, 15, 30 and 60 days of implantation. At 7 (3a-3d) and 15 (3e-3h) days, several inflammatory cells (arrows) are dispersed throughout the capsules. Numerous inflammatory cells (arrows) are seen in close contact with the Bio-C Repair (3f) and MTA HP (3g) after 15 days. At 30 (3i-3l) and 60 (3m-3p) days, fibroblasts (Fb) are present between collagen fibres (asterisk) and few inflammatory cells (arrows). T, space of implanted polyethylene tube; BV, blood vessel; thick arrow, material particle. HE. Bars: 30 μm. **Figures 3q and 3r –** Number of inflammatory cells per mm^2 (2q) and number of fibroblasts (2r) per mm^2 in the capsules of TCS + $CaWO_4$, Bio-C Repair, MTA HP and CG. Superscript letters indicate the comparison among the groups; different letters = significant difference. Superscript numbers indicate the analysis of each group over time; different numbers = significant difference. Tukey's test. ($p<0.05$).

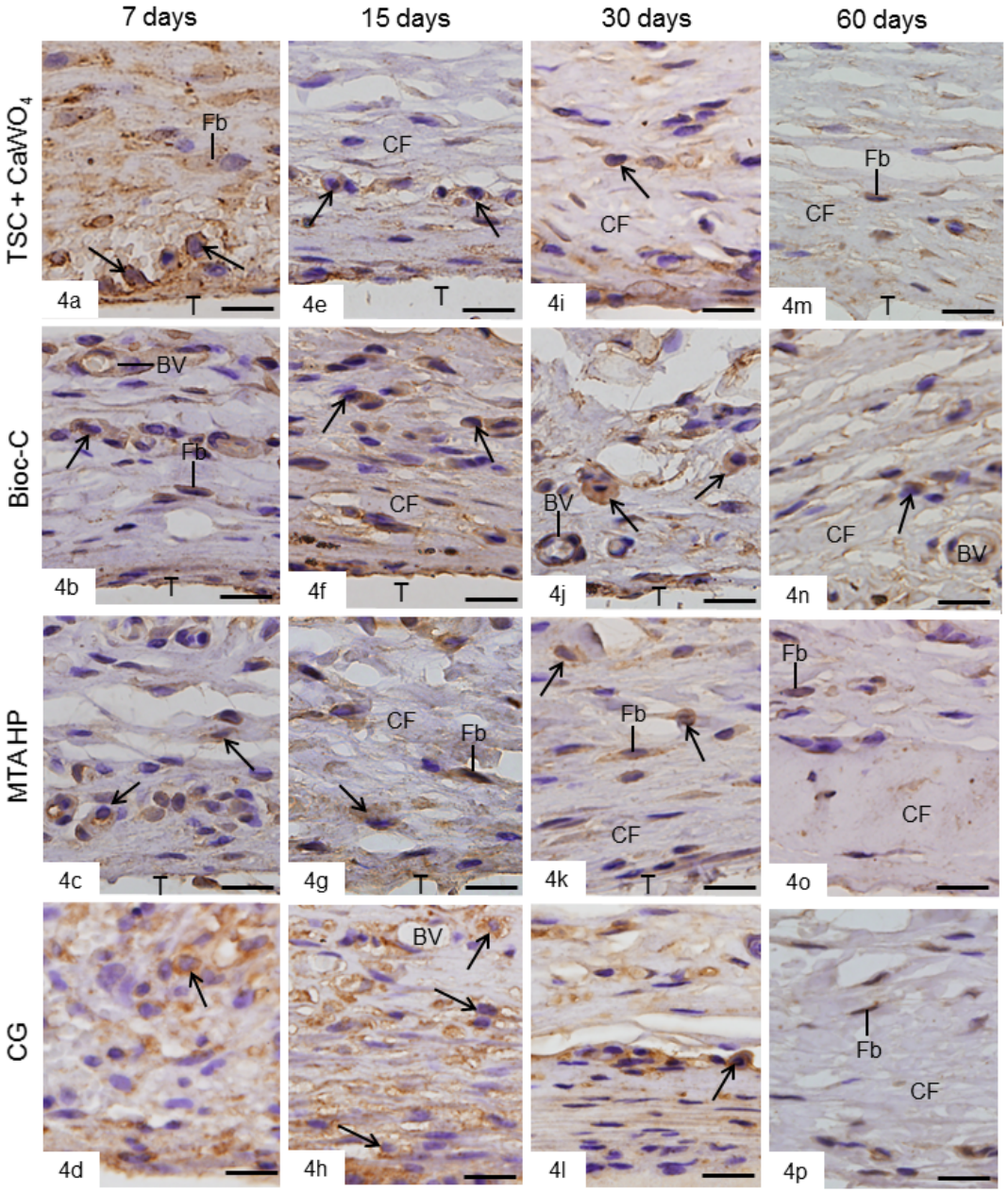
7 days
15 days
30 days
60 days
TSC + CaWO4
Bioc-C
MTA HP
CG
Fb
CF
BV
T
4a
4b
4c
4d
4e
4f
4g
4h
4i
4j
4k
4l
4m
4n
4o
4p

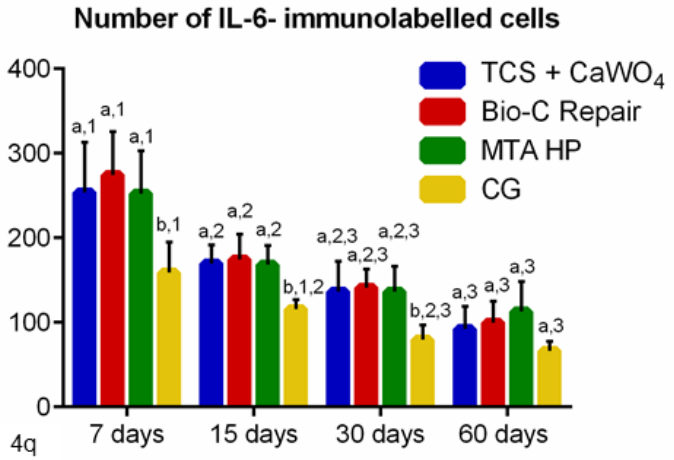
Number of IL-6- immunolabelled cells
TCS + CaWO4
Bio-C Repair
MTA HP
CG
400
300
200
100
0
7 days
15 days
30 days
60 days
4q

Figures 4a-4p – Light micrographs of sections of capsules of TCS + $CaWO_4$ (4a, 4e, 4i and 4m), Bio-C Repair (4b, 4f, 4j and 4n), MTA HP (4c, 4g, 4k and 4o) and CG specimens (4d, 4h, 4l and 4p) after 7, 15, 30 and 60 days of implantation. Sections were subjected to immunohistochemistry for detection of IL-6 (brown-yellow colour) and counterstained with haematoxylin. IL-6-immunolabelled inflammatory cells (arrows) and some fibroblasts (Fb) are seen in the capsules of all groups. BV, blood vessels; CF, collagen fibres. Bars: 22 μm. **Figure 4q -** Number of IL-6-immunolabelled cells in the capsules of TCS + $CaWO_4$, Bio-C Repair, MTA HP and CG groups at 7, 15, 30 and 60 days. Superscript letters indicate the comparison among the groups in each time point; different letters = significant difference. Superscript numbers indicate the analysis of each group over time; different numbers = significant difference. Tukey's test ($p<0.05$).

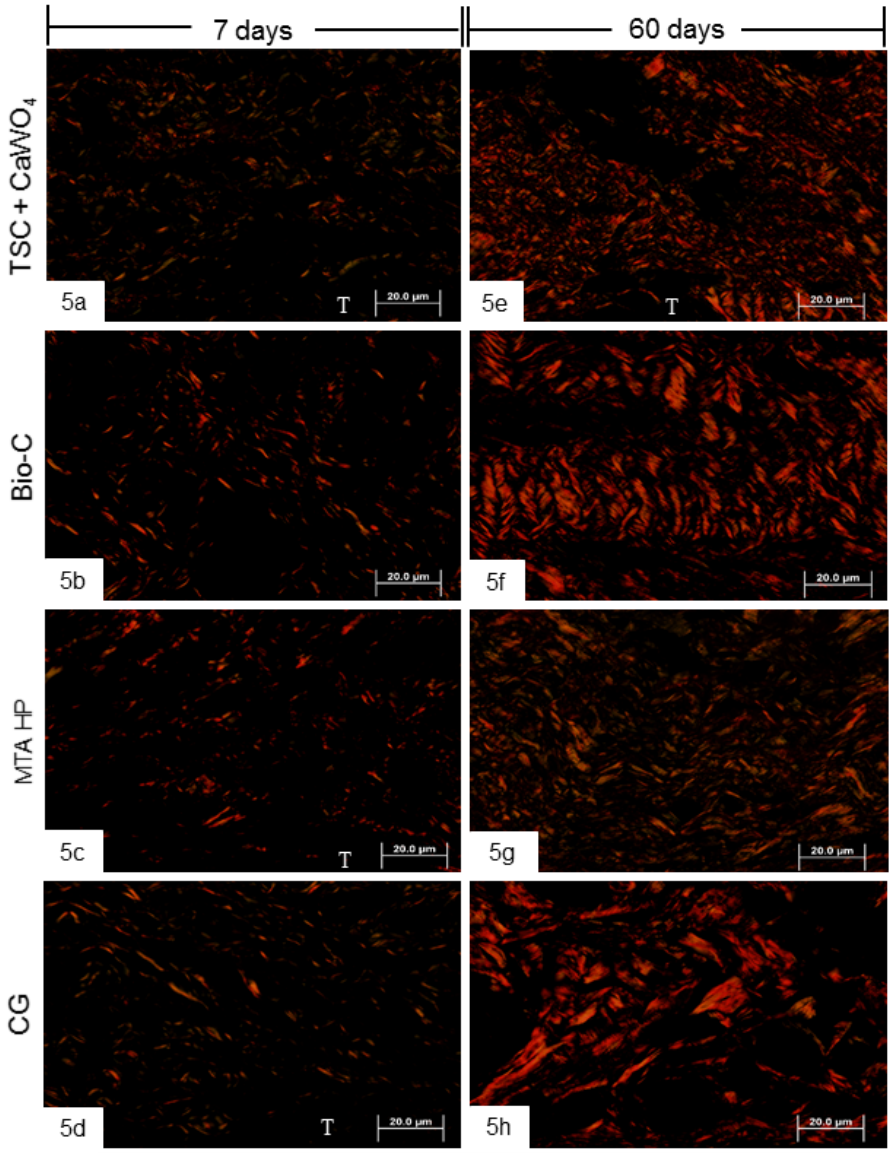
7 days
60 days
TSC + CaWO4
Bio-C
MTA HP
CG
5a
5b
5c
5d
5e
5f
5g
5h
T
20.0 µm

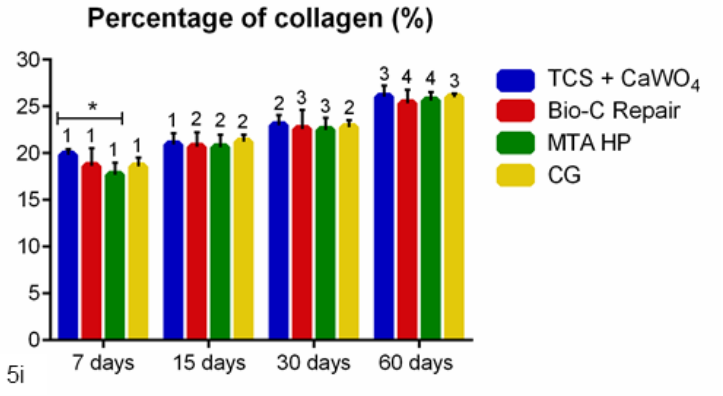
Percentage of collagen (%)
30
25
20
15
10
5
0
7 days
15 days
30 days
60 days
TCS + CaWO4
Bio-C Repair
MTA HP
CG
5i

Figures 5a-5h – Light micrographs of sections of capsules of TCS + $CaWO_4$ (5a and 5e), Bio-C Repair (5b and 5f), MTA HP (5c and 5g) and CG specimens (5d and 5h) after 7, 15, 30 and 60 days of implantation. The sections were stained with picrosirius-red and photographed under polarized illumination. At 7 days (5a-5d), few birefringent collagen fibres (orange/red colors) are seen in the capsules. At 60 days (5e-5h), an evident increase in the birefringence is observed in the capsules of all groups. T, space of implanted polyethylene tube. Bars: 20 μm. **Figure 5i –** Birefringent collagen content (in percentage) in TCS + $CaWO_4$, Bio-C Repair, MTA HP and CG groups at 7, 15, 30 and 60 days. Superscript asterisk indicates significant difference between the TCS + $CaWO_4$ and MTA HP groups at 7 days. Superscript numbers indicate the analysis of each group over time; different numbers = significant difference. Tukey's test ($p<0.05$).

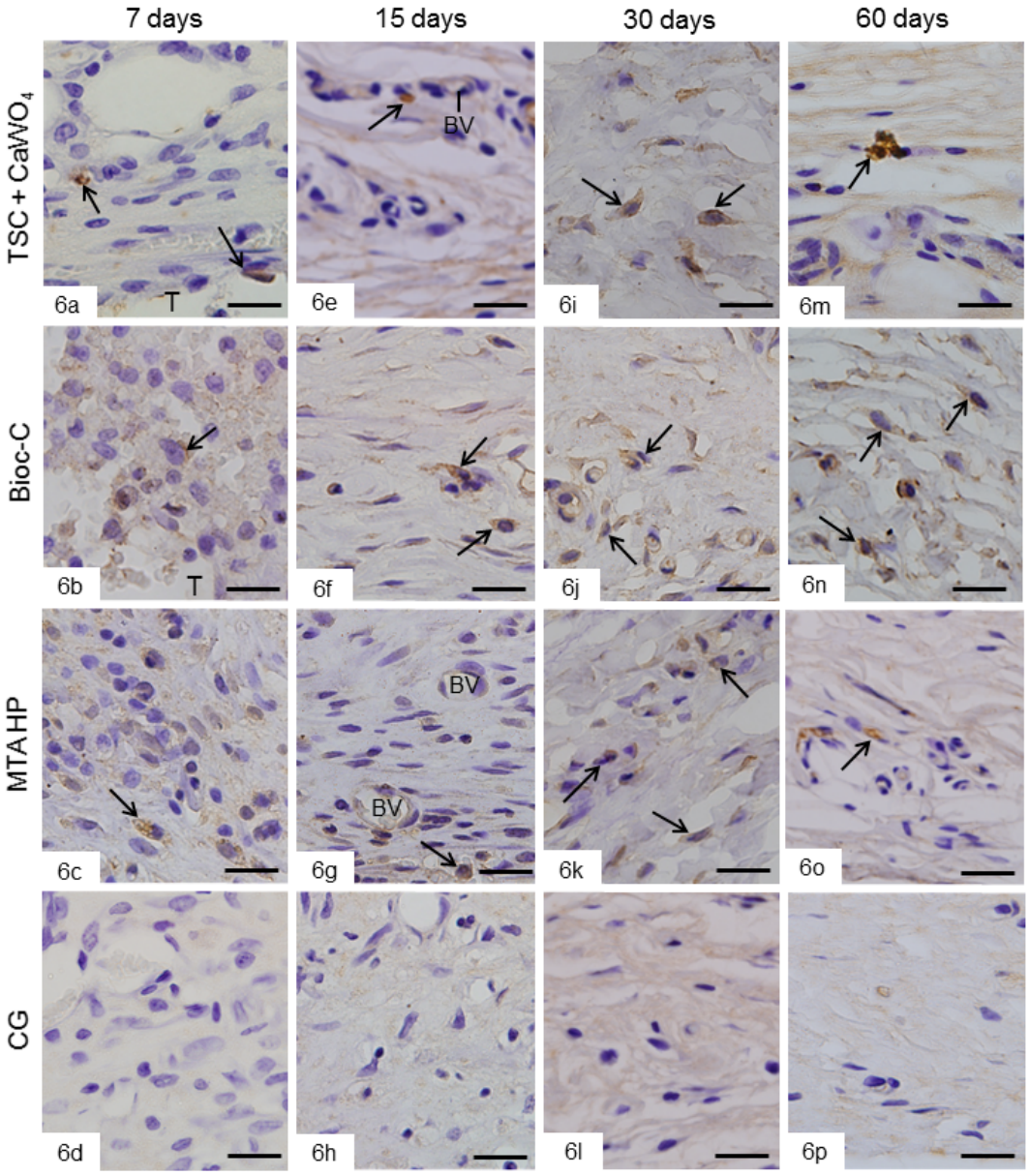
7 days
15 days
30 days
60 days
TSC + CaWO4
Bioc-C
MTA HP
CG
T
BV
6a
6b
6c
6d
6e
6f
6g
6h
6i
6j
6k
6l
6m
6n
6o
6p

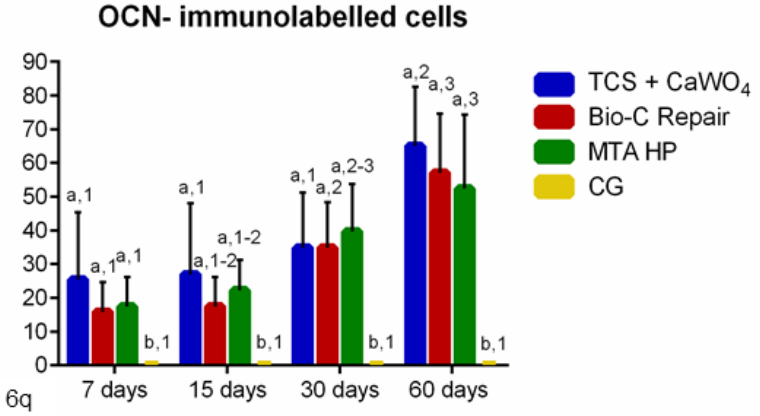
OCN- immunolabelled cells
TCS + CaWO4
Bio-C Repair
MTA HP
CG
7 days
15 days
30 days
60 days
6q

Figures 6a-6p – Light micrographs of sections of capsules of TCS + $CaWO_4$ (6a, 6e, 6i and 6m), Bio-C Repair (6b, 6f, 6j and 6n), MTA HP (6c, 6g, 6k and 6o) and CG specimens (6d, 6h, 6l and 6p) after 7, 15, 30 and 60 days of implantation. Sections were subjected to immunohistochemistry for detection of OCN (brown-yellow colour) and counterstained with haematoxylin. In 6a-6c, 6e-6g, 6i-6k and 6m-6o, some cells exhibiting cytoplasmic immunolabelling are seen in the capsules around the materials. In 6d, 6h, 6l and 6p (CG), OCN-immunolabelled cells are not observed. Bars: 20 μm. **Figure 6q –** Number of OCN-immunolabelled cells in the capsules of TCS + $CaWO_4$, Bio-C Repair, MTA HP and CG groups at 7, 15, 30 and 60 days. Superscript letters indicate the comparison among the groups in each time point; different letters = significant difference. Superscript numbers indicate the analysis of each group over time; different numbers = significant difference. Tukey's test ($p<0.05$).

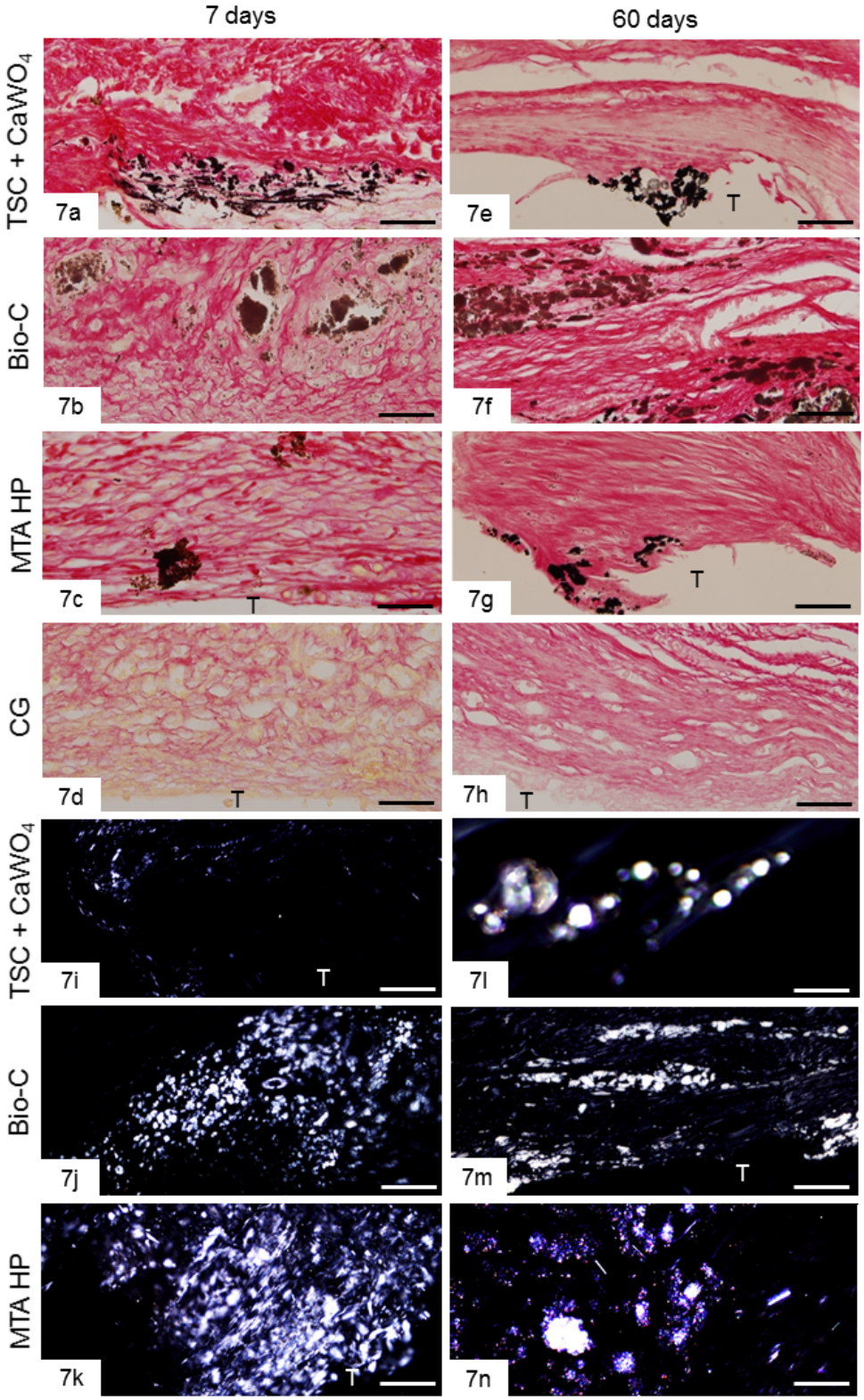
7 days
60 days
TSC + CaWO4
Bio-C
MTA HP
CG
TSC + CaWO4
Bio-C
MTA HP
7a
7b
7c
7d
7e
7f
7g
7h
7i
7j
7k
7l
7m
7n
T

Figures 7a-7h – Light micrographs of portions of capsule juxtaposed to the opening of the polyethylene tubes after 7 (7a-7d) and 60 (7e-7h) days of implantation into the subcutaneous. The sections were subjected to von Kossa histochemical reaction (black colour) and counterstained with picrosirius-red (red colour). von Kossa-positive structures (in black colour) are seen in the capsules of TCS + $CaWO_4$ (7a and 7e), Bio-C Repair (7b and 7f) and MTA HP (7c and 7g). No reactivity is observed in the capsules of CG specimens (7d and 7h). **Figs. 7i-7n –** Light micrographs of portions of capsules of unstained sections under polarized light. Birefringent material with granular aspect is seen in the capsules of TCS + $CaWO_4$ (7i and 7l), Bio-C Repair (7j and 7m) and MTA HP (7k and 7n). T, space of implanted polyethylene tube. Bars: 120 μm.

3.2 Publicação 2*

Bioactive potential of Bio-C Pulpo is evidenced by the presence of birefringent calcite and osteocalcin immunoexpression in the tissue rat subcutaneous

Address for all correspondence:
Prof. Dr. Paulo Sérgio Cerri
Laboratory of Histology and Embryology – Dental School
São Paulo State University (UNESP), Araraquara, SP, Brazil.
Phone: +55 16 33016497
Fax: +55 16 33016433
e-mail: paulo.cerri@unesp.br

ORCID

Marcela B. Queiroz https://orcid.org/0000-0002-2140-1095

*O artigo segue as normas do periódico *Journal of biomedical materials research. Part B, Applied biomaterials*, ao qual foi aceito para publicação.

Abstract

To evaluate the tissue reaction and bioactive potential of Bio-C Pulpo (Angelus, Brazil) in comparison with Biodentine (Septodont, France) and White MTA (WMTA; Angelus, Brazil). In thirty-two rats, 148 polyethylene tubes filled with Bio-C Pulpo, Biodentine or WMTA, and empty (CG, control group) were implanted into subcutaneous tissues for 7, 15, 30 and 60 days. The samples were removed and embedded in paraffin. The capsule thickness, numerical density of inflammatory cells (IC) and fibroblasts (Fb), amount of collagen, immunohistochemistry detection of interleukin-6 (IL-6) and osteocalcin (OCN), von Kossa and analysis of unstained sections under polarized light were performed. Data were subjected to two-way ANOVA followed by Tukey's test ($p \leq 0.05$). At 7 and 15 days, the capsules around Bio-C Pulpo were thicker than in WMTA while no significant difference was found between Bio-C Pulpo and Biodentine ($p=0.8987$). At 30 and 60 days, significant differences in the thickness of capsules were not observed among the groups. Although at 7 days the number of IC was greater around Biodentine than in Bio-C Pulpo ($p=0.0046$) and WMTA ($p=0.0139$), no significant difference was detected among the materials in other periods. At 7, 15 and 30 days, a greater number of IL-6-immunostained cells was found in Bio-C Pulpo and Biodentine than in WMTA specimens while, at 60 days, no significant difference was detected among the groups. In all groups, the number of Fb and collagen content increased significantly over time. In all periods, the capsules around materials exhibited von Kossa-positive and birefringent structures, and OCN-immunostained cells whereas, in the CG, these structures and immunolabelled cells were not observed. Bio-C Pulpo, similarly to Biodentine and WMTA, is biocompatible and allows the connective tissue repair as well as induces the immunoexpression of osteocalcin and deposition of calcite suggesting that this material may present a bioactive potential.

KEYWORDS

Bioactive material, tissue reaction, immunohistochemistry, interleukin-6, osteocalcin, bioceramic materials, repair materials

1 INTRODUCTION

The success of pulpotomy treatment is directly influenced by the biological properties of the endodontic material, which must be biocompatible and induce the differentiation of cells able to synthesize proteins of mineralized tissues, such as dentine and bone[1,2,3]. The tricalcium silicate-based materials, including the White MTA (WMTA; Angelus Indústria de Produtos Odontológicas S/A, Brazil), are biocompatible[4,5,6] and induce the hard tissue bridge formation[7,8,9,10]. Thus, WMTA Angelus is a tricalcium silicate-based material considered the gold standard for the pulpotomy treatment[11,12,13]. WMTA exhibits good physicochemical properties such as radiopacity, solubility, setting time, as well as provides an alkaline pH to the microenvironment[5] and releases calcium ions[14,15,16,17]. The replacement of its radiopacifying agent (bismuth oxide) by calcium tungstate seems to avoid tooth discoloration[5,18], being indicated as a repair material in the treatment of pulpotomy vital pulp treatment[19], in addition to maintaining its biocompatibility and bioactive potential[6].

Biodentine TM (Septodont, Saint Maur des Fossés, France) was developed in 2009, being indicated as a repair material in the treatment of pulpotomy and acting as a substitute for dentine[20,21,22]. Biodentine is a tricalcium silicate-based material containing zirconium oxide as radiopacifier agent[23,24]. This tricalcium silicate-based material is biocompatible[25,26,27,28,29] and stimulates the fibroblast proliferation and formation of collagen fibers, leading to connective tissue repair[27]. Moreover, it has been demonstrated that Biodentine presents fast setting time, ease of handling and insertion into cavities and no dental discoloration[30]. The alkaline pH provided by Biodentine (approximately 10) has been associated with antimicrobial activity against *E. faecalis* planktonic cells and capacity to induce the production of mineralization nodules[31]. An in vivo study has demonstrated that Biodentine induced the formation of mineralized tissue in the teeth of dogs with furcation perforation[29]. Moreover, the Biodentine implanted into subcutaneous tissues induced the precipitation of calcium in the capsules[32,32] as well as the presence of calcium and phosphorus were detected by scanning electron microscopy and spectroscopy X-rays by energy dispersion (SEM/EDX), supporting the concept that Biodentine has bioactive potential[33].

Bio-C Pulpo（Angelus Indústria de Produtos Odontológicas S/A, Brazil）has been developed by Angelus for the treatment of pulpectomy, lining cavity and protecting the pulp-dentine complex. Bio-C Pulpo is a bioceramic material containing tricalcium and dicalcium silicate, calcium aluminate, calcium hydroxide, calcium fluoride, silicon dioxide, iron oxide, and zirconium oxide in its powder whereas the liquid contains distilled water, plasticizer,

calcium chloride (catalyst), and methylparaben [9,18,34,35]. Thus, the mixture of powder/liquid provides a material with consistency similar to "modelling putty"[6,18], which facilitates handling and insertion into dental cavities, an advantageous feature of Bio-C Pulpo compared to WMTA. Studies comparing Bio-C Pulpo with WMTA have demonstrated that Bio-C Pulpo, besides alterations in its chemical composition, maintains the biocompatibility and bioactive potential, expected features from a bioceramic material[6,18]. Moreover, no change in the structural integrity of liver as well as in the serum glutamic-oxaloacetic transaminase and glutamic-pyruvic transaminase levels, biochemical parameters of liver function, indicates that Bio-C Pulpo does not promote systemic changes[6].

In the present study, the tissue response induced by Bio-C Pulpo was compared with Biodentine and WMTA, focusing on the inflammatory reaction, connective tissue repair and bioactivity of the bioceramic materials. The null hypothesis was that Bio-C Pulpo would induce intense tissue injury when compared with Biodentine and WMTA after implantation in the connective tissue of rat subcutaneous.

2 MATERIALS AND METHODS

2.1 Experimental design

The research was approved by the Ethical Committee for Animal Research of São Paulo State University (UNESP/FOAr, SP, Brazil).

Thirty-two male Holtzman rats (*Rattus norvegicus albinus*) aged 3 months, weighing 220-250 g, were maintained in the room at a controlled temperature (23 ± 2ºC) and humidity (55 ± 10%) under a light-dark 12:12 cycle. The animals were housed in polyethylene cages (40x30x15 cm) containing a layer of white pine shavings, and were provided with water and food *ad libitum*.

After anesthesia with a solution containing 80 mg ketamine hydrochloride (Virbac do Brasil Indústria e Comércio Ltda, São Paulo, São Paulo, Brazil) and 8 mg xylazine hydrochloride (União Química Farmacêutica Nacional S / A, São Paulo, São Paulo, Brazil) per 100 g of body weight via the intraperitoneal route, the animals had the dorsal region shaved. After antisepsis of dorsal region with a 5% iodine solution, a 2 cm incision was made in the cranio-caudal plane using a n° 15 scalpel blade (Fibra Cirúrgica, Joinville, Santa Catarina, Brazil). With blunt-ended scissors, a pocket was created in the subcutaneous, and the polyethylene tubes (measuring 10 mm length x 1.5 mm diameter) filled with Bio-C Pulpo (Angelus, Londrina, Brazil), Biodentine (Septodont, Saint Maur-des-Fosses, France) or WMTA

Angelus (White MTA Angelus, Londrina, Brazil) were implanted (Table 1). Polyethylene tubes without material were used as control group (CG). In each animal, four implants (one of each material and one empty polyethylene tube) were placed in the subcutaneous pocket. After 7, 15, 30 and 60 days, eight animals were killed in each time point, totaling thirty-two animals.

2.2 Histological processing

The implants and surrounding tissues were removed and fixed in a 4% formaldehyde solution (prepared from paraformaldehyde) buffered with 0.1 M sodium phosphate with pH 7.2 at room temperature. After 48 hours, the specimens were dehydrated in graded concentrations of ethanol, treated with xylene and immersed for 4 hours in liquid paraffin. Forty longitudinal sections (6 μm thick) were obtained of each implant. From non-serial sections stained with haematoxylin and eosin (HE), the histopathological description and quantitative analyses were carried out. The amount of collagen in the capsules was measured using sections stained with picrosirius-red and analyzed under polarized illumination. The von Kossa histochemical reaction and analysis of unstained sections with polarization microscope were performed to evaluate the presence of calcite crystals in the capsules. The sections were also subjected to the immunohistochemistry reactions for detection of interleukin-6 (IL-6), a pro-inflammatory cytokine[26,36], and osteocalcin (OCN), a glycoprotein involved in the mineralization process[37].

2.2.1 - Histopathological and quantitative analyses

The capsules adjacent to the polyethylene tube opening were analyzed according to the following parameters: predominant cell types (inflammatory cells or fibroblasts), collagen fibers and blood vessels as well as structural integrity of adjacent tissues (muscular tissue and loose connective tissue) to the capsules. All morphological and quantitative analyses were performed by a blinded examiner.

The extension of the inflammatory reaction promoted by implants was estimated measuring the thickness of capsules. To measure the thickness of capsules, three HE-stained non-serial sections (the smallest distance between the sections was 100 μm) of each specimen was used. In each section, the image was captured at x40 using a digital camera attached to a light microscope (BX-51, Olympus, Tokyo, Japan). Using an image analysis program (Image-Pro Express 6.0, Olympus), the thickness of capsule was measured from the capsule surface until the adjacent tissues[38] and the average value of the three measurements was calculated for each specimen. The capsules measuring until 150 μm were categorized as thin while capsules measuring over 150 μm were considered thick[6,38,39].

In addition, to evaluate the inflammatory infiltrate degree and whether the bioceramic materials induce the connective tissue repair, the number of inflammatory cells and fibroblasts was obtained in the capsules. In each specimen, three non-serial HE-stained sections (with minimum interval between sections of 100 μm) were used to estimate the number of inflammatory cells and number of fibroblasts. In each section, a standardized field (0.09 mm^2) of the capsule adjacent to the implanted tube opening was captured using x40 objective lens (x695 final magnification). Using an image analysis program (Olympus Image-Pro Express 6.0 software, Tokyo, Japan) the inflammatory cells (neutrophils, plasma cells, mast cells, macrophages and lymphocytes) and fibroblasts were identified according to morphological characteristics[26,27,36,38,40]. The total number of inflammatory cells and fibroblasts computed from three fields per specimen was divided by total area (0.27 mm^2) and, the number of inflammatory cells and fibroblasts per mm^2 was obtained in each specimen. This analysis was performed in all specimens in the different periods.

2.2.2 - Detection of IL-6 and OCN

Sections adhered to the slides treated previously with 3-aminoprpyl-triethoxysilane (Sigma-Aldrich Chemie, GmbH, Steihenheim, Germany) were deparaffinized and hydrated. For antigen retrieval, the slides were immersed in 0.001 M sodium citrate buffer with pH 6.0 and heated at 94-98º C in microwave oven for 30 min. The sections were washed in 0.05 M Tris-HCl buffer at pH 7.4 and immersed for 20 min in 5% aqueous hydrogen peroxide solution to inactivate the endogenous peroxidase. After incubation in 2% bovine serum albumin (BSA; Sigma-Aldrich Co., Saint Louis, Missouri, USA) for 30 minutes at room temperature, the sections were incubated overnight at 4 ° C with the primary antibodies: mouse monoclonal anti-IL-6 antibody (Abcam Inc., Cambridge, MA, USA; code: ab9324; 1:100 dilution) and rabbit anti-osteocalcin antibody (Sigma-Aldrich Co., Saint Louis, Missouri, USA; code: SAB 1306277-40TST; 1:500 dilution). After washings in Tris-HCl buffer, the sections were incubated for 1 hour at room temperature with HRP-labelled polymer (EnVision + Dual Link System-HRP, Dako Inc., Carpinteria, CA, USA; K4061). The sections were washed in buffer and the peroxidase activity was revealed by the 3,3'-diaminobenzidine chromogen (DAB, Dako Inc., Carpinteria, California, USA) for 3 min, and counterstained with Carazzi's haematoxylin. In the negative controls, the primary antibodies were replaced by mouse or rabbit non-immune serum.

The number of IL-6- and OCN-immunostained cells (yellow/brown colour) was counted in all specimens. In each specimen, a standardized field of capsule adjacent to the polyethylene

tube opening was captured at x40 magnification (area of 0.09 mm^2). Using an image analysis program (Image Pro-Express 6.0, Olympus), the immunolabelled cells were counted and the number of IL-6- and OCN-immunostained cells per mm^2 was calculated[6,26,38].

2.2.3 - Birefringent collagen in the capsules

To estimate the amount of collagen in the capsules, three non-serial sections per specimen were stained for 1 hour with 0.1% picrosirius-red solution. After washing, the sections were dehydrated and mounted in resinous medium (Permount®, Fisher Scientific, New Jersey, USA). In each section, a standardized field was captured at x40 magnification using a light microscope equipped with polarized filters. All images were captured based on rigorously standardized parameters (light intensity, diaphragm aperture, condenser position and exposition time).

The amount of birefringent collagen in the capsules was measured using an image analysis software (ImageJ®; http://rsbweb.nih.gov/ij), which was adjusted according to the hue following parameters: red/orange, 2–38 and 230–256; yellow, 39–51; and green, 52–128[41,42]. The amount of collagen in each specimen was equivalent to the percentage of birefringent areas in the total area (expressed in pixels) provided by image analysis program[29].

2.3 von Kossa reaction and birefringent calcite structures

In each specimen, three-serial sections were subjected to the von Kossa reaction for detection of calcium/phosphate deposits in the capsules. After hydration, the sections were incubated for 1 hour in 5% silver nitrate solution, washed in distilled water and immersed in 5% sodium hyposulfite solution for 5 min. Afterwards, the sections were stained with picrosirius-red[6,36,43] and analyzed using light microscope Olympus (BX-51, Olympus, Tokyo, Japan).

As calcite crystals exhibit birefringence[4,6,14,36,37,44], sections were dewaxed and mounted in resinous medium. These unstained sections were analyzed under polarized illumination (BX-51, Olympus, Tokyo, Japan) to evaluate the presence of birefringent structures in the capsules.

2.4 Statistical analysis

The data were subjected to the two-way ANOVA analysis followed by the Tukey *post-hoc* test (Prism 6.0 software; GraphPad, San Diego, CA, USA). Significance level was set at 5% ($p<0.05$).

3 RESULTS

3.1 - Morphological and quantitative analyses: HE-stained sections

The morphological analysis revealed thick capsules of all groups at 7 and 15 days. In these periods, an evident inflammatory reaction was seen in the capsules adjacent to the opening of the polyethylene tubes. Numerous inflammatory cells, identified by strong basophilia, were seen particularly in the Biodentine specimens (Figs. 1B and 1F). Otherwise, no change was observed in the adjacent loose connective and muscular tissues (Figs. 1A-1H). At 30 and 60 days, the implants were surrounded by a thin capsule (Figs. 1I-1P).

According to Figure 1Q, there was no significant difference in the thickness of capsules between Biodentine and WMTA ($p=0.7988$) after 7 days. At 7 and 15 days, no significant difference was also detected between Bio-C Pulpo and Biodentine specimens ($p=0.8987$). At 15 days, the capsules around WMTA were significantly thinner than Bio-C Pulpo ($p=0.0358$) and Biodentine ($p=0.0047$). At 30 and 60 days, significant differences in the thickness of capsules were not observed among the groups ($p>0.05$).

The morphological analysis of HE-stained sections under high magnification revealed that, at 7 and 15 days, the capsules of all groups contained several mononuclear inflammatory cells (Figs. 2A-2H). In the Biodentine specimens, some necrotic areas containing cells with accentuated basophilia were observed in the capsules in close juxtaposition to the material surface, particularly at 7 days (Fig. 2B). After 30 and 60 days, the capsules of all groups contained mainly fibroblasts among collagen fibers (Figs. 2I-2P). The quantitative analysis (Fig. 2Q) revealed that the greatest density of inflammatory cells was found in the capsule of all groups at 7 days. In this period, the number of inflammatory cells was significantly greater around Biodentine specimens than Bio-C Pulpo ($p=0.0046$) and WMTA ($p=0.0139$). However, no significant difference was detected among Bio-C Pulpo, Biodentine and WMTA at 15, 30 and 60 days ($p>0.05$). There was no significant difference in the number of inflammatory cells between Bio-C Pulpo and CG specimens at 15 ($p=0.0794$), 30 ($p=0.8725$) and 60 ($p=0.3429$) days. WMTA and CG specimens had no significant difference in the intensity of inflammatory reaction at 30 ($p=0.2043$) and 60 ($p=0.9717$) days. Only on 60th day, Biodentine specimens showed no significant difference in the number of inflammatory cells in comparison with CG.

Regarding to the number of fibroblasts (Fig. 2R), a significant increase was observed in the capsules of all groups over time. In Bio-C Pulpo specimens, the number of fibroblasts was significantly lower in comparison to WMTA at 15 days ($p = 0.0061$). In all periods, no significant difference in the number of fibroblasts was detected between Bio-C Pulpo and

Biodentine. At 30 and 60 days, significant differences in the number of fibroblasts were not observed among all specimens, including the CG specimens.

3.2 - Immunoexpression of IL-6

The capsules around all specimens contained IL-6-immunostained cells (brown-yellow colour) in all periods. However, an evident reduction in these cells was seen in all specimens over time (Figs. 3A-3P). No immunolabelling was seen in the negative controls (data not shown). As shown in Fig. 3Q, the number of IL-6-immunolabelled cells was significantly greater in the capsules of Bio-C Pulpo and Biodentine than in WMTA specimens at 7, 15 and 30 days. Moreover, significant differences were not observed between Bio-C Pulpo and Biodentine at 7 ($p=0.2988$), 15 ($p=0.9957$), 30 ($p=0.7914$) and 60 ($p=0.9994$) days. At 7, 15 and 30 days, the CG specimens showed a reduced immunoexpression in comparison with Bio-C Pulpo, Biodentine and WMTA specimens ($p<0.0001$). Otherwise, no significant difference was detected between bioceramic materials and CG specimens at 60 days.

3.3 - Birefringent collagen in the capsules

In all groups, the capsules contained few and thin birefringent collagen fibers in the period of 7 days (Figs. 4A-4D). At 60 days, an apparent increase in the birefringence was observed in the capsules around all specimens (Figs. 4E-4H). In all time points, no significant difference was found in the amount of collagen among the implants of bioceramic materials. At 15, 30 and 60 days, there no was significant difference between Bio-C Pulpo and CG specimens ($p>0.05$). At 60 days, significant differences in the amount of birefringent collagen were not observed ($p>0.05$) among the bioceramic materials and CG specimens (Fig. 4I).

3.4 - OCN detection

Although OCN-immunolabelled cells were found in the capsules around bioceramic materials in all periods, a more intense immunolabelling was observed at 30 and 60 days (Figs. 5A-5C, 5E-5G, 5I-5K and 5M-5O). In all time points, OCN-immunolabelled cells were not observed in the capsules of CG (Figs. 5D, 5H, 5L and 5P).

The quantitative analysis (Fig. 5Q) revealed a significant increase in the number of OCN-immunolabelled cells in the capsules around bioceramic materials over time. In all periods, no significant difference in the immunoexpression of OCN among bioceramic materials was observed.

3.5 - von Kossa reaction and birefringent calcite structures

Sections of Bio-C Pulpo, Biodentine and WMTA specimens exhibited von Kossa-positive structures (in black or brown colour) while no von Kossa-positive structure was seen in the CG specimens (Figs. 6A-6H).

Deparaffinized unstained sections analyzed under polarized illumination revealed birefringent irregular structures dispersed through the capsules around Bio-C Pulpo, Biodentine and WMTA (Figs. 6I-6N). Birefringent structures were not observed in the capsules of CG specimens (data not shown).

4 DISCUSSION

In the present study, the implantation of Bio-C Pulpo and Biodentine materials in the subcutaneous connective tissue induced initially (at 7 and 15 days) the formation of thick capsules in comparison with those around CG specimens. At 15 days, the thickness of capsules around Bio-C Pulpo and Biodentine was also significantly greater than in WMTA specimens. The thickness of capsules has been widely used as a parameter to estimate the extent of the inflammatory reaction and, consequently, the tissue injury caused by materials[6,36,38]. Although the capsules around Bio-C Pulpo and Biodentine measured 2 to 3 folds more than in the CG specimens, the inflammatory reaction was only seen around Bio-C Pulpo and Biodentine materials i.e., no inflammatory reaction was noted in the muscular and loose connective tissues. The evident reaction initially promoted by these bioceramic materials was reduced gradually culminating in the capsules with similar thickness to those found in the WMTA and CG specimens at 30 and 60 days.

The quantitative analysis concerning the inflammatory cells revealed that, at 7 days, Biodentine induced a greater recruitment of inflammatory cells than Bio-C Pulpo and WMTA, whereas significant differences in the number of inflammatory cells were not detected between Bio-C Pulpo and WMTA. An accentuated irritant potential of Biodentine has been demonstrated after implantation into subcutaneous tissues[26,27,45]. Tissue injury initially caused by Biodentine has been attributed, at least in part, to the calcium chloride and/or polycarboxylate (hydrosoluble polymer) present in its liquid[46,47,48]. High pH provided by Biodentine during its setting time may also be responsible for the recruitment of inflammatory cells since alkaline pH stimulates the recruitment of inflammatory cells[26,40,49,50]. In fact, Biodentine provides a pH about 10.8 to the microenvironment after 7 days[31] while the pH medium with Bio-C Pulpo vary from 8.5 (at 24 hours) to 8.4 (at 28 days) and with WMTA from 7.9 (at 24 hours) to 7.9 (at 28 days)[4]. However, the irritant effect exerted by Biodentine seems

to occur for short time since a significant reduction in the number of inflammatory cells was observed at 15 days in the capsules around this repair material. Thus, no significant difference in the degree of inflammatory infiltrate was found among bioceramic materials after 15, 30 and 60 days. It is possible that the high pH provided by Biodentine[31] may be at least in part responsible for necrosis areas seen in the capsules around this material, at 7 and 15 days. Furthermore, Biodentine also showed greater calcium leaching than TCS + 20% ZrO_2, and calcium hydroxide is formed as a by-product of the hydration reaction of the material[51]. Calcium hydroxide on dental pulp causes an inflammatory reaction as well as a necrosis in the surface of pulp tissue[52].

Although no significant difference was detected in the number of inflammatory cells in the capsules around Bio-C Pulpo, Biodentine and WMTA at 15, 30 and 60 days, the immunohistochemistry for detection of IL-6 revealed significant differences among the groups. At 7, 15 and 30 days, the number of IL-6-immunolabelled cells was significantly greater around Bio-C Pulpo and Biodentine specimens than in WMTA specimens. However, it is important to emphasize that IL-6 is a pro-inflammatory cytokine detected in endothelial cells, fibroblasts and inflammatory cells[38,27,53]. In the present study, immunoexpression of IL-6 was computed in different cell types (inflammatory cells, endothelial cells and fibroblasts). From an in vitro study that evaluated the cell viability of Saos-2 using the MTT method after 24 hours of exposure to the Biodentine extracts showed that this material is cytocompatible in dilutions greater than 1:8, 1:16 and 1:32, being cytotoxic in the initial dilutions of 1:1, 1:2 and 1:4 when compared to the control samples[31]. Bio-C Pulpo and WMTA showed similar cytocompatibility when fibroblasts were co-cultured with extracts of these materials for 24 hours[5]. Thus, in vitro studies have been suggested that these bioceramic materials induce a similar cellular response. Here, our findings indicate that Bio-C Pulpo and Biodentine promoted a similar tissue damage after subcutaneous implantation in rats. Besides the differences found in the initial tissue response to Bio-C Pulpo and Biodentine in comparison with WMTA, our results suggest that irritant potential of Bio-C Pulpo and Biodentine may be transient since, no evident difference was seen in the inflammatory reaction (number of inflammatory cells and IL-6 imunoexpression) among these materials and WMTA at 60 days.

Despite the highest values of IL-6-immunostained cells detected in Bio-C Pulpo and Biodentine at 7, 15 and 30 days, the significant reduction in the immunoexpression of this cytokine in these groups over time points to a regression in the inflammatory reaction since IL-6 plays an important role in the recruitment of inflammatory cells from the bloodstream[54,55]. Several studies have demonstrated that IL-6 is responsible for the maintenance of inflammatory

reaction and, the reduction of this cytokine is associated with tissue connective remodeling, allowing the formation of extracellular matrix components and fibroblasts proliferation[27,36,38,53,56]. In fact, no significant difference in the number of IL-6-immunostained cells and inflammatory cells was observed among the groups, including in the CG specimens, at 60 days, indicating that bioceramic materials are biocompatible.

Besides the reduction in the inflammatory infiltrate and in the pro-inflammatory cytokine (IL-6), the significant increase in the number of fibroblasts verified in the capsules of all groups over time supports the concept that the bioceramic materials allow the healthy connective tissue neoformation. The quantitative analysis of birefringent collagen in the capsules revealed a significant increase in the amount of collagen in parallel to the increase in the number of fibroblasts, indicating the formation of fibrous capsules around bioceramic materials. The fibroblast proliferation accompanied by collagen formation suggests that Bio-C Pulpo, Biodentine and WMTA may allow the connective tissue repair.

Our findings revealed von Kossa-positive structures around the bioceramic materials suggesting, therefore, the presence of calcium/phosphate deposits in the capsules. It is known that during the hydration of tricalcium silicate-based materials, the release of calcium ions takes place[16,37,57,58]; these ions may react with carbonate dioxide from tissue fluids, giving rise to calcium carbonate[16,59,60]. Moreover, the birefringent structures seen in the unstained sections are suggestive of amorphous calcite[4,6,14,50]. von Kossa-positive deposits and birefringent amorphous calcite structures has been demonstrated around bioceramic materials, such as WMTA[7,17], MTA Repair HP[4,6,37] and Biodentine[32,33]. Since the calcium carbonate may act as a nucleus of mineralization[59], the calcium ions released by materials may be responsible, at least in part, for the bioactivity of these bioceramic cements[57,61]. Immunoexpression of alkaline phosphatase, an enzyme involved with the mineralization process, was detected in cells closely juxtaposed to von Kossa-positive structures in capsules around Bio-C Pulpo, WMTA and MTA Repair HP, pointing to a bioactive potential of these bioceramic materials[6]. *In vivo* studies have demonstrated the formation of mineralized tissues in perforated pulp chamber floor of rat molars filled with WMTA[8] and dog teeth[29,62]. Here, our findings reinforce the concept that this new Bio-C Pulpo material, similarly to Biodentine and WMTA, may present bioactivity. However, the bioactivity of a dental material is assured by its ability to induce the formation of hydroxyapatite crystals[29,33,63], which can be evaluated using Fourier transform infrared (FTIR) microspectroscopy and dark field electron microscopy[64,65,66].

In addition to von Kossa-positive structures and birefringent deposits, OCN was also seen in Bio-C Pulpo, Biodentine and WMTA specimens. OCN is a no-collagen protein present

in the extracellular matrix of mineralized tissues and, therefore, is synthetized by their own cells[67]. Considering that OCN has high binding affinity for hydroxyapatite crystals and seems to play an important role in the growth of these crystals[68], this protein has been pointed as essential in the mineralization process[69]. Therefore, the immunoexpression of OCN in the connective tissue around bioceramic materials indicates that this protein could have a participation in the formation of birefringent amorphous calcite. Moreover, our findings clearly showed an increase in the immunoexpression of OCN over time in the bioceramic materials specimens. In contrast, no immunoexpression was seen in the capsules of CG specimens, indicating that Bio-C Pulpo, Biodentine and WMTA materials stimulate the production of OCN by the connective tissue cells. These results, taken together, support the concept that these bioceramic materials present bioactive potential.

Our findings indicate that the changes made in Bio-C Pulpo and Biodentine to improve the handling of bioceramic materials may be responsible for highest immunoexpression of IL-6 pro-inflammatory cytokine initially detected in the connective tissue in comparison with WMTA. However, significant reduction of immunoexpression of IL-6 and in the inflammatory reaction around Bio-C Pulpo and Biodentine parallel to the increase in the number of fibroblasts and in the amount in the collagen fibers, indicate that these bioceramic materials are biocompatible as well as may allow the connective tissue repair. Furthermore, the presence of von Kossa-positive deposits, birefringent calcite structures and osteocalcin-immunolabelled cells suggest that Bio-C Pulpo and Biodentine may present bioactive potential. Thus, the Bio-C Pulpo may be used as an alternative repair material.

REFERENCES

1. Okiji T, Yoshiba K. Reparative dentinogenesis induced by mineral trioxide aggregate: a review from the biological and physicochemical points of view. *Int. J. Dent.* 2009; *2009:* 464280.
2. Hanna SN, Perez Alfayate R, Prichard J. Vital pulp therapy an insight over the available literature and future expectations. *Eur. Endod. J.* 2020; *5:* 46-53.
3. Ferreira CMA, Sassone LM, Gonçalves AS, de Carvalho JJ, Tomás-Catalá CJ, García-Bernal D, Oñate-Sánchez RE, Rodríguez-Lozano FJ, Silva EJNL. Physicochemical, cytotoxicity and in vivo biocompatibility of a high-plasticity calcium-silicate based material. *Sci. Rep.* 2019; *9:* 3933.
4. Cintra L, Benetti F, de Azevedo Queiroz ÍO et al. Cytotoxicity, biocompatibility, and biomineralization of the new high-plasticity MTA material. *J. Endod.* 2017; *43:* 774-778.
5. Pelepenko LE, Saavedra F, Antunes TBM, Bombarda GF, Gomes BPFA, Zaia AA, Marciano MA. Investigation of a modified hydraulic calcium silicate-based material - Bio-C Pulpo. *Braz. Oral. Res.* 2021; *35:* e077.
6. Delfino MM, de Abreu Jampani JL, Lopes CS *et al.* Comparison of Bio-C Pulpo and MTA Repair HP with White MTA: effect on liver parameters and evaluation of biocompatibility and bioactivity in rats. *Int. Endod. J.* 2021; *54:* 1597-1613.
7. Parirokh M, Torabinejad M. Mineral trioxide aggregate: a comprehensive literature review--Part III: Clinical applications, drawbacks, and mechanism of action. *J. Endod.* 2010; *36:* 400-413.
8. da Silva GF, Guerreiro-Tanomaru JM, Sasso-Cerri E, Tanomaru-Filho M, Cerri PS. Histological and histomorphometrical evaluation of furcation perforations filled with MTA, CPM and ZOE. *Int. Endod. J.* 2011; *44:* 100-110.
9. Koutroulis A, Kuehne SA, Cooper PR, Camilleri J. The role of calcium ion release on biocompatibility and antimicrobial properties of hydraulic cements. *Sci. Rep.* 2019; *9:* 19019.
10. Yoon JH, Choi SH, Koh JT, Lee BN, Chang HS, Hwang IN, Oh WM, Hwang YC. Hard tissue formation after direct pulp capping with osteostatin and MTA *in vivo*. *Restor. Dent. Endod.* 2021; *46:* e17.

11. Gomes-Filho JE, Rodrigues G, Watanabe S, Estrada Bernabé PF, Lodi CS, Gomes AC, Faria MD, Domingos Dos Santos A, Silos Moraes JC. Evaluation of the tissue reaction to fast endodontic cement (CER) and Angelus MTA. *J. Endod.* 2009; *35:* 1377-1380.
12. Torabinejad M, Parirokh M. Mineral trioxide aggregate: a comprehensive literature review--part II: leakage and biocompatibility investigations. *J. Endod.* 2010; *36:* 190-202.
13. Torabinejad M, Parirokh M, Dummer PMH. Mineral trioxide aggregate and other bioactive endodontic cements: an updated overview - part II: other clinical applications and complications. *Int. Endod. J.* 2018; *51:* 284-317.
14. Holland R, de Souza V, Nery MJ, Otoboni Filho JA, Bernabé PF, Dezan Júnior E. Reaction of rat connective tissue to implanted dentin tubes filled with mineral trioxide aggregate or calcium hydroxide. *J. Endod.* 1999; *25:* 161-166.
15. Duarte MA, Demarchi AC, Yamashita JC, Kuga MC, Fraga SC. pH and calcium ion release of 2 root-end filling materials. *Oral Surg. Oral Med. Oral Pathol. Oral Radiol. Endod.* 2003; *95:* 345-347.
16. Silva GF, Tanomaru-Filho M, Bernardi MI, Guerreiro-Tanomaru JM, Cerri PS. Niobium pentoxide as radiopacifying agent of calcium silicate-based material: evaluation of physicochemical and biological properties. *Clin. Oral Investig.* 2015; *19:* 2015-2025.
17. Duarte MAH, Marciano MA, Vivan RR, Tanomaru Filho M, Tanomaru JMG, Camilleri J. Tricalcium silicate-based cements: properties and modifications. *Braz. Oral Res.* 2018; *32:* e70.
18. Cosme-Silva L, Gomes-Filho JE, Benetti F, Dal-Fabbro R, Sakai VT, Cintra LTA, Ervolino E, Viola NV. Biocompatibility and immunohistochemical evaluation of a new calcium silicate-based cement, Bio-C Pulpo. *Int. Endod. J.* 2019; *52:* 689-700.
19. Sanz JL, Soler-Doria A, López-García S, García-Bernal D, Rodríguez-Lozano FJ, Lozano A, Llena C, Forner L, Guerrero-Gironés J, Melo M. Comparative Biological Properties and Mineralization Potential of 3 Endodontic Materials for Vital Pulp Therapy: Theracal PT, Theracal LC, and Biodentine on Human Dental Pulp Stem Cells. *J. Endod.* 2021; *47:* 1896-1906.
20. Laurent P, Camps J, About I. Biodentine (TM) induces TGF-β1 release from human pulp cells and early dental pulp mineralization. *Int. Endod. J.* 2012; *45:* 439-448.

21. Malkondu Ö, Karapinar Kazandağ M, Kazazoğlu E. A review on biodentine, a contemporary dentine replacement and repair material. *Biomed. Res. Int.* 2014; *2014:* 160951.
22. De Rossi A, Silva LA, Gatón-Hernández P, Sousa-Neto MD, Nelson-Filho P, Silva RA, de Queiroz AM. Comparison of pulpal responses to pulpotomy and pulp capping with biodentine and mineral trioxide aggregate in dogs. *J. Endod.* 2014; *40:* 1362-1369.
23. Camilleri J, Sorrentino F, Damidot D. Investigation of the hydration and bioactivity of radiopacified tricalcium silicate cement, Biodentine and MTA Angelus. *Dent. Mater.* 2013; *29:* 580-593.
24. Araújo LB, Cosme-Silva L, Fernandes AP, Oliveira TM, Cavalcanti BDN, Gomes Filho JE, Sakai VT. Effects of mineral trioxide aggregate, BiodentineTM and calcium hydroxide on viability, proliferation, migration and differentiation of stem cells from human exfoliated deciduous teeth. *J. Appl. Oral Sci.* 2018; *26:* e20160629.
25. Mori GG, Teixeira LM, de Oliveira DL, Jacomini LM, da Silva SR. Biocompatibility evaluation of biodentine in subcutaneous tissue of rats. *J. Endod.* 2014; *40:* 1485-1488.
26. da Fonseca TS, da Silva GF, Tanomaru-Filho M, Sasso-Cerri E, Guerreiro-Tanomaru JM, Cerri PS. In vivo evaluation of the inflammatory response and IL-6 immunoexpression promoted by Biodentine and MTA Angelus. *Int. Endod. J.* 2016; *49:* 145-153.
27. da Fonseca TS, Silva GF, Guerreiro-Tanomaru JM, Sasso-Cerri E, Tanomaru-Filho M, Cerri PS. Mast cells and immunoexpression of FGF-1 and Ki-67 in rat subcutaneous tissue following the implantation of Biodentine and MTA Angelus. *Int. Endod. J.* 2019; *52:* 54-67.
28. Daltoé MO, Paula-Silva FW, Faccioli LH, Gatón-Hernández PM, De Rossi A, Bezerra Silva LA. Expression of Mineralization Markers during Pulp Response to Biodentine and Mineral Trioxide Aggregate. *J. Endod.* 2016; *42:* 596-603.
29. Silva LAB, Pieroni KAMG, Nelson-Filho P, Silva RAB, Hernandéz-Gatón P, Lucisano MP, Paula-Silva FWG, de Queiroz AM. Furcation Perforation: Periradicular Tissue Response to Biodentine as a Repair Material by Histopathologic and Indirect Immunofluorescence Analyses. *J. Endod.* 2017; *43:* 1137-1142.
30. Kaur M, Singh H, Dhillon JS, Batra M, Saini M. MTA versus Biodentine: Review of Literature with a Comparative Analysis. *J. Clin. Diagn. Res.* 2017; *11:* ZG01-ZG05.
31. Queiroz MB, Torres FFE, Rodrigues EM, Viola KS, Bosso-Martelo R, Chavez-Andrade GM, Souza MT, Zanotto ED, Guerreiro-Tanomaru JM, Tanomaru-Filho M.

Development and evaluation of reparative tricalcium silicate-ZrO_2 -Biosilicate composites. *J. Biomed. Mater. Res.: B Appl. Biomater.* 2021; *109:* 468-476.

32. Souza TA, Bezerra MM, Silva PGB, Costa JJN, Carneiro RFLA, Barcelos JOF, Vasconcelos BC, Chaves HV. Bone morphogenetic proteins in biomineralization of two endodontic restorative cements. *J. Biomed. Mater. Res.: B Appl. Biomater.* 2021; *109:* 348-357.
33. Talabani RM, Garib BT, Masaeli R, Zandsalimi K, Ketabat F. Biomineralization of three calcium silicate-based cements after implantation in rat subcutaneous tissue. *Restor. Dent. Endod.* 2020; *46:* e1.
34. Cosme-Silva L, Santos AFD, Lopes CS, Dal-Fabbro R, Benetti F, Gomes-Filho JE, Queiroz IOA, Ervolino E, Viola NV. Cytotoxicity, inflammation, biomineralization, and immunoexpression of IL-1β and TNF-α promoted by a new bioceramic cement. *J. Appl. Oral Sci.* 2020; *28:* e20200033.
35. Lima SPR, Santos GLD, Ferelle A, Ramos SP, Pessan JP, Dezan-Garbelini CC. Clinical and radiographic evaluation of a new stain-free tricalcium silicate cement in pulpotomies. *Braz. Oral. Res.* 2020; *34:* e102.
36. Delfino MM, Guerreiro-Tanomaru JM, Tanomaru-Filho M, Sasso-Cerri E, Cerri PS. Immunoinflammatory response and bioactive potential of GuttaFlow bioseal and MTA Fillapex in the rat subcutaneous tissue. *Sci. Rep.* 2020; *10:* 7173.
37. Benetti F, Queiroz ÍOA, Cosme-Silva L, Conti LC, Oliveira SHP, Cintra LTA. Cytotoxicity, Biocompatibility and Biomineralization of a New Ready-for-Use Bioceramic Repair Material. *Braz. Dent. J.* 2019; *30:* 325-332.
38. Saraiva JA, da Fonseca TS, da Silva GF, Sasso-Cerri E, Guerreiro-Tanomaru JM, Tanomaru-Filho M, Cerri PS. Reduced interleukin-6 immunoexpression and birefringent collagen formation indicate that MTA Plus and MTA Fillapex are biocompatible. *Biomed. Mater.* 2018; *13:* 035002.
39. Yaltirik M, Ozbas H, Bilgic B, Issever H. Reactions of connective tissue to mineral trioxide aggregate and amalgam. *J. Endod.* 2004; *30:* 95-99.
40. Silva GF, Bosso R, Ferino RV, Tanomaru-Filho M, Bernardi MI, Guerreiro-Tanomaru JM, Cerri PS. Microparticulated and nanoparticulated zirconium oxide added to calcium silicate cement: Evaluation of physicochemical and biological properties. *J. Biomed. Mater. Res. A.* 2014; *102:* 4336-4345.

41. Koshimizu JY, Beltrame FL, de Pizzol JP Jr, Cerri PS, Caneguim BH, Sasso-Cerri E. NF-kB overexpression and decreased immunoexpression of AR in the muscular layer is related to structural damages and apoptosis in cimetidine-treated rat vas deferens. *Reprod. Biol. Endocrinol.* 2013; *11:* 29.
42. de Pizzol Júnior JP, Sasso-Cerri E, Cerri PS. Matrix Metalloproteinase-1 and Acid Phosphatase in the Degradation of the Lamina Propria of Eruptive Pathway of Rat Molars. *Cells.* 2018; *7:* 206.
43. Viola NV, Guerreiro-Tanomaru JM, da Silva GF, Sasso-Cerri E, Tanomaru-Filho M, Cerri PS. Biocompatibility of an experimental MTA sealer implanted in the rat subcutaneous: quantitative and immunohistochemical evaluation. *J. Biomed. Mater. Res.: B Appl. Biomater.* 2012; *100:* 1773-1781.
44. Bueno CRE, Vasques AMV, Cury MTS, Sivieri-Araújo G, Jacinto RC, Gomes-Filho JE, Cintra LTA, Dezan-Júnior E. Biocompatibility and biomineralization assessment of mineral trioxide aggregate flow. *Clin. Oral Investig.* 2019; *23:* 169-177.
45. Andrade AS, Silva GF, Camilleri J, Cerri ES, Guerreiro-Tanomaru JM, Cerri PS, Tanomaru-Filho M. Tissue Response and Immunoexpression of Interleukin 6 Promoted by Tricalcium Silicate-based Repair Materials after Subcutaneous Implantation in Rats. *J. Endod.* 2018; *44:* 458-463.
46. Han L, Okiji T. Uptake of calcium and silicon released from calcium silicate-based endodontic materials into root canal dentine. *Int. Endod. J.* 2011; *44:* 1081-1087.
47. Camilleri J, Kralj P, Veber M, Sinagra E. Characterization and analyses of acid-extractable and leached trace elements in dental cements. *Int. Endod. J.* 2012; *45:* 737-743.
48. Kang JY, Lee BN, Son HJ, Koh JT, Kang SS, Son HH, Chang HS, Hwang IN, Hwang YC, Oh WM. Biocompatibility of mineral trioxide aggregate mixed with hydration accelerators. *J. Endod.* 2013; *39:* 497-500.
49. Williams DF. On the mechanisms of biocompatibility. *Biomaterials.* 2008; *29:* 2941-*29*53.
50. Hoshino RA, Silva GFD, Delfino MM, Guerreiro-Tanomaru JM, Tanomaru-Filho M, Sasso-Cerri E, Filho IB, Cerri PS. Physical Properties, Antimicrobial Activity and In Vivo Tissue Response to Apexit Plus. *Materials (Basel)*. 2020; *13:* 1171.
51. Camilleri J, Laurent P, About I. Hydration of Biodentine, Theracal LC, and a prototype tricalcium silicate-based dentin replacement material after pulp capping in entire tooth cultures. *J. Endod.* 2014; *40:* 1846-1854.

52. Li Z, Cao L, Fan M, Xu Q. Direct Pulp Capping with Calcium Hydroxide or Mineral Trioxide Aggregate: A Meta-analysis. *J. Endod.* 2015; *41:* 1412–1417.
53. Barbosa DD, Delfino MM, Guerreiro-Tanomaru JM, Tanomaru-Filho M, Sasso-Cerri E, Silva GF, Cerri PS. Histomorphometric and immunohistochemical study shows that tricalcium silicate cement associated with zirconium oxide or niobium oxide is a promising material in the periodontal tissue repair of rat molars with perforated pulp chamber floors. *Int. Endod. J.* 2021; *54:* 736-752.
54. Scheller J, Chalaris A, Schmidt-Arras D, Rose-John S. The pro- and anti-inflammatory properties of the cytokine interleukin-6. *Biochim. Biophys. Acta.* 2011; *1813:* 878-888.
55. Del Giudice M, Gangestad SW. Rethinking IL-6 and CRP: Why they are more than inflammatory biomarkers, and why it matters. *Brain Behav. Immun.* 2018; *70:* 61-75.
56. Hoshino RA, Delfino MM, da Silva GF, Guerreiro-Tanomaru JM, Tanomaru-Filho M, Sasso-Cerri E, Cerri PS. Biocompatibility and bioactive potential of the NeoMTA Plus endodontic bioceramic-based sealer. *Restor. Dent. Endod.* 2020; *46:* e4.
57. Camilleri J, Gandolfi MG, Siboni F, Prati C. Dynamic sealing ability of MTA root canal sealer. *Int. Endod. J.* 2011; *44:* 9-20.
58. Marciano MA, Duarte MA, Camilleri J. Calcium silicate-based sealers: Assessment of physicochemical properties, porosity and hydration. *Dent. Mater.* 2016; *32:* e30-40.
59. Seux D, Couble ML, Hartmann DJ, Gauthier JP, Magloire H. Odontoblast-like cytodifferentiation of human dental pulp cells in vitro in the presence of calcium hydroxide cement. *Arch. Oral Biol.* 1991; *36:* 117–128.
60. Gandolfi MG, Siboni F, Primus CM, Prati C. Ion release, porosity, solubility, and bioactivity of MTA Plus tricalcium silicate. *J. Endod.* 2014; *40:* 1632-1637.
61. Abou ElReash A, Hamama H, Abdo W, Wu Q, Zaen El-Din A, Xiaoli X. Biocompatibility of new bioactive resin composite versus calcium silicate cements: an animal study. *BMC Oral Health.* 2019; *19:* 194.
62. Song W, Sun W, Chen L, Yuan Z. *In vivo*Biocompatibility and Bioactivity of Calcium Silicate-Based Bioceramics in Endodontics. *Front. Bioeng. Biotechnol.* 2020; *8:* 580954.
63. Xuereb M, Vella P, Damidot D, Sammut CV, Camilleri J. In situ assessment of the setting of tricalcium silicate-based sealers using a dentin pressure model. *J. Endod.* 2015; *41:* 111-124.

64. Katchburian E, Antoniazzi MM, Jared C, Faria FP, Souza Santos H, Freymüller E. Mineralized dermal layer of the Brazilian tree-frog Corythomantis greeningi. *J. Morphol.* 2001; *248:* 56-63.
65. Bonewald LF, Harris SE, Rosser J, Dallas MR, Dallas SL, Camacho NP, Boyan B, Boskey A. von Kossa staining alone is not sufficient to confirm that mineralization in vitro represents bone formation. *Calcif. Tissue Int.* 2003; *72:* 537-547.
66. Gandolfi MG, Taddei P, Siboni F, Modena E, De Stefano ED, Prati C. Biomimetic remineralization of human dentin using promising innovative calcium-silicate hybrid "smart" materials. *Dent. Mater.* 2011; *27:* 1055-1069.
67. Blanquer A, Musilkova J, Barrios L, Ibáñez E, Vandrovcova M, Pellicer E, Sort J, Bacakova L, Nogués C. Cytocompatibility assessment of Ti-Zr-Pd-Si-(Nb) alloys with low Young's modulus, increased hardness, and enhanced osteoblast differentiation for biomedical applications. *J Biomed. Mater. Res.: B Appl. Biomater.* 2018; *106:* 834-842.
68. Boskey AL, Gadaleta S, Gundberg C, Doty SB, Ducy P, Karsenty G. Fourier transform infrared microspectroscopic analysis of bones of osteocalcin-deficient mice provides insight into the function of osteocalcin. *Bone.* 1998; *23:* 187-196.
69. Hosseini S, Naderi-Manesh H, Vali H, Baghaban Eslaminejad M, Azam Sayahpour F, Sheibani S, Faghihi S. Contribution of osteocalcin-mimetic peptide enhances osteogenic activity and extracellular matrix mineralization of human osteoblast-like cells. *Colloids Surf. B Biointerfaces.* 2019; *173:* 662-671.

TABLE 1 Bioceramic materials, manufacturers, chemical composition and proportions.

Materials	Composition	Ratio Powder/Liquid
Bio-C Pulpo (Angelus, Londrina, Brazil)	**Powder:** tricalcium silicate, dicalcium silicate, calcium aluminate, calcium hydroxide, zirconium oxide, calcium fluoride, silicon dioxide and iron oxide. **Liquid:** distilled water, plasticizer, calcium chloride and methylparaben.	0.17g : 3 drops
Biodentine (Septodont, Saint-Maur-des-Fosses, France)	**Powder:** tricalcium silicate, zirconium oxide, calcium oxide, calcium carbonate, yellow pigment, red pigment and brown iron oxide. **Liquid:** Calcium chloride dihydrate, Areo and purified water.	1 capsule : 5 drops
White MTA (Angelus, Londrina, Brazil)	**Powder:** tricalcium silicate, dicalcium silicate, tricalcium aluminate, calcium oxide, calcium tungstate. **Liquid:** distilled water.	1 g : 300 µl

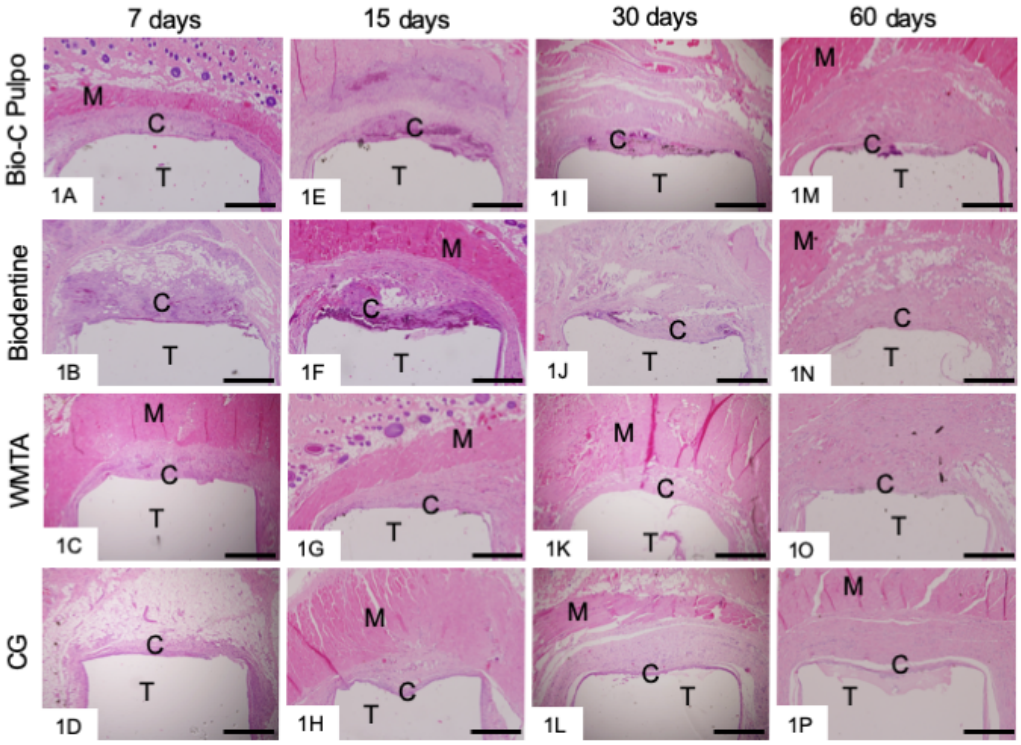
7 days
15 days
30 days
60 days
Bio-C Pulpo
Biodentine
WMTA
CG
M
C
T
1A
1E
1I
1M
1B
1F
1J
1N
1C
1G
1K
1O
1D
1H
1L
1P

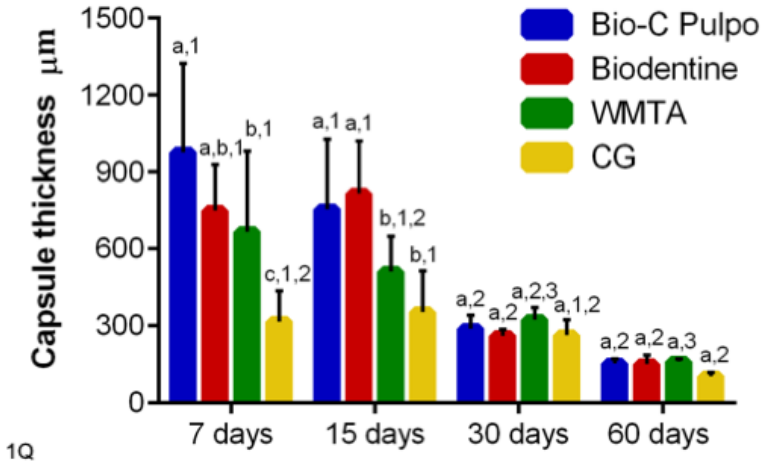
Capsule thickness µm
1500
1200
900
600
300
0
Bio-C Pulpo
Biodentine
WMTA
CG
a,1
a,b,1
b,1
c,1,2
a,1 a,1
b,1,2
b,1
a,2
a,2
a,2,3
a,1,2
a,2 a,2 a,3
a,2
7 days
15 days
30 days
60 days

1Q

Figures 1A-1P - Light micrographs showing a general view of capsules (C) of Bio-C Pulpo, Biodentine, WMTA and CG specimens at 7, 15, 30 and 60 days. At 7 days (Figs. 1A-1D), the thick capsules (C) exhibit evident inflammatory reaction (intense basophilia). At 15 days, the inflammatory reaction is particularly evident in the capsules around Bio-C Pulpo (Fig. 1E) and Biodentine (Fig. 1F). **Figures 1I-1P** (30 and 60 days) – thin capsules are seen. M, muscle; T, space of implanted polyethylene tube. Bars: 900 μm. HE.

Figure 1Q - Thickness of capsules (μm) of Bio-C Pulpo, Biodentine, WMTA and CG groups at 7, 15, 30 and 60 days. Different superscript letters denote significant difference between among in the period. Different superscript numbers denote significant difference in a group over time. Tukey's test ($p \leq 0.05$).

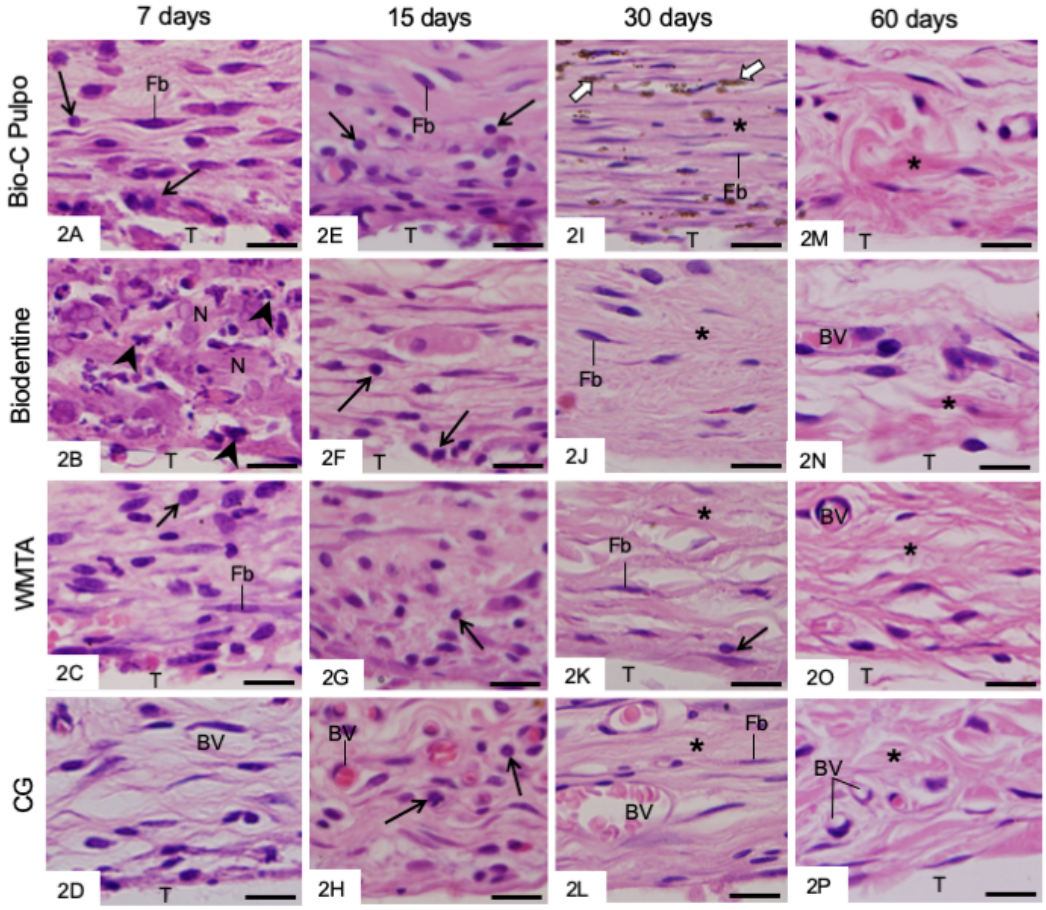
7 days
15 days
30 days
60 days
Bio-C Pulpo
Biodentine
WMTA
CG
Fb
T
N
BV
2A
2B
2C
2D
2E
2F
2G
2H
2I
2J
2K
2L
2M
2N
2O
2P

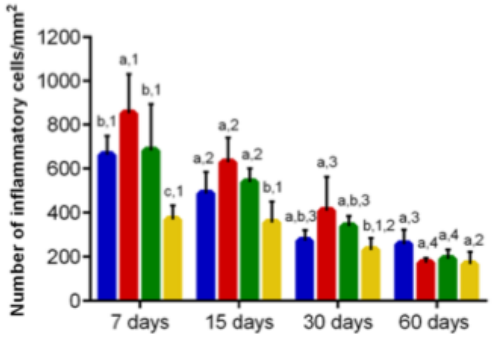
Number of inflammatory cells/mm²
1200
1000
800
600
400
200
0
7 days
15 days
30 days
60 days

2Q

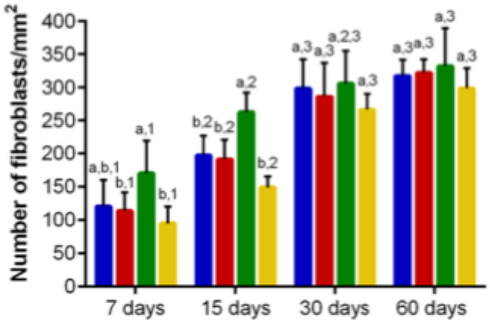
Number of fibroblasts/mm²
400
350
300
250
200
150
100
50
0
7 days
15 days
30 days
60 days

2R

Figures 2A-2P - Light micrographs showing portions of capsules (C) of Bio-C Pulpo, Biodentine, WMTA and CG specimens at 7, 15, 30 and 60 days. Inflammatory cells (arrows), fibroblasts (Fb), collagen fibres (asterisks) and material particles (empty arrows) are seen in the capsules. In Fig. 2B, nuclei strongly stained by haematoxylin (arrowheads) and acidophilic and amorphous material (N) suggesting necrosis areas. T, space of implanted polyethylene tube; BV, blood vessel. Bars: 30 μm. HE.

Figures 2Q and 2R - Numerical density of inflammatory cells (Fig. 2Q) and of fibroblasts (Fig. 2R) in the capsules of Bio-C Pulpo, Biodentine, WMTA and CG specimens at 7, 15, 30 and 60 days. Different superscript letters denote significant difference among groups in the period. Different superscript numbers denote significant difference in a group over time. Tukey's test ($p \leq 0.05$).

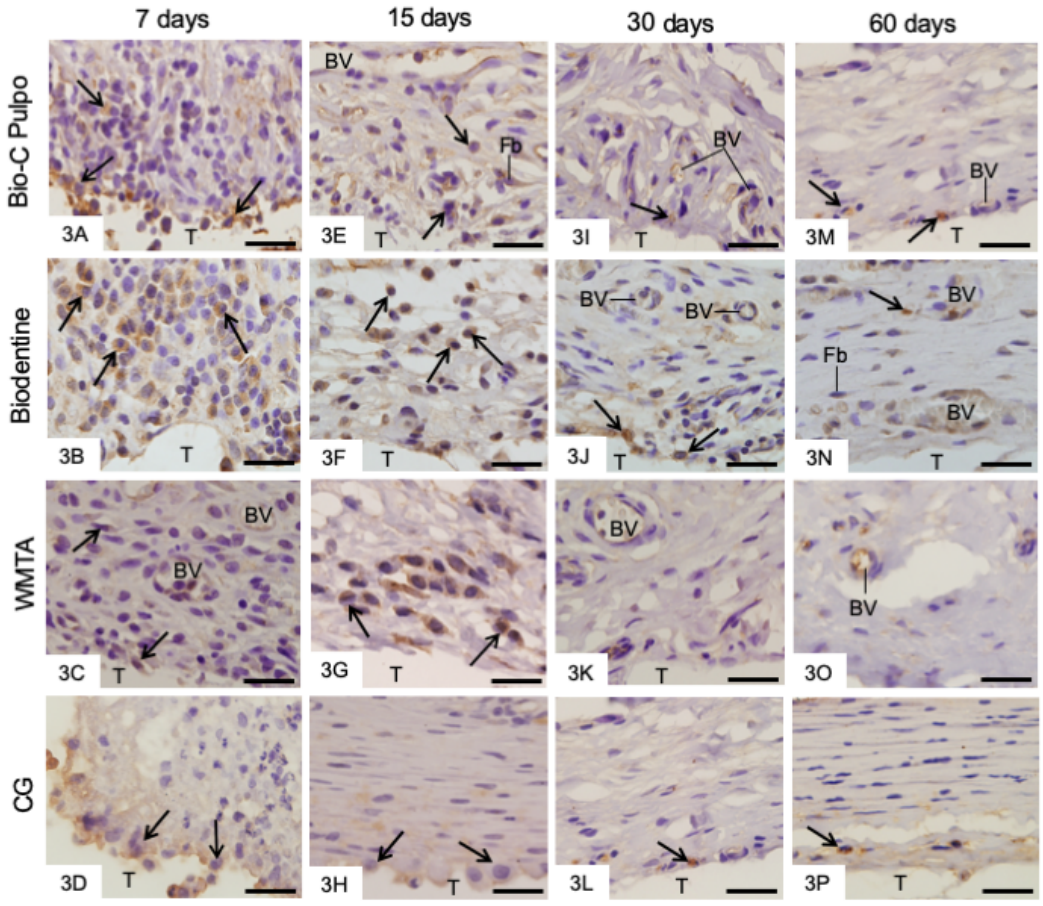
7 days
15 days
30 days
60 days
Bio-C Pulpo
Biodentine
WMTA
CG
BV
Fb
T
3A
3B
3C
3D
3E
3F
3G
3H
3I
3J
3K
3L
3M
3N
3O
3P

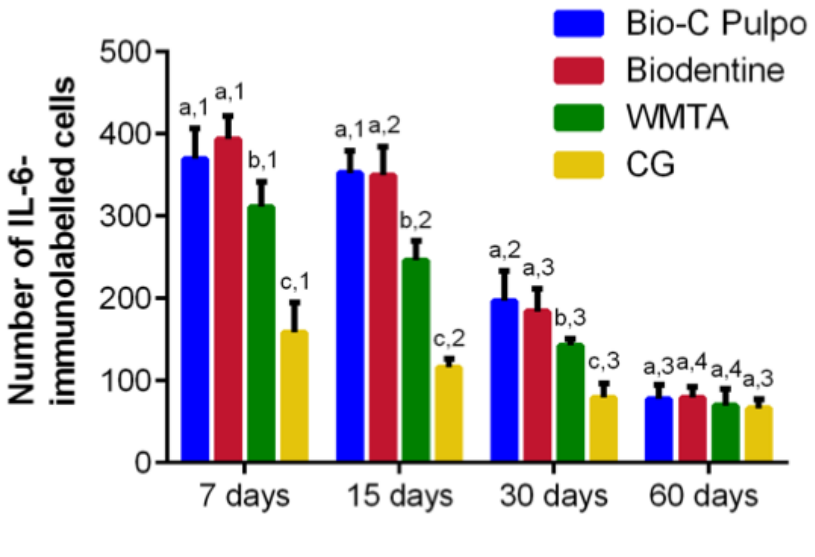
Bio-C Pulpo
Biodentine
WMTA
CG
Number of IL-6-immunolabelled cells
500
400
300
200
100
0
7 days
15 days
30 days
60 days
a,1
a,1
b,1
c,1
a,1
a,2
b,2
c,2
a,2
a,3
b,3
c,3
a,3
a,4
a,4
a,3

2O

Figures 3A-3P – Light micrographs of sections showing portions of capsules (C) of Bio-C Pulpo, Biodentine, WMTA and CG groups. The sections were submitted to immunohistochemistry for IL-6 detection (brown-yellow colour) and counterstained with haematoxylin. Inflammatory cells (arrows) exhibit strong immunolabelling in their cytoplasm; some IL-6-immunostained fibroblasts (Fb) are also observed. Note scarce immunolabelling in capsules of CG specimens. BV, blood vessels; T, space of implanted polyethylene tube. Bars: 22 μm.

Figure 3Q – Number of IL-6-immunolabelled cells in the capsules of Bio-C Pulpo, Biodentine, WMTA and CG groups at 7, 15, 30 and 60 days. Different superscript letters denote significant difference among groups in the period. Different superscript numbers denote significant difference in a group over time. Tukey's test ($p \leq 0.05$).

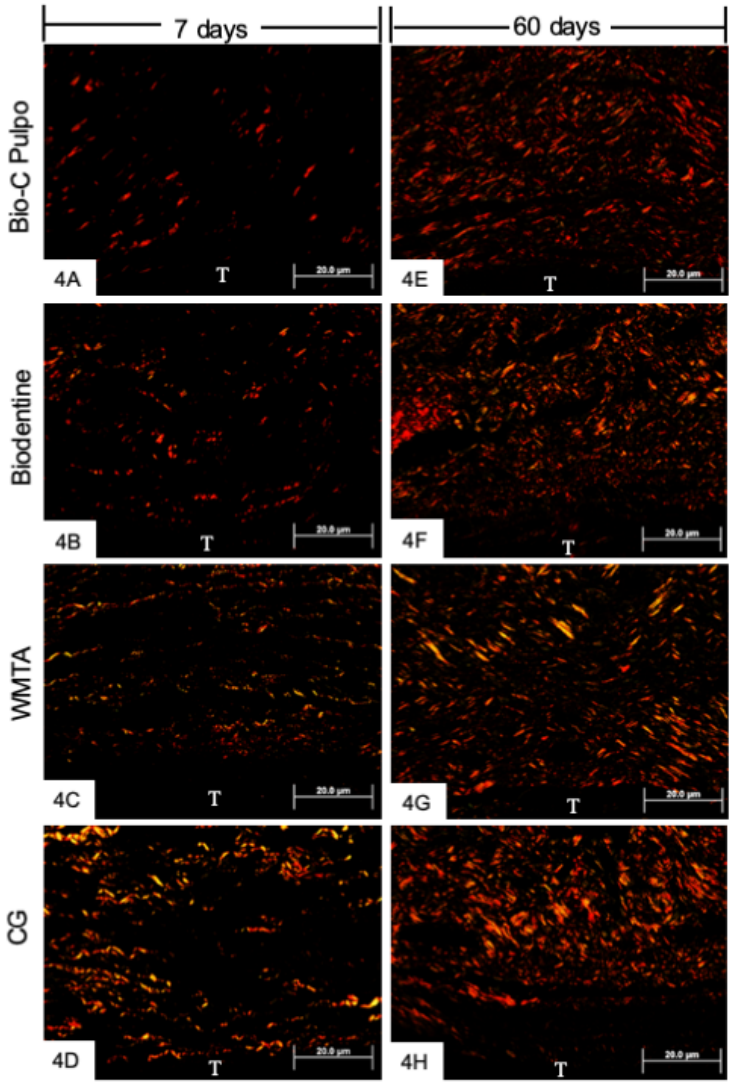
7 days
60 days
Bio-C Pulpo
Biodentine
WMTA
CG
4A
4B
4C
4D
4E
4F
4G
4H
T
20.0 µm

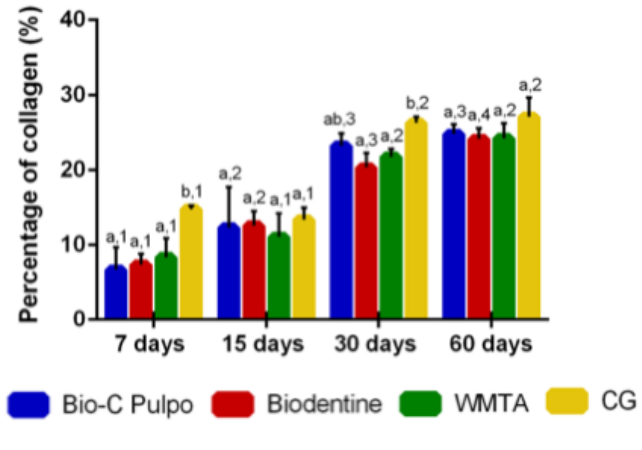
Percentage of collagen (%)
40
30
20
10
0
a,1
a,1
a,1
b,1
a,2
a,2
a,1
a,1
ab,3
a,3
a,2
b,2
a,3
a,4
a,2
a,2
7 days
15 days
30 days
60 days
Bio-C Pulpo
Biodentine
WMTA
CG

4I

Figures 4A-4H - Light micrographs showing portions of capsules of Bio-C Pulpo, Biodentine, WMTA and CG specimens at 7 and 60 days. The sections were subjected to the picrosirius-red and analyzed under polarized illumination. Birefringent collagen fibres (orange/red/yellow colours) are seen in the capsules. T, space of implanted polyethylene tube.
Figure 4I - Amount of birefringent collagen (in percentage) in the capsules of Bio-C Pulpo, Biodentine, WMTA and CG groups at 7, 15, 30 and 60 days. Different superscript letters denote significant difference among groups in the period. Different superscript numbers denote significant difference in a group over time. Tukey's test ($p \leq 0.05$).

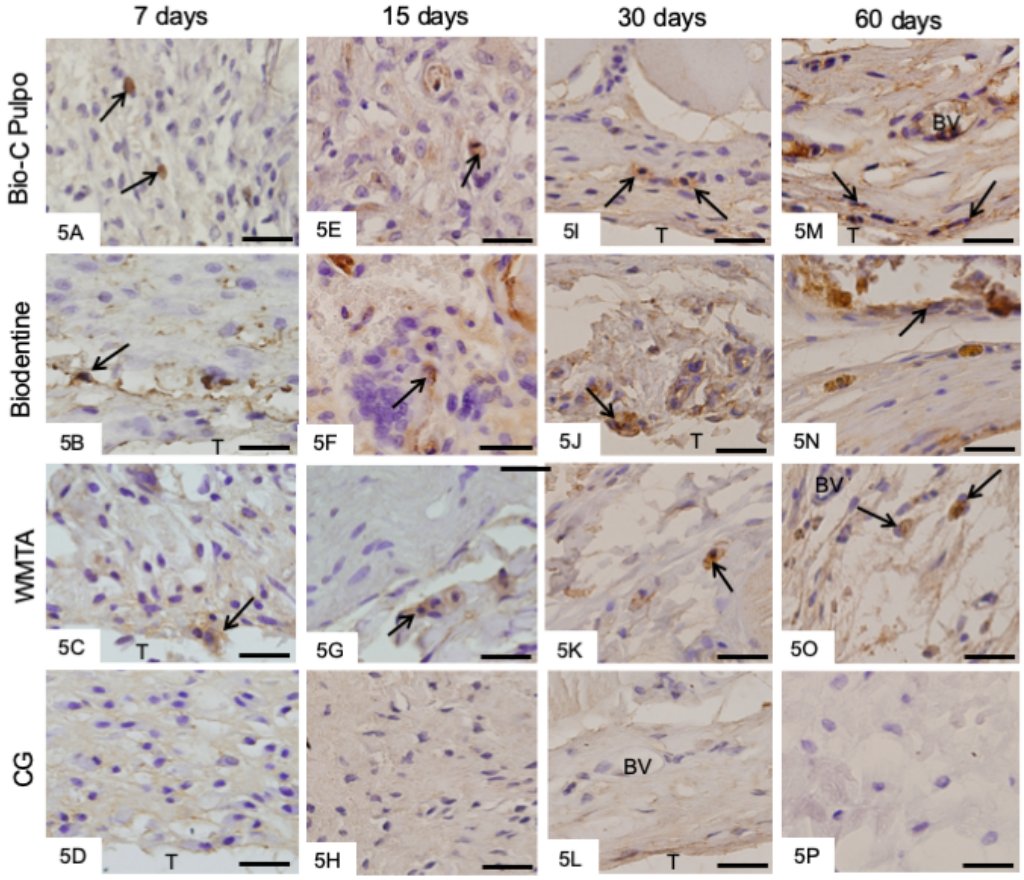
7 days
15 days
30 days
60 days
Bio-C Pulpo
Biodentine
WMTA
CG
5A
5E
5I
5M
5B
5F
5J
5N
5C
5G
5K
5O
5D
5H
5L
5P
T
BV

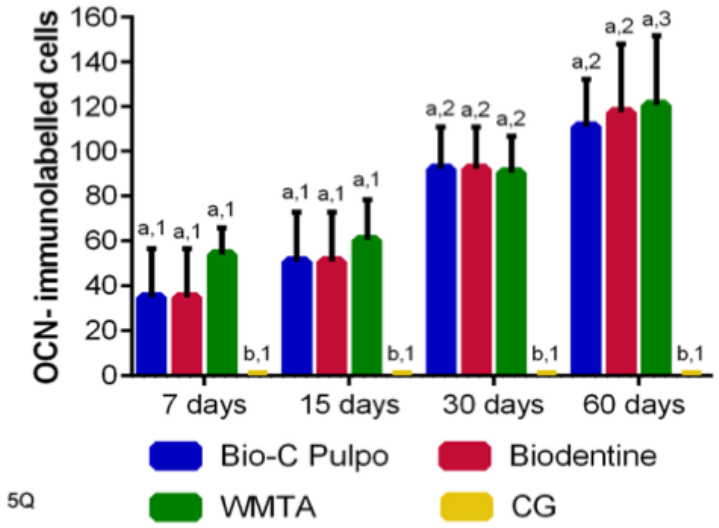
OCN- immunolabelled cells
160
140
120
100
80
60
40
20
0
a,1
a,2
a,3
b,1
7 days
15 days
30 days
60 days
Bio-C Pulpo
Biodentine
WMTA
CG

5Q

Figures 5A-5P – Light micrographs of sections showing portions of capsules (C) of Bio-C Pulpo, Biodentine, WMTA and CG groups. The sections were submitted to immunohistochemistry for OCN detection (brown-yellow colour) and counterstained with haematoxylin. OCN-immunolabelled cells (arrows) are present in the capsules around bioceramic materials. Note absence of OCN-immunolabelled cells in capsules of CG specimens. BV, blood vessels; T, space of implanted polyethylene tube. Bars: 22 μm.

Figure 5Q – Number of OCN-immunolabelled cells in the capsules of Bio-C Pulpo, Biodentine, WMTA and CG groups at 7, 15, 30 and 60 days. Different superscript letters denote significant difference among groups in the period. Different superscript numbers denote significant difference in a group over time. Tukey's test ($p \leq 0.05$).

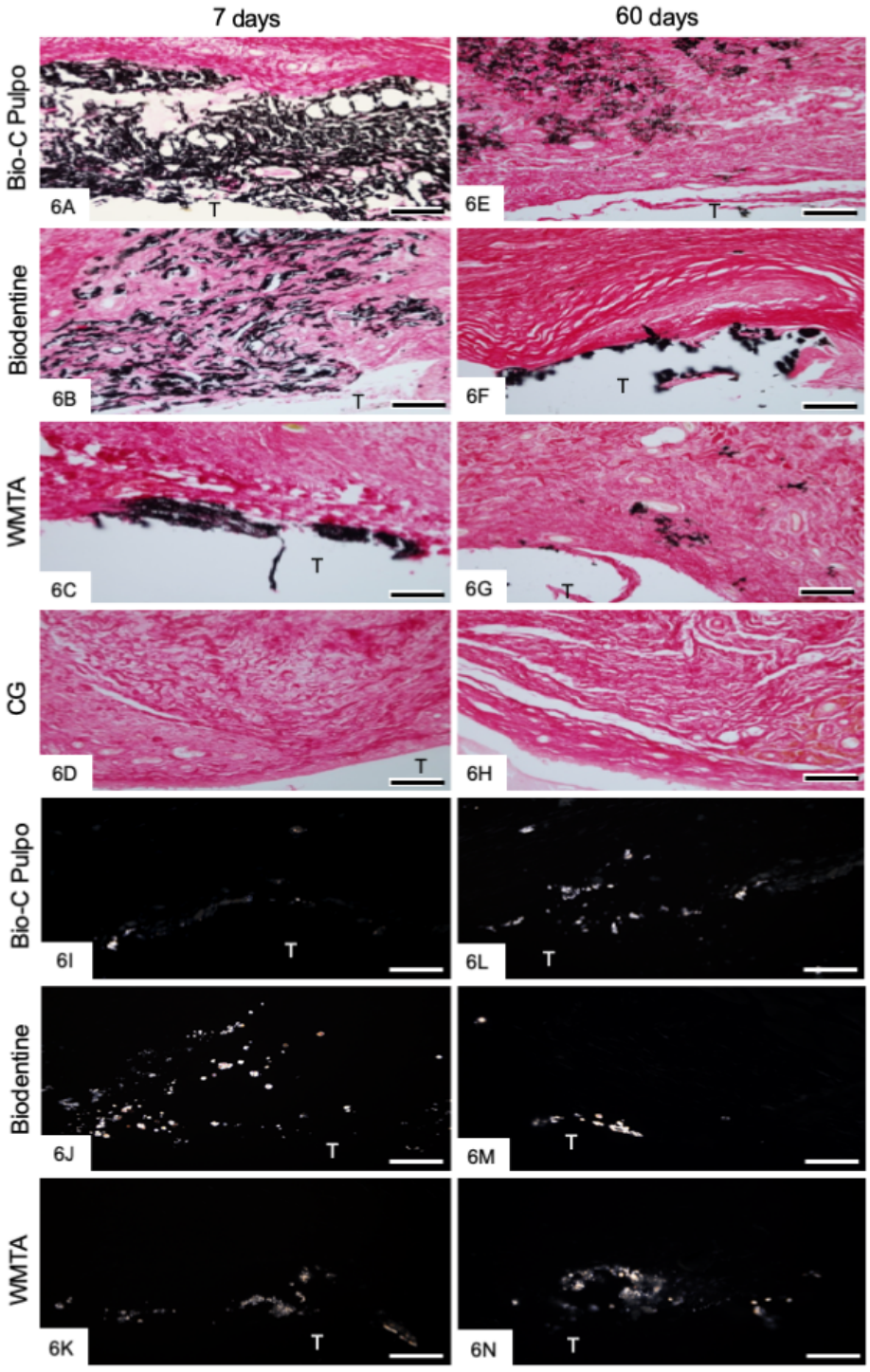
7 days
60 days
Bio-C Pulpo
Biodentine
WMTA
CG
Bio-C Pulpo
Biodentine
WMTA
6A
6B
6C
6D
6E
6F
6G
6H
6I
6J
6K
6L
6M
6N
T

Figures 6A-6H - Light micrographs showing portions of capsule of Bio-C Pulpo, Biodentine, WMTA and CG specimens at 7 and 60 days. The sections were subjected to von Kossa histochemical reaction (black colour) and counterstaining with picrosirius-red (red colour). The capsules around Bio-C Pulpo, Biodentine and WMTA exhibit von Kossa reactivity in black colour structures. Note that in CG specimens (Figs. 6D and 6H), no positive structure is present.
Figures 6I-6N – Light micrographs of unstained sections under polarized light. Birefringent material is dispersed through the capsules around the materials. T, space of implanted polyethylene tube. Bars: 120 μm.

4 DISCUSSÃO

O TCS puro foi associado à 30% de tungstato de cálcio ($CaWO_4$), usado como radiopacificador, uma vez que essa associação forneceu 4,61 (mm de alumínio) de radiopacidade[28], portanto, em conformidade com a norma ISO (International Organization for Standardization) 6876/2012. A radiopacidade é importante para distinguir o material endodôntico das estruturas anatômicas adjacentes[96,97]. Biomateriais contendo silicato tricálcico sintetizado puro têm sido propostos[23-28], a fim de evitar a presença de contaminantes.

As análises morfológica e quantitativa revelaram que o TCS + $CaWO_4$ induziu uma reação inflamatória moderada, semelhante ao Bio-C e MTA HP, quando implantados no tecido conjuntivo do subcutâneo. Aos 7 e 15 dias, o infiltrado inflamatório observado nas cápsulas ao redor dos materiais de reparo, foi significativamente maior do que nos espécimes do GC, indicando que substâncias liberadas por esses materiais podem ser responsáveis, pelo menos em parte, pelo dano tecidual. Além da composição química dos materiais, as suas propriedades físico-químicas devem também exercer influência na resposta tecidual, dentre elas o tempo de presa, solubilidade e pH parecem ter uma íntima associação com a biocompatibilidade dos materiais. O MTA HP apresenta tempo de presa inicial de aproximadamente 17 minutos[98] a 32,5 minutos[28], enquanto que o tempo de presa inicial do TCS + $CaWO_4$ foi aproximadamente de 61,78 minutos[28]. Em contraposição, o Bio-C apresenta tempo de presa inicial de aproximadamente 7 minutos[60] a 12 minutos[99], onde podemos sugerir que as substâncias que foram liberadas durante o tempo de presa podem ter sido prejudiciais ao tecido. Com relação ao pH, os materiais apresentaram valores de pH alcalino, sendo que nas primeiras horas, o pH do TCS + $CaWO_4$ foi de aproximadamente 9,5[28], o Bio-C Repair de aproximadamente 7[100] e o MTA HP de aproximadamente 9,3[28]. Sabe-se que o pH alcalino estimula o recrutamento de leucócitos[40,85,88,98], exercendoportanto um papel importante na resposta inflamatória em resposta aos materiais. A solubilidade e a radiopacidade dos materiais apresentaram valores de acordo com a norma ISO 6876/2012, que preconiza que a solubilidade do material esteja a baixo de 3% e a radiopacidade seja de no mínimo 3 mm Al.

No estudo 2, o Bio-C Pulpo, um material biocerâmico contendo silicato tricálcico e dicálcico, aluminato de cálcio, hidróxido de cálcio, fluoreto de cálcio, dióxido de

silício, óxido de ferro e óxido de zircônio em seu pó, enquanto o líquido contém água destilada, plastificante, cloreto de cálcio (catalisador) e metilparabeno[60,82,99,101], foi comparado ao Biodentine e ao WMTA (Angelus). O Bio-C Pulpo foi manipulado na proporção de 0,17 g de pó para 3 gotas de líquido por aproximadamente 60 segundos, quando o cimento adquiriu a consistência de uma massa homogênea, de consistência semelhante a massa de modelagem. A manipulação e inserção deste material foi relativamente simples e fácil. Apesar do Biodentine também ser de fácil manipulação, pois a sua mistura é feita no dispositivo amalgamador, a desvantagem é que este material é disponibilizado em cápsulas (com aproximadamente 1g), que após a mistura apresenta um tempo de trabalho relativamente curto, o que pode levar a perda do material[70]. O WMTA (Angelus) após a manipulação apresenta uma consistência de aspecto arenoso e, portanto, há uma dificuldade de inserção deste material em cavidades[3,62].

Como esperado, nos períodos iniciais (7 e 15 dias), os materiais reparadores (Bio-C Pulpo, Biodentine e WMTA) estimularam o recrutamento de células inflamatórias no tecido conjuntivo adjacente à abertura dos tubos de polietileno implantados no subcutâneo. Nestes períodos, as cápsulas que envolviam os materiais Bio-C Pulpo e Biodentine apresentaram-se mais espessas em comparação àquelas adjacentes ao WMTA. A evidente reação inicialmente promovida por esses materiais biocerâmicos foi reduzida gradativamente culminando nas cápsulas com espessuras semelhantes às encontradas nos espécimes WMTA e CG aos 30 e 60 dias. A análise quantitativa das células inflamatórias revelou que, aos 7 dias, Biodentine induziu um maior recrutamento de células inflamatórias do que Bio-C Pulpo e WMTA, enquanto que não foram detectadas diferenças significativas no número de células inflamatórias entre Bio-C Pulpo e WMTA. Um acentuado potencial irritante de Biodentine foi demonstrado após a implantação em tecidos subcutâneos[39,74,83]. A injúria tecidual causada inicialmente pelo Biodentine tem sido atribuída, pelo menos em parte, ao cloreto de cálcio e/ou policarboxilato (polímero hidrossolúvel) presente em seu líquido[102-104]. O pH elevado proporcionado pelo Biodentine nas primeiras horas, em torno de 11.7[50], que durante seu tempo de presa também pode ser responsável pelo recrutamento de células inflamatórias, uma vez que o pH alcalino estimula o recrutamento de células inflamatórias[36,83,85,105]. No entanto, o efeito irritante exercido pelo Biodentine parece ocorrer por pouco tempo, uma vez que uma redução significativa no número de células inflamatórias foi observada aos 15 dias nas

cápsulas ao redor desse material de reparo. Assim, não foi encontrada diferença significante no grau de infiltrado inflamatório entre os materiais biocerâmicos após 15, 30 e 60 dias. Aos 7 e 15 dias, Biodentine apresentou áreas de necrose nas cápsulas ao redor do material. O hidróxido de cálcio contido nos materiais biocerâmicos inclui inflamação e necrose da superfície da polpa[106].

Os materiais foram colocados no tecido subcutâneo imediatamente após a inserção nos tubos de polietileno, portanto, é razoável sugerir que as substâncias liberadas durante o tempo de presa foram prejudiciais ao tecido. Além disso, um produto da reação à base de silicato de cálcio é a hidroxila (OH), que proporciona um pH alcalino ao microambiente. Sabe-se que o pH alcalino estimula o recrutamento de leucócitos[40,85,88,98] que migram dos vasos sanguíneos em direção à superfície dos materiais, causando espessamento das cápsulas como observados nos períodos iniciais. No entanto, uma redução significativa no número de células inflamatórias ao redor dos materiais à base de silicato de cálcio foi observada ao longo do tempo indicando uma supressão da injúria tecidual induzida por esses materiais.

A imuno-histoquímica para detecção de IL-6, uma interleucina que atua como citocina pró-inflamatória, revelou também uma redução significativa no número de células imunomarcadas com IL-6 em cápsulas ao redor dos materiais TCS + $CaWO_4$, Bio-C e MTA HP ao longo do tempo. A IL-6 é uma citocina produzida por uma variedade de células, incluindo macrófagos, linfócitos, plasmócitos, células endoteliais, fibroblastos e mastócitos[83,88]. Há evidências de que esta citocina é responsável pela manutenção da reação inflamatória, uma vez que a IL-6 desempenha um papel na maturação de plasmócitos, bem como na ativação e diferenciação das células T[88,89]. Portanto, o número de células imunomarcadas com IL-6 nas cápsulas parece estar diretamente associado ao grau de reação inflamatória induzida pelos materiais endodônticos[83,84,86,87]. Não foi observada diferença significativa na imunoexpressão de IL-6 entre os materiais Bio-C Pulpo, Biodentine e WMTA em todos os períodos, assim como os resultados referentes à densidade numérica de células inflamatórias, indicando que os danos no tecido conjuntivo causado por TCS + $CaWO_4$, Bio- C e MTA HP são transitórios. Apesar dos maiores valores de células imunomarcadas com IL-6 detectados em Bio-C Pulpo e Biodentine aos 7, 15 e 30 dias, a redução significativa na imunoexpressão desta citocina nestes grupos ao longo do tempo aponta para uma regressão na reação inflamatória.

Em relação ao estudo 2, o número de células imunomarcadas à IL-6 foi significativamente maior em torno de espécimes Bio-C Pulpo e Biodentine em comparação às dos espécimes do WMTA, aos 7, 15 e 30 dias. É importante ressaltar que a redução da reação inflamatória foi acompanhada por um aumento significante no número de fibroblastos e quantidade de fibras colágenas nas cápsulas ao redor de todos os espécimes ao longo do tempo. Em geral, várias células inflamatórias e poucos fibroblastos foram observados nas cápsulas aos 7 dias enquanto, no período de 60 dias, os fibroblastos foram o principal tipo celular observado nas cápsulas ricas em colágeno, reforçando a ideia de que houve regressão da reação inflamatória ao longo do tempo[84,86]. Portanto, nossos achados mostraram claramente que fibroblastos e fibras colágenas, componentes típicos do tecido conjuntivo saudável, substituíram a reação inflamatória inicialmente induzida por materiais de silicato de cálcio.

Além da biocompatibilidade, nossos achados sugerem que TCS + CaWO4, Bio-C Repair e MTA HP, Bio-C Pulpo, Biodentine e WMTA expressam potencial bioativo no tecido conjuntivo do subcutâneo de ratos. No presente estudo, estruturas positivas de von Kossa foram observadas ao redor dos espécimes indicando precipitação de cálcio nas cápsulas[40,54,87]. A análise de cortes não corados das cápsulas formadas em resposta aos revelou estruturas birrefringentes, que são sugestivas de calcita amorfa[52,62,77,86,94,95]. Sabe-se que quando os materiais de silicato de cálcio são hidratados, os íons cálcio são liberados[24,36,40,107,108] e reagem com o carbonato dióxido do líquido intersticial dando origem ao carbonato de cálcio[24,109], uma calcita amorfa birrefringente[52,86,90,94]. Além disso, as cápsulas de TCS + $CaWO_4$, Bio-C e MTA HP foram imunorreativas à osteocalcina, uma glicoproteína sintetizada por células de tecidos mineralizados, como linhagem de células osteogênicas[77]. Embora células imunomarcadas com OCN tenham sido observadas nas cápsulas em todos os períodos, um aumento significativo na imunoexpressão foi observado nas cápsulas ao redor de materiais de silicato de cálcio ao longo do tempo. Esses achados indicam que TCS + $CaWO_4$, Bio-C e MTA HP, O Bio-C Pulpo, o Biodentine e o WMTA podem promover a precipitação de cálcio estimulando a produção de OCN por células mesenquimais derivadas do tecido conjuntivo subcutâneo. Esta hipótese é corroborada pelo fato de que estruturas von Kossa positivas e birrefringentes, bem como células imunomarcadas com OCN, não foram observadas nas cápsulas do GC. Esses resultados, em conjunto, sustentam o conceito de que esses materiais biocerâmicos apresentam potencial bioativo.

A escolha de um material de reparo, é importante ressaltar que os produtos de reação do material entram em contato direto com os tecidos[111,112]. Nossos achados indicam que o material experimental TCS + $CaWO_4$ e os demais materiais MTA HP, Bio-C, Bio-C Pulpo, Biodentine e WMTA são biocompatíveis e induzem o reparo do tecido conjuntivo quando implantados no subcutâneo de ratos. Além disso, os materiais TCS + $CaWO_4$, MTA HP, Bio-C Pulpo, Biodentine e WMTA parecem exercer potencial bioativo no tecido conjuntivo. Porém, futuras pesquisas devem ser conduzidas para confirmar se o material experimental TCS+ $CaWO_4$ é capaz de estimular a diferenciação e atividade de células produtoras de tecidos mineralizados.

5 CONCLUSÃO

O TCS + 30% $CaWO_4$ constitui uma alternativa como material de reparo, pois este material biocerâmico permite a proliferação de fibroblastos e a formação de colágeno ao longo do tempo. Além disso, este material biocerâmico experimental permite a precipitação de cristais de calcita e estimula a produção de osteocalcina, sugerindo que este material possui potencial bioativo.

As alterações feitas no Bio-C Pulpo e Biodentine para melhorar o manuseio de materiais biocerâmicos possivelmente devem ser responsáveis, pelo menos em parte, pela acentuada imunoexpressão da citocina pró-inflamatória IL-6 inicialmente detectada no tecido conjuntivo. No entanto, a redução significante da imunoexpressão de IL-6 e da reação inflamatória ao redor de Bio-C Pulpo e Biodentine paralelamente ao aumento do número de fibroblastos e da quantidade nas fibras de colágeno, indicam que esses materiais biocerâmicos são biocompatíveis e também podem permitir o reparo do tecido conjuntivo. A presença de depósitos positivos ao von Kossa, estruturas de calcita birrefringentes e células imunomarcadas à osteocalcina sugerem que Bio-C Pulpo e Biodentine apresentam potencial bioativo.

REFERÊNCIAS*

1. Camilleri J, Pitt Ford TR. Mineral trioxide aggregate: a review of the constituents and biological properties of the material. Int Endod J. 2006; 39(10):747–54.
2. Roberts HW, Toth JM, Berzins DW, Charlton DG. Mineral trioxide aggregate material use in endodontic treatment: a review of the literature. Dent Mater. 2008; 24(2):149-64.
3. Parirokh M, Torabinejad M. Mineral trioxide aggregate: a comprehensive literature review-Part I: chemical, physical, and antibacterial properties. J Endod. 2010; 36(1): 16-27.
4. Camilleri J. Hydration mechanisms of mineral trioxide aggregate. Int Endod J. 2007; 40(6):462-70.
5. Camilleri J. The physical properties of accelerated Portland cement for endodontic use. Int Endod J. 2008; 41(2):151-7.
6. Gandolfi MG, Ciapetti G, Taddei P, Perut F, Tinti A, Cardoso MV, et al. Apatite formation on bioactive calcium-silicate cements for dentistry affects surface topography and human marrow stromal cells proliferation. Dent Mater. 2010; 26(10):974-92.
7. Glickman GN, Koch KA. 21st-century. Endod J Am Dent Assoc 1939. 2000; 131:39S–46S.
8. Sienko MJ, Plane RA. Chemistry. McGraw-Hill, New York. 1961.
9. Parirokh M, Torabinejad M, Dummer PMH. Mineral trioxide aggregate and other bioactive endodontic cements: an updated overview - part I: vital pulp therapy. Int Endod J. 2018; 51(2): 177-205.
10. Asgary S, Parirokh M, Eghbal MJ, Brink F. Chemical differences between white and gray mineral trioxide aggregate. J Endod. 2005; 31(2): 101–103.
11. Darvell BW, Wu RC. "MTA"- a hydraulic silicate cement: review update and setting reaction. Dent Mater. 2011; 27(5): 407-22.

* De acordo com o Guia de Trabalhos Acadêmicos da FOAr, adaptado das Normas Vancouver. Disponível no site da Biblioteca: http://www.foar.unesp.br/Home/Biblioteca/guia-de-normalizacao-atualizado.pdf

12. Camilleri J, Montesin FE, Di Silvio L, Pitt Ford TR. The chemical constitution and biocompatibility of accelerated Portland cement for endodontic use. Int Endod J. 2005; 38(11): 834–42.
13. Schembri Wismayer P, Lung CY, Rappa F, Cappello F, Camilleri J. Assessment of the interaction of Portland cement-based materials with blood and tissue fluids using an animal model. Sci Rep. 2016; 6: 34547.
14. Moinzadeh AT, Farack L, Wilde F, Shemesh H, Zaslansky P. Synchrotron-based phase contrast-enhanced micro-computed tomography reveals delaminations and material tearing in water-expandable root fillings ex vivo. J Endod. 2016; 42(5): 776–81.
15. Meschi N, Li X, Van Gorp G, Camilleri J, Van Meerbeek B, Lambrechts P. Bioactivity potential of Portland cement in regenerative endodontic procedures: from clinic to lab. Dent Mater. 2019; 35(9):1342–50.
16. Xuereb M, Vella P, Damidot D, Sammut CV, Camilleri J. In situ assessment of the setting of tricalcium silicate-based sealers using a dentin pressure model. J Endod. 2015; 41(1):111–24.
17. Li Z, Cao L, Fan M, Xu Q. Direct pulp capping with calcium hydroxide or mineral trioxide aggregate: a meta-analysis. J Endod. 2015; 41(9):1412–17.
18. Camiller J. Classification of hydraulic cements used in dentistry. Front in Dent Med. 2020; 1:9.
19. Oliveira MG, Xavier CB, Demarco FF, Pinheiro AL, Costa AT, Pozza DH. Comparative chemical study of MTA and Portland cements. Braz Dent J. 2007; 18(1):3–7.
20. Chang SW, Shon WJ, Lee W, Kum KY, Baek SH, Bae KS. Analysis of heavy metal contents in gray and white MTA and 2 kinds of Portland cement: a preliminary study. Oral Surg Oral Med Oral Pathol Oral Radiol Endod. 2010; 109(4):642-6.
21. Schembri M, Peplow G, Camilleri J. Analyses of heavy metals in mineral trioxide aggregate and Portland cement. J Endod. 2010; 36(7):1210–15.
22. Camilleri J. Evaluation of the effect of intrinsic material properties and ambient conditions on the dimensional stability of white mineral trioxide aggregate and Portland cement. J Endod. 2011; 37(2):239-45.

23. Camilleri J, Sorrentino F, Damidot D. Investigation of the hydration and bioactivity of radiopacified tricalcium silicate cement, Biodentine and MTA Angelus. Dent Mater. 2013; 29(5):580-93.
24. Camilleri J, Laurent P, About I. Hydration of Biodentine, Theracal LC, and a proto- type tricalcium silicate-based dentin replacement material after pulp capping in entire tooth cultures. J Endod 2014; 40:1846–54.
25. Taha NA, Safadi RA, Alwedaie MS. Biocompatibility evaluation of endosequence root repair paste in the connective tissue of rats. J Endod. 2016; 42(10):1523-8.
26. Bosso-Martelo R, Guerreiro-Tanomaru JM, Viapiana R, Berbert FL, Duarte MA, Tanomaru-Filho M. Physicochemical properties of calcium silicate cements associated with microparticulate and nanoparticulateradiopacifiers. Clin Oral Investig. 2016; 20(1): 83-90.
27. Barbosa DD, Delfino MM, Guerreiro-Tanomaru JM, Tanomaru-Filho M, Sasso-Cerri E, Silva GF, et al. Histomorphometric and immunohistochemical study shows that tricalcium silicate cement associated with zirconium oxide or niobium oxide is a promising material in the periodontal tissue repair of rat molars with perforated pulp chamber floors. Int Endod J. 2021; 54(5):736-52.
28. Queiroz MB, Torres FFE, Rodrigues EM, Viola KS, Bosso-Martelo R, Chavez-Andrade GM, et al. Physicochemical, biological, and antibacterial evaluation of tricalcium silicate-based reparative cements with different radiopacifiers. Dent Mater. 2021; 37(2):311-20.
29. Demirkaya K, Demirdöğen BC, Torun ZÖ, Erdem O, Çırak E, Tunca YM. Brain aluminium accumulation and oxidative stress in the presence of calcium silicate dental cements. Hum Exp Toxicol. 2017; 36(10):1071–80.
30. Simsek N, Bulut ET, Ahmetoğlu F, Alan H. Determination of trace elements in rat organs implanted with endodontic repair materials by ICP-MS. J Mater Sci. Mater Med. 2016; 27(3):46.
31. Demirkaya K, Demirdöğen BC, Torun ZÖ, Erdem O, Çırak E, Tunca YM. Brain aluminium accumulation and oxidative stress in the presence of calcium silicate dental cements. Hum Exp Toxicol. 2017; *36*(10):1071–80.

32. Coomaraswamy K, Lumley PJ, Hofmann MP. Effect of bismuth oxide radiopacifier content on the material properties of an endodontic Portland cement–based (MTA-like) System. J Endod. 2007; 33(3):295-8.
33. Camilleri J, Mallia B. Evaluation of the dimensional changes of mineral trioxide aggregate sealer. Int Endod J. 2011; 44(5):416-24.
34. Coutinho-Filho T, De-Deus G, Klein L, Manera G, Peixoto C, Gurgel-Filho ED. Radiopacity and histological assessment of Portland cement plus bismuth oxide. Oral Surg Oral Med Oral Pathol Oral Radiol Endod. 2008; 106(6):e69-77.
35. Hwang YC, Lee SH, Hwang IN, Kang IC, Kim MS, Kim SH, et al. Chemical composition, radiopacity, and biocompatibility of Portland cement with bismuth oxide. Oral Surg Oral Med Oral Pathol Oral Radiol Endod. 2009; 107(3):e96-102.
36. Silva GF, Bosso R, Ferino RV, Tanomaru-Filho M, Bernardi MI, Guerreiro-Tanomaru JM, et al. Microparticulated and nanoparticulated zirconium oxide added to calcium silicate cement: evaluation of physicochemical and biological properties. J Biomed Mater Res A. 2014; 102(12):4336-45.
37. Slompo C, Peres-Buzalaf C, Gasque KC, Damante CA, Ordinola-Zapata R, Duarte MA, et al.-Experimental calcium silicate-based cement with and without zirconium oxide modulates fibroblasts viability. Braz Dent J. 2015; *26*(6):587–91.
38. Silva GF, Guerreiro-Tanomaru JM, da Fonseca TS, Bernardi MIB, Sasso-Cerri E, Tanomaru-Filho M, et al. Zirconium oxide and niobium oxide used as radiopacifiers in a calcium silicate-based material stimulate fibroblast proliferation and collagen formation. Int Endod J. 2017; 50 Suppl 2:e95-e108.
39. Andrade GM, Bonetti-Filho I, Guerreiro-Tanomaru JM. A novel model for evaluating the flow of endodontic materials using micro-computed tomography. J Endod. 2017; 43(5):796–800.
40. Silva GF, Tanomaru-Filho M, Bernardi MI, Guerreiro-Tanomaru JM, Cerri PS. Niobium pentoxide as radiopacifying agent of calcium silicate-based material: evaluation of physicochemical and biological properties. Clin Oral Investig. 2015; 19(8):2015-25.

41. Tomás-Catalá CJ, Collado-González M, García-Bernal D, Oñate-Sánchez RE, Forner L, Llena C, et al. Biocompatibility of new pulp-capping materials neomta plus, MTA Repair HP, and Biodentine on human dental pulp stem cells. J Endod. 2018; 44(1):126-32.
42. Galarça AD, Da Rosa WLO, Da Silva TM, da Silveira Lima G, Carreño NLV, Pereira TM, et al. Physical and biological properties of a high-plasticity tricalcium silicate cement. Biomed Res Int. 2018; 27:2018:8063262.
43. Marciano MA, Duarte MA, Camilleri J. Calcium silicate-based sealers: assessment of physicochemical properties, porosity and hydration. Dent Mater. 2016; 32(2): 30-40.
44. Camilleri J. Tricalcium silicate cements with resins and alternative radiopacifiers. J Endod. 2014; 40(12):2030–5.
45. Marciano MA, Duarte MA, Camilleri J. Dental discoloration caused by bismuth oxide in MTA in the presence of sodium hypochlorite. Clin Oral Investi. 2015; 19(9):2201–9.
46. Felman D, Parashos P. Coronal tooth discoloration and white mineral trioxide aggregate. J Endod. 2013; 39(4):484–7.
47. Húngaro Duarte MA, de Oliveira El, Kadre GD, Vivan RR, Guerreiro Tanomaru JM, Tanomaru Filho M. Radiopacity of portland cement associated with different radiopacifying agents. J Endod. 2009; 35(5):737-40.
48. Torabinejad M, Hong CU, McDonald F, Pitt Ford TR. Physical and chemical properties of a new root-end filling material. J Endod. 1995; 21(7):349–53.
49. Marciano MA, Duarte MA, Camilleri J. Calcium silicate-based sealers: assessment of physicochemical properties, porosity and hydration. Dent Mater. 2016; 32(2): 30-40.
50. Queiroz MB, Torres FFE, Rodrigues EM, Viola KS, Bosso-Martelo R, Chavez-Andrade GM, et al. Development and evaluation of reparative tricalcium silicate-ZrO_2 - Biosilicate composites. J Biomed Mater Res B Appl Biomater. 2021; 109(4):468-76.
51. Alves Silva EC, Tanomaru-Filho M, da Silva GF, Delfino MM, Cerri PS, Guerreiro-Tanomaru JM. Biocompatibility and bioactive potential of new calcium silicate-based endodontic sealers: Bio-C Sealer and Sealer Plus BC. J Endod. 2020; 46(10):1470-77.

52. Delfino MM, de Abreu Jampani JL, Lopes CS, Guerreiro-Tanomaru JM, Tanomaru-Filho M, Sasso-Cerri E, Cerri PS. Comparison of Bio-C Pulpo and MTA Repair HP with White MTA: effect on liver parameters and evaluation of biocompatibility and bioactivity in rats. Int Endod J. 2021; 54(9):1597-613.
53. Camilleri J, Gandolfi MG, Siboni F, Prati C. Dynamic sealing ability of MTA root canal sealer. Int Endod J. 2011; 44(1):9-20.
54. Viola NV, Guerreiro-Tanomaru JM, da Silva GF, Sasso-Cerri E, Tanomaru-Filho M, Cerri PS. Biocompatibility of an experimental MTA sealer implanted in the rat subcutaneous: quantitative and immunohistochemical evaluation. J Biomed Mater Res B Appl Biomater. 2012; 100(7):1773-81.
55. Hungaro-Duarte MA, Minotti PG, Rodrigues CT, Zapata RO, Bramante CM, Tanomaru Filho M, et al. Effect of different radiopacifying agents on the physicochemical properties of white Portland cement and white mineral trioxide aggregate. J Endod. 2012; 38(3):394-7.
56. Tanomaru-Filho M, Torres F, Bosso-Martelo R, Chávez-Andrade GM, Bonetti-Filho I, Guerreiro-Tanomaru JM. A novel model for evaluating the flow of endodontic materials using micro-computed tomography. J Endod. 2017; 43(5):796–800.
57. Guerreiro-Tanomaru JM, Vázquez-García FA, Bosso-Martelo R, Bernardi MI, Faria G, Tanomaru-Filho M. Effect of addition of nano-hydroxyapatite on physico-chemical and antibiofilm properties of calcium silicate cements. J Appl Oral Sci. 2016; 24(3):204-10.
58. Gomes-Cornélio AL, Rodrigues EM, Salles LP, Mestieri LB, Faria G, Guerreiro-Tanomaru JM, et al. Bioactivity of MTA Plus, Biodentine and an experimental calcium silicate-based cement on human osteoblast-like cells. Int Endod J. 2017; 50(1):39-47.
59. Bosso-Martelo R, Guerreiro-Tanomaru JM, Viapiana R, Berbert FL, Basso Bernardi MI, Tanomaru-Filho M. Calcium silicate-based cements associated with micro- and nanoparticle radiopacifiers: physicochemical properties and bioactivity. Int Sch Res Notices. 2015; 23; 2015:874283.
60. Koutroulis A, Kuehne SA, Cooper PR, Camilleri J. The role of calcium ion release on biocompatibility and antimicrobial properties of hydraulic cements. Sci Rep. 2019; 13;9(1):19019.

61. Torabinejad M, Parirokh M, Dummer PMH. Mineral trioxide aggregate and other bioactive endodontic cements: an updated overview - part II: other clinical applications and complications. Int Endod J. 2018; 51(3):284-317.
62. Cintra LTA, Benetti F, de Azevedo Queiroz ÍO, de Araújo Lopes JM, Penha de Oliveira SH, et al. Cytotoxicity, biocompatibility, and biomineralization of the new high-plasticity MTA material. J Endod. 2017; 43(5): 774-8.
63. Cutajar A, Mallia B, Abela S, Camilleri J. Replacement of radiopacifier in mineral trioxide aggregate; characterization and determination of physical properties. Dent Mater. 2011; 27(9): 879–91.
64. Antonijevic D, Medigovic I, Zrilic M, Jokic B, Vukovic Z, Todorovic L. The influence of different radiopacifying agents on the radiopacity, compressive strength, setting time, and porosity of Portland cement. Clin Oral Investig. 2014; 18 (6):1597-604.
65. Camilleri J, Grech L, Galea K, Keir D, Fenech M, Formosa L, Damidot D, Mallia B. Porosity and root dentine to material interface assessment of calcium silicate-based root-end filling materials. Clin Oral Investig. 2014; 18(5):1437-46.
66. Laurent P, Camps J, De Meo M, Dejou J, About I. Induction of specific cell responses to a Ca(3) SiO(5)-based posterior restorative material. Dent Mater. 2008; 24(11):1486–94.
67. Laurent P, Camps J, About I. Biodentine (TM) induces TGF-beta1 release from human pulp cells and early dental pulp mineralization. Int Endod J. 2012; 45(5):439-48.
68. Koubi S, Elmerini H, Koubi G, Tassery H, Camps J. Quantitative evaluation by glucose diffusion of microleakage in aged calcium silicate-based open-sandwich restorations. Int J Dent. 2012; 2012:105863.
69. Tran XV, Gorin C, Willig C, Baroukh B, Pellat B, Decup F, et al. Effect of a calcium-silicate-based restorative cement on pulp repair. J Dent Res. 2012; 91(12):1166-71.
70. Koubi G, Colon P, Franquin JC, Hartmann A, Richard G, Faure MO, *et al.* Clinical evaluation of the performance and safety of a new dentine substitute, Biodentine, in the restoration of posterior teeth - a prospective study. Clin Oral Investig. 2013; 17(1):243-9.

71. Butt N, Talwar S, Chaudhry S, Nawal RR, Yadav S, Bali A. Comparison of physical and mechanical properties of mineral trioxide aggregate and Biodentine. Indian J Dent Res. 2014; 25(6):692-7.
72. Lucas CP, Viapiana R, Bosso-Martelo R, Guerreiro-Tanomaru JM, Camilleri J, Tanomaru-Filho M. Physicochemical properties and dentin bond strength of a tricalcium silicate-based retrograde material. Braz Dent J. 2017; 28(1):51-6.
73. Rodrigues EM, Gomes-Cornélio AL, Soares-Costa A, Salles LP, Velayutham M, Rossa-Junior C, et al. An assessment of the overexpression of BMP-2 in transfected human osteoblast cells stimulated by mineral trioxide aggregate and Biodentine. Int Endod J. 2017; 50(2): e9-e18.
74. da Fonseca TS, Silva GF, Guerreiro-Tanomaru JM, Delfino MM, Sasso-Cerri E, Tanomaru-Filho M, et al. Biodentine and MTA modulate immunoinflammatory response favoring bone formation in sealing of furcation perforations in rat molars. Clin Oral Invest. 2019; 23(3):1237–52.
75. Talabani RM, Garib BT, Masaeli R, Zandsalimi K, Ketabat F. Biomineralization of three calcium silicate-based cements after implantation in rat subcutaneous tissue. Restor Dent Endod. 2020; 46(1):e1.
76. Souza TA, Bezerra MM, Silva P, Costa J, Carneiro R, Barcelos J, et al. Bone morphogenetic proteins in biomineralization of two endodontic restorative cements. J Biomed Mater Res B Appl Biomater. 2021; 109(3):348–57.
77. Benetti F, Queiroz ÍOA, Cosme-Silva L, Conti LC, Oliveira SHP, Cintra LTA. Cytotoxicity, biocompatibility and biomineralization of a new ready-for-use bioceramic repair material. Braz Dent J. 2019; 30(4):325-32.
78. López-García S, Lozano A, García-Bernal D, Forner L, Llena C, Guerrero-Gironés J, et al. Biological effects of new hydraulic materials on human periodontal ligament stem cells. J Clin Med. 2019; 8(8):1216.
79. Ghilotti J, Sanz JL, López-García S, Guerrero-Gironés J, Pecci-Lloret MP, Lozano A, et al. Comparative surface morphology, chemical composition, and cytocompatibility of bio-c repair, biodentine, and proroot mta on hDPCs. Materials (Basel). 2020; 13(9):2189.

80. Oliveira LV, de Souza GL, da Silva GR, Magalhães TEA, Freitas GAN, Turrioni AP, de Rezende Barbosa GL, Moura CCG. Biological parameters, discolouration and radiopacity of calcium silicate-based materials in a simulated model of partial pulpotomy. Int Endod J. 2021; 54(11):2133-44.
81. Pelepenko LE, Saavedra F, Antunes TBM, Bombarda GF, Gomes BPFA, Zaia AA, Marciano MA. Investigation of a modified hydraulic calcium silicate-based material - Bio-C Pulpo. Braz Oral Res. 2021; 16;35:e077.
82. Cosme-Silva L, Gomes-Filho JE, Benetti F, Dal-Fabbro R, Sakai VT, Cintra L, et al. Biocompatibility and immunohistochemical evaluation of a new calcium silicate-based cement, Bio-C Pulpo. Int Endod J. 2019; 52(5):689–700.
83. da Fonseca TS, da Silva GF, Tanomaru-Filho M, Sasso-Cerri E, Guerreiro-Tanomaru JM, Cerri PS. In vivo evaluation of the inflammatory response and IL-6 immunoexpression promoted by Biodentine and MTA Angelus. Int Endod J. 2016; 49(2):145-53.
84. Saraiva JA, da Fonseca TS, da Silva GF, Sasso-Cerri E, Guerreiro-Tanomaru JM, Tanomaru-Filho M, et al. Reduced interleukin-6 immunoexpression and birefringent collagen formation indicate that MTA Plus and MTA Fillapex are biocompatible. Biomed Mater. 2018; 20;13(3):035002.
85. Hoshino RA, Delfino MM, da Silva GF, Guerreiro-Tanomaru JM, Tanomaru-Filho M, Sasso-Cerri E, et al. Biocompatibility and bioactive potential of the NeoMTA Plus endodontic bioceramic-based sealer. Restorative dentistry & endodontics. 2020; 46(1):e4.
86. Delfino MM, Guerreiro-Tanomaru JM, Tanomaru-Filho M, Sasso-Cerri E, Cerri PS. Immunoinflammatory response and bioactive potential of GuttaFlow bioseal and MTA Fillapex in the rat subcutaneous tissue. Sci Rep. 2020; 10(1):7173.
87. Hoshino RA, Silva G, Delfino MM, Guerreiro-Tanomaru JM, Tanomaru-Filho M, Sasso-Cerri E, et al. Physical properties, antimicrobial activity and in vivo tissue response to apexit plus. Materials (Basel). 2020; 13(5):1171.
88. Scheller J, Chalaris A, Schmidt-Arras D, Rose-John S. The pro- and anti-inflammatory properties of the cytokine interleukin-6. Biochim Biophys Acta. 2011; 1813(5):878-88.

89. Tanaka T, Narazaki M, Kishimoto T. IL-6 in inflammation, immunity, and disease. Cold Spring Harb Perspect Biol. 2014; 4,6(10):a016295.
90. Silva ECA, Tanomaru-Filho M, Silva GF, Lopes CS, Cerri PS, Guerreiro Tanomaru JM. Evaluation of the biological properties of two experimental calcium silicate sealers: an in vivo study in rats. Int Endod J. 2021; 54(1):100-11.
91. Gericke A, Qin C, Spevak L, Fujimoto Y, Butler WT, Sørensen ES, Boskey AL. Importance of phosphorylation for osteopontin regulation of biomineralization. Calcif Tissue Int. 2005; 77(1):45–54.
92. Wei F, Wang C, Zhou G, Liu D, Zhang X, Zhao Y, et al. The effect of centrifugal force on the mRNA and protein levels of ATF4 in cultured human periodontal ligament fibroblasts. Arch Oral Biol. 2008; 53(1):35–43.
93. Puchtler H, Meloan SN. On the chemistry of formaldehyde fixation and its effects on immunohistochemical reactions. Histochemistry. 1985; 82(3):201-4.
94. Holland R, de Souza V, Nery MJ, Otoboni Filho JA, Bernabé PFE, Dezan Junior E. Reaction of rat connective tissue to implanted dentin tubes filled with mineral trioxide aggregate or calcium hydroxide. J Endod. 1999; 25(3): 161-6.
95. Bueno CRE, Vasques AMV, Cury MTS, Sivieri-Araújo G, Jacinto RC, Gomes-Filho JE, et al. Biocompatibility and biomineralization assessment of mineral trioxide aggregate flow. Clin Oral Investig. 2019; 23(1):169-77.
96. Beyer-Olsen EM, Orstavik D. Radiopacity of root canal sealers. Oral Surg Oral Med Oral Pathol. 1981; 51(3):320–28.
97. Laghios CD, Benson BW, Gutmann JL, Cutler CW. Comparative radiopacity of tetracalcium phosphate and other root-end filling materials. Int Endod J. 2000; 33(4):311–15.
98. Ferreira C, Sassone LM, Gonçalves AS, de Carvalho JJ, Tomás-Catalá C. J, García-Bernal D, et al. Physicochemical, cytotoxicity and in vivo biocompatibility of a high-plasticity calcium-silicate based material. Sci Rep. 2019; 9(1): 3933.
99. Lima SPR, Santos GLD, Ferelle A, Ramos SP, Pessan JP, Dezan-Garbelini CC. Clinical and radiographic evaluation of a new stain-free tricalcium silicate cement in pulpotomies. Braz Oral Res. 2020; 34:e102.

100. Oliveira LV, de Souza GL, da Silva GR, Magalhães T, Freitas G, Turrioni AP, et al. Biological parameters, discolouration and radiopacity of calcium silicate-based materials in a simulated model of partial pulpotomy. Int Endod J. 2021; 54(11): 2133–44.

101. Cosme-Silva L, Santos A, Lopes CS, Dal-Fabbro R, Benetti F, Gomes-Filho JE, et al. Cytotoxicity, inflammation, biomineralization, and immunoexpression of IL-1β and TNF-α promoted by a new bioceramic cement. Journal of applied oral science. 2020; 28: e20200033.

102. Han L, Okiji T. Uptake of calcium and silicon released from calcium silicate-based endodontic materials into root canal dentine. Int Endod J. 2011; 44(12): 1081–87.

103. Camilleri J, Kralj P, Veber M, Sinagra E. Characterization and analyses of acid-extractable and leached trace elements in dental cements. Int Endod J. 2012; 45(8):737–43.

104. Kang JY, Lee BN, Son HJ, Koh JT, Kang SS, Son HH, et al. Biocompatibility of mineral trioxide aggregate mixed with hydration accelerators. J Endod. 2013; 39(4):497–500.

105. Williams DF. On the mechanisms of biocompatibility. Biomaterials. 2008; 29(20):2941-53.

106. Liu S, Wang S, Dong Y. Evaluation of a bioceramic as a pulp capping agent in vitro and in vivo. J Endod. 2015; 41(5):652-7.

107. Gandolfi MG, Siboni F, Primus CM, Prati C. Ion release, porosity, solubility, and bioactivity of MTA Plus tricalcium silicate. J Endod. 2014; *40*(10):1632–37.

108. Niu LN, Jiao K, Wang TD, Zhang W, Camilleri J, Bergeron BE, et al. A review of the bioactivity of hydraulic calcium silicate cements. J Dent. 2014; 42(5):517–33.

109. Seux D, Couble ML, Hartmann DJ, Gauthier JP, Magloire H. Odontoblast-like cytodifferentiation of human dental pulp cells in vitro in the presence of calcium hydroxide cement. Arch Oral Biol. 1991; 36:117–28.

110. Camilleri J, Grech L, Galea K, Keir D, Fenech M, Formosa L, Damidot D, Mallia B. Porosity and root dentine to material interface assessment of calcium silicate-based root-end filling materials. Clin Oral Investig. 2014; 18(5):1437-46.

111. Peters OA. Research that matters - biocompatibility and cytotoxicity screening. Int Endod J. 2013; 46(3): 195–97.

112. Collado-González M, López-García S, García-Bernal D, Oñate-Sánchez RE, Tomás-Catalá CJ, Moraleda JM, et al. Biological effects of acid-eroded MTA Repair HP and ProRoot MTA on human periodontal ligament stem cells. Clin Oral Investig. 2019; 23(10):3915–24.

APÊNDICE A – METODOLOGIA EXPANDIDA DOS ARTIGOS 1 E 2

Animais

O projeto foi aprovado pelo Comitê de Ética no Uso de Animais (CEUA) da Faculdade de Odontologia de Araraquara – FOAr/UNESP (Processo nº 03/2019 – ANEXO A).

Foram utilizados 64 ratos Holtzman machos e adultos (*Rattus norvegicus albinus*), pesando em média 220 g. Os animais foram mantidos em ambiente sob ciclo claro-escuro 12:12 horas, com temperatura (23 ± 2ºC) e umidade (55 ± 10%) controladas, e com ração e água fornecidas *ad libitum*. Os animais foram alojados em gaiolas de polietileno (40x30x15 cm) forradas com uma camada de aparas de pinho branco (maravalha); em cada gaiola foram colocados quatro ratos. Os animais foram distribuídos em oito grupos, sendo 4 grupos para cada pesquisa. **Pesquisa 1:** TCS + $CaWO_4$ (cimento de silicato tricálcico + 30% de tungstato de cálcio), Bio-C Repair (Bio-C Repair, Angelus, Londrina, Brasil), MTA HP (MTA Repair HP, Angelus, Londrina, Brasil) e Grupo Controle (GC, tubos vazios de polietileno). **Pesquisa 2:** Bio-C Pulpo (Angelus, Londrina, Brasil), Biodentine (Septodont, Saint Maur-des-Fosses, França), MTA Branco Angelus (Angelus, Londrina, Brasil) e Grupo Controle (GC, tubos vazios de polietileno). A Tabela 1 descreve a procedência, composição química e proporção utilizada no preparo dos materiais.

Tabela 1- Materiais biocerâmicos, fabricante, composição química e proporção.

Materiais	Composição	Proporção
TCS + 30% $CaWO_4$ (TCS, Mineral Research Processing, Meyzieu, França e $CaWO_4$, Sigma Aldrich, St Louis, MO, USA)	Pó: 70% silicate tricálcico puro (TCS) + 30% tungstato de cálcio ($CaWO_4$). Liquido: água destilada.	1g : 330 µl (Pó/Líquido)
Bio-C Repair (Angelus, Londrina, Brasil)	Silicatos de cálcio, aluminato de cálcio, óxido de cálcio, óxido de zircônio, óxido de ferro, dióxido de silício e agente dispersante (pronto para uso).	Seringa (pronto para uso)
MTA Repair HP (Angelus, Londrina, Brasil)	Pó: silicato tricálcico, silicato dicálcico, aluminato tricálcico, óxido de cálcio e tungstato de cálcio. Líquido: água e plastificante.	1g : 340 µl (Pó/Líquido)
Bio-C Pulpo (Angelus, Londrina, Brasil)	Pó: silicato tricálcico, silicato dicálcico, cálcio aluminato, hidróxido de cálcio, óxido de zircônio, fluoreto de cálcio, dióxido de silicone e óxido de ferro. Líquido: água destilada, plastificante, cloreto de cálcio e metilparabeno.	0,17g : 3 gotas (Pó/Líquido)
Biodentine (Septodont, Saint Maur-des-Fosses, França)	Pó: Silicato tricálcico, óxido de zircônio, óxido de cálcio, carbonato de cálcio, pigmento amarelo, pigmento vermelho e óxido de ferro marrom. Líquido: Cloreto de cálcio dihidratado, Areo e água purificada.	1 cápsula : 5 gotas (Pó/Líquido)
MTA Branco Angelus (Angelus, Londrina, Brasil)	Pó: Silicato tricálcico, silicato dicálcico, aluminato tricálcico, óxido de cálcio, tungstato de cálcio. Líquido: água destilada.	1 g : 300 µl (Pó/Líquido)

Fonte: Elaboração própria do autor

Manipulação dos materiais

O material experimental (TCS + $CaWO_4$) foi previamente preparado na proporção de 70% de TCS (Mineral Research Processing, Meyzieu, França) e 30% de tungstato de cálcio ($CaWO_4$; Sigma Aldrich, St Louis, MO, EUA) em peso. Este material experimental foi misturado na proporção de 1g de pó e 330 µl de água destilada durante 60 segundos, quando o material apresentava consistência de massa. O Bio-C Repair é fornecido pelo fabricante pronto para uso; este material exibe uma consistência cremosa. O MTA HP foi preparado na proporção de mistura pó / líquido de 1 g: 340 µl de veículo (água e plastificante) por 40 segundos, obtendo-se um cimento semelhante a uma argila de modelagem. O Bio-C Pulpo é também fornecido pelo fabricante pronto para uso; esse material apresenta consistência viscosa. O Biodentine foi preparado com o auxílio de um aparelho amalgamador digital (Ultramat-S SDI; SDI Brasil Indústria e Comércio LTDA), com agitação de 15 segundos, na proporção de uma cápsula para cinco gotas do líquido, exibindo consistência levemente arenosa. O MTA Branco Angelus foi manipulado com 1g de pó para 300 µl de água destilada, apresentando consistência arenosa. Todos os materiais foram preparados para serem utilizados como materiais reparadores. Os materiais foram manipulados dentro de uma câmara de fluxo laminar em condições assépticas, com placa de vidro e espátula esterilizados. Os materiais foram inseridos em tubos de polietileno (Figuras 1 e 2; Embramed Indústria e Comércio Ltda., São Paulo, SP, Brasil), previamente esterilizados em óxido de etileno[1,2]. Os tubos de polietileno usados no experimento continham 1,5 mm de diâmetro e foram cortados com 10 mm de comprimento.

Tubos com os materiais da pesquisa 1

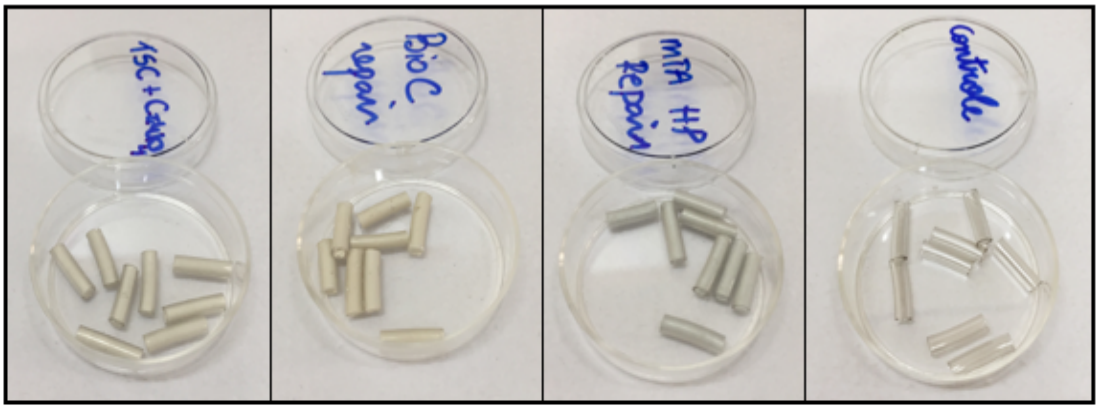

Figura 1- Tubos de polietileno estéreis contendo os materiais utilizados (TCS + $CaWO_4$, Bio-C Repair e MTA HP) e tubos sem material (GC).
Fonte: Própria do autor.

Tubos com os materiais da pesquisa 2

Figura 2- Tubos de polietileno estéreis contendo os materiais utilizados (MTA Branco Angelus, Biodentine e Bio-C Pulpo) e tubos sem material (GC).
Fonte: Própria do autor.

Procedimentos cirúrgicos

Os animais foram anestesiados com uma solução contendo 0,08 mL de cloridrato de cetamina 10% (Virbac do Brasil Indústria e Comércio Ltda, São Paulo, São Paulo, Brasil) e 0,04 mL de cloridrato de xilazina 2% (União Química Farmacêutica Nacional S / A, São Paulo, São Paulo, Brasil) por 100 g de peso corporal, administrado com seringa e agulha de insulina por via intraperitoneal (Figura 3A). Após a sedação, foi realizada a tricotomia na região dorsal e a antissepsia feita com solução de iodo a 5% (Figura 3B). Após a assepsia, foi realizada uma incisão de 2 cm no plano crânio-caudal (Figura 3C) com auxílio de uma lâmina de bisturi nº 15 (Fibra Cirúrgica, Joinville, Santa Catarina, Brasil). A pele foi divulsionada com tesoura de ponta romba (Figura 3D) e, a seguir, os tubos de polietileno foram inseridos no tecido conjuntivo subcutâneo (Figura 3E). Em cada animal, quatro tubos de polietileno (um tubo de cada grupo) foram colocados na bolsa criada no subcutâneo de cada animal (Figura 3F) de maneira que sua posição fosse alternada nos animais, ou seja, a implantação dos tubos foi realizada no sistema de “rodízio” (Figuras 5 e 6).

Duzentos e cinquenta e seis tubos de polietileno foram implantados em sessenta e quatro animais (quatro implantes em cada animal). O local da pele incisada foi suturado (Figura 3G) com pontos simples com fio de seda 4-0 (Ethicon Inc., São José dos Campos, São Paulo, Brasil). Após 7, 15, 30 e 60 dias de implantação, oito animais em cada período foram anestesiados e os implantes com os tecidos adjacentes foram removidos (Figura 4). Subsequentemente, os animais foram sacrificados com uma *overdose* de anestésico.

Sequência cirúrgica de inserção dos tubos

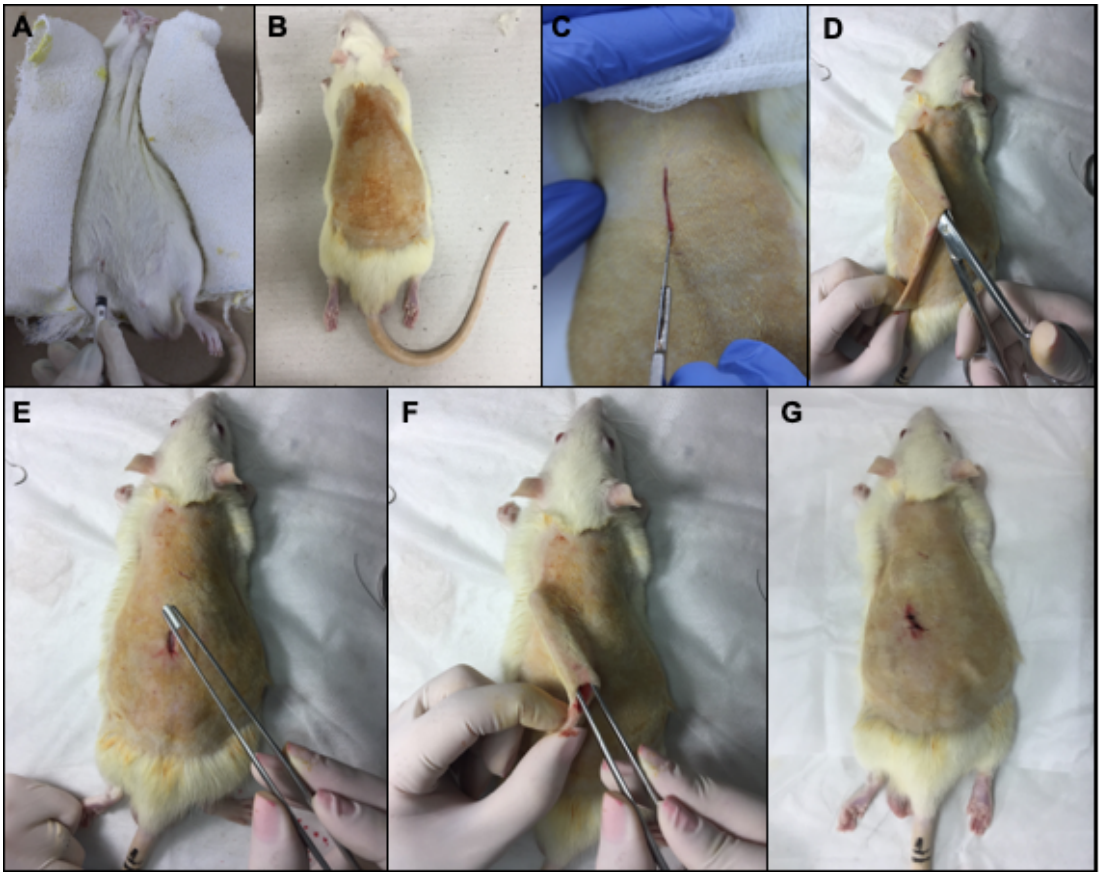

Figura 3- Imagens do procedimento cirúrgico de inserção dos implantes no subcutâneo dorsal do rato. **A-** Anestesia do animal. **B-** Tricotomia e antissepsia feita com solução de iodo a 5%. **C-** Incisão craniocaudal com a lâmina de bisturi. **D-** Divulsão da pele usando uma tesoura de ponta romba. **E e F –** Inserção do implante na bolsa criada no subcutâneo. **G-** Sutura.
Fonte: Própria do autor.

Amostra

Figura 4- Amostra de um implante com os tecidos adjacentes que foi retirada do animal.
Fonte: Própria do autor.

Esquema de Alternância de implantação do tubos da pesquisa 1

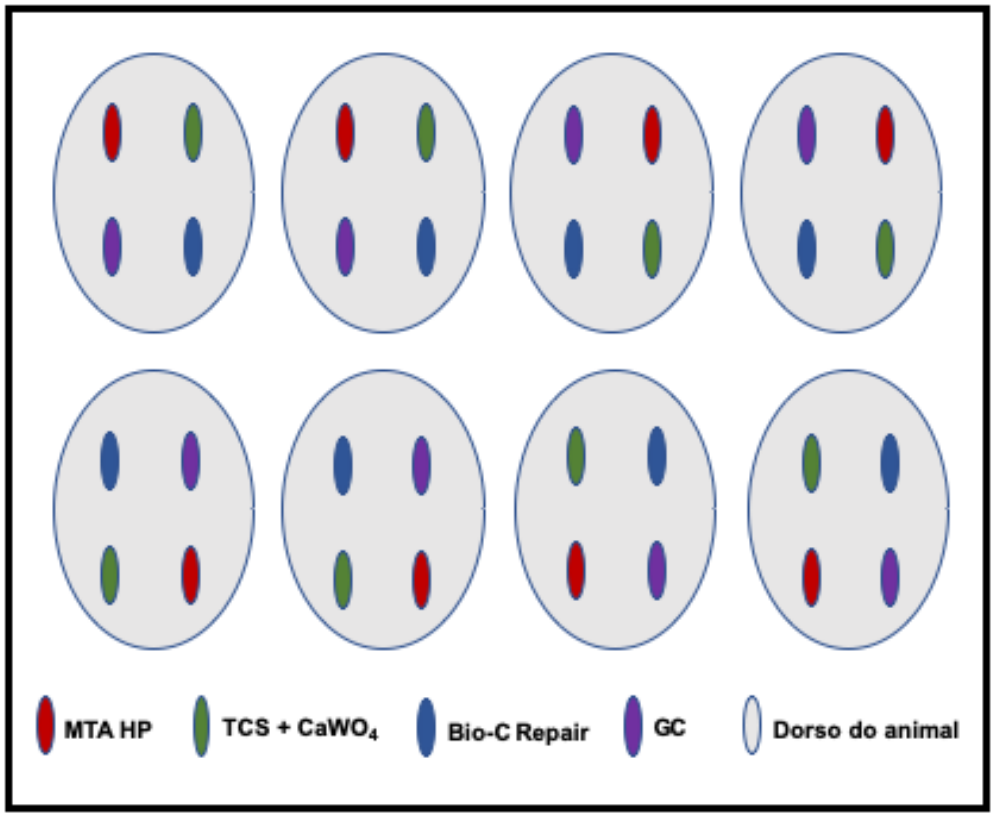

Figura 5- Organograma ilustrando os locais de implantação no dorso de cada animal e a alternância no sítio de implantação de cada material da pesquisa 1.
Fonte: Própria do autor.

Esquema de Alternância de implantação do tubos da pesquisa 2

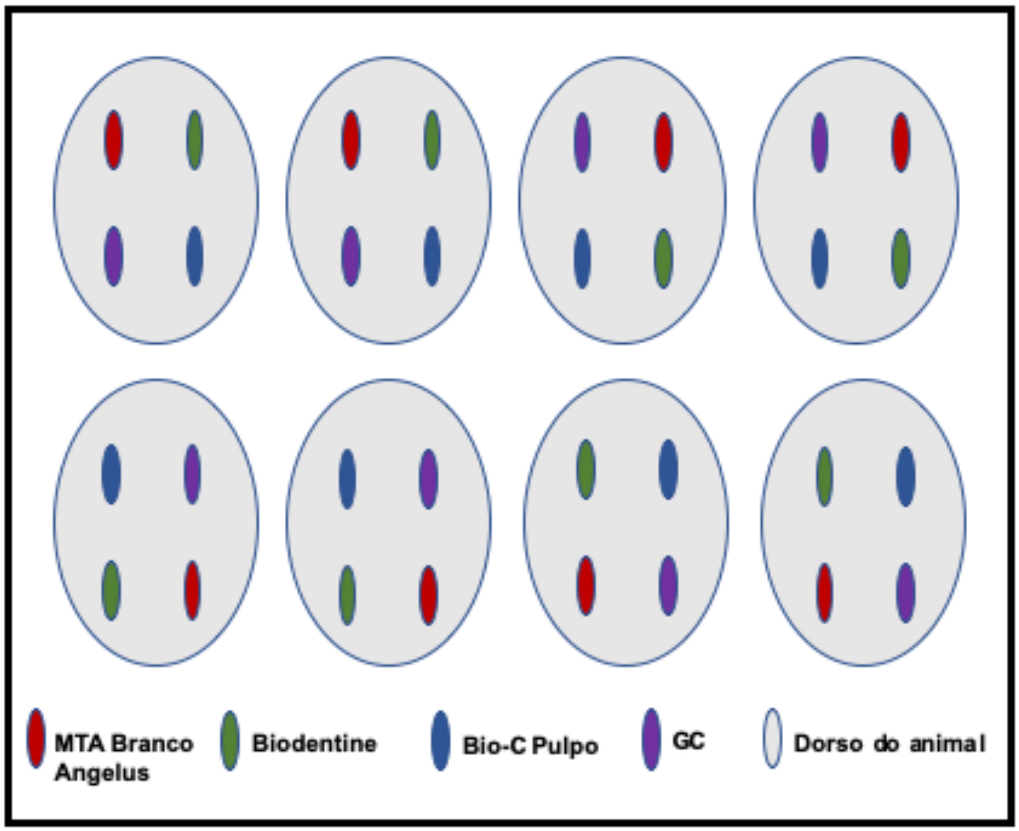

Figura 6- Organograma ilustrando os locais de implantação no dorso de cada animal e a alternância no sítio de implantação de cada material da pesquisa 2. Fonte: Própria do autor.

Processamento histológico

Após a remoção, os implantes com os tecidos adjacentes foram armazenados em cassetes com a identificação do grupo e período e, imediatamente, imersos em solução de formaldeído a 4% (preparada a partir do paraformaldeído) tamponada com fosfato de sódio 0,1 M com pH 7,2 à temperatura ambiente. Após 48 horas, as amostras foram desidratadas, diafanizadas com xilol (3 banhos de 1 hora e 30 min cada) e imersas em parafina líquida a 60ºC durante 4 horas, com 3 trocas de parafina. Subsequentemente, as amostras foram incluídas em parafina sendo posicionada para obtenção dos cortes longitudinais dos implantes (Figura 7). Após a inclusão, o tubo de polietileno foi cuidadosamente removido com auxílio de uma lâmina de bisturi e o seu espaço foi preenchido com parafina (Figura 8). Usando um micrótomo rotativo (Leica, modelo RM2125 RST, Heidelberg, Alemanha) e navalhas de aço inoxidável descartáveis (Leica, modelo 818, Heidelberg, Alemanha), quarenta cortes com 6 µm

de espessura foram colados em lâminas de vidro; em cada lâmina foram colocadas dois cortes. A adesão dos cortes às lâminas de vidro foi realizada em estufa a 60 º C durante, aproximadamente, 45 min.

Cinco lâminas contendo cortes não seriados foram coradas com hematoxilina e eosina (HE) para análise morfológica, mensuração da espessura da cápsula, estimativa do número de células inflamatórias e do número de fibroblastos nas cápsulas (Figura 7). Três cortes não seriados foram corados com picrosirius-red para análise quantitativa do colágeno birrefringente e três cortes não seriados foram submetidos ao von Kossa para avaliar a presença de cálcio nas cápsulas. Ainda, cortes foram desparafinizados e montados para análise sob luz polarizada. Os cortes aderidos as lâminas tratadas com 3-aminopropiltrietoxisilano 4% (Sigma-Aldrich Co., Saint Louis, Missouri, EUA) foram submetidos as reações de imuno-histoquímica para detecção de interleucina-6 (IL-6) e osteocalcina (OCN).

Durante o processo de remoção dos implantes dos animais e de processamento histológico das amostras, algumas foram “danificadas” e dessa maneira tivemos que definir o *n* do estudo como sendo n=7 (sendo utilizado 7 amostras de cada implante para cada período).

Fluxograma do processamento histológico das amostras

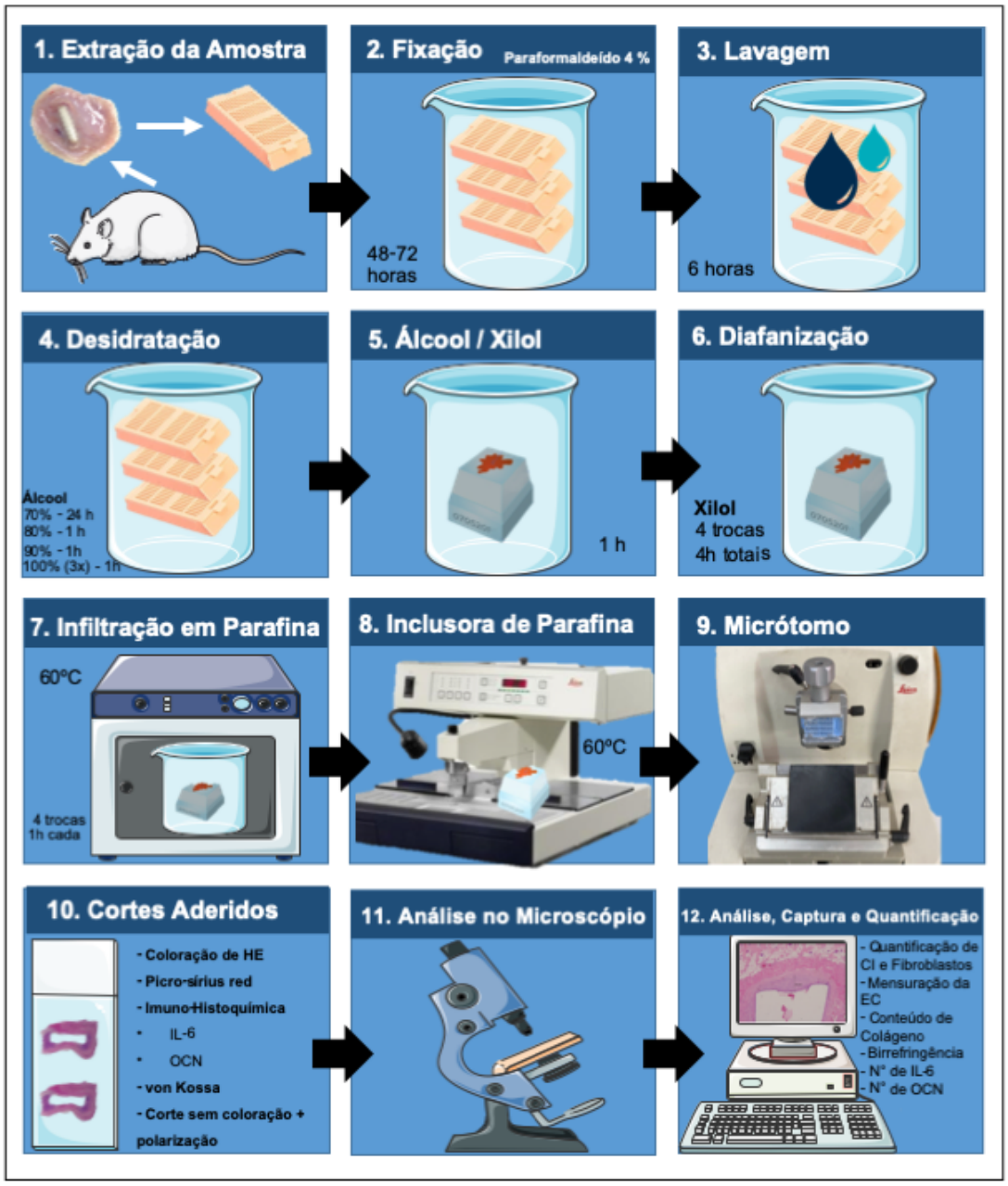

Figura 7- Fluxograma ilustrando o processamento histológico das amostras e as análises realizadas.
Fonte: Elaboração própria do autor.

Ilustração do implante e do corte histológico

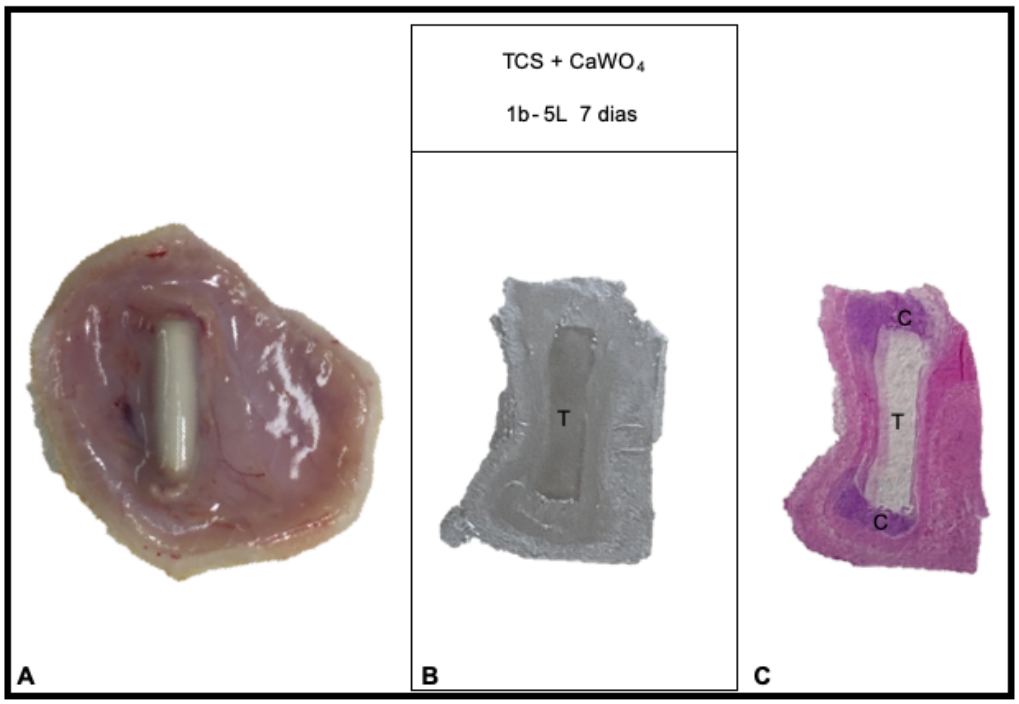

Figura 8- A- Imagens ilustrando o implante com os tecidos adjacentes removido do animal. **B-** imagem mostrando um corte da amostra sem coloração. Note que o tubo de polietileno (T) foi removido permanecendo o seu espaço envolvido pelo tecido conjuntivo. Em **C-** corte corado com HE, mostra a cápsula (C) adjacente a abertura do tubo de polietileno (T) que representa a região de interesse nas análises morfológica, histoquímica, morfométrica e imuno-histoquímica.
Fonte: Própria do autor.

Avaliação da biocompatibilidade

- Análise morfológica dos cortes corados com HE

Na análise descritiva foram considerados os principais constituintes das cápsulas, como tipos de células (células inflamatórias e fibroblastos), presença de fibras de colágeno, vasos sanguíneos e extensão da reação inflamatória. Para estimar se os tecidos adjacentes foram danificados e a extensão da reação inflamatória, a espessura das cápsulas foi mensurada. A análise e captura das imagens foram realizadas com um microscópio Olympus (modelo BX 51, Olympus, Tóquio, Japão) com uma câmera digital acoplada (DP-72, Olympus, Tóquio, Japão). As análises quantitativas foram realizadas com o auxílio de um sistema de análise de imagens (Image-Pro Express 6.0, Olympus, Tóquio, Japão). A análise foi realizada por um examinador treinado e “cego” aos grupos.

Mensuração da espessura da cápsula (EC)

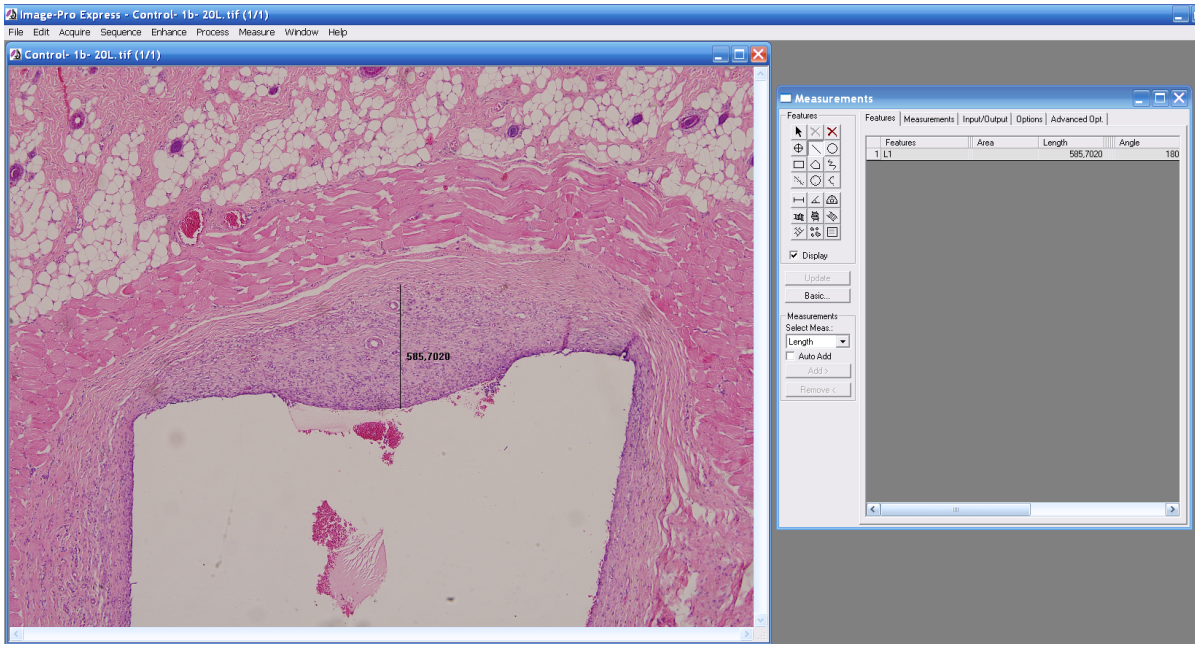

Figura 9- A figura mostra um *print sreen* da imagem capturada com a objetiva de 4x e transferida para o programa de análise de imagem (Image-Pro Express 6,0, Olympus). Após a calibração do sistema, seleciona-se a ferramenta que se pretende usar (tela à direita; *Features*). Nesse caso, seleciona-se a "linha" que permite mensurar distância de um ponto ao outro. Uma vez selecionada a ferramenta apropriada, traça-se a linha desde à superfície interna da cápsula até o seu limite com os tecidos adjacentes e o programa fornece a extensão da cápsula (em micrômetros).
Fonte: Própria do autor.

- Mensuração da espessura das cápsulas

Em cada amostra, a espessura da cápsula foi medida a partir de três cortes não seriados corados com HE (a menor distância entre os cortes foi de 100 µm). Em cada corte, a imagem foi capturada com a objetiva de 4x (aumento final de 65x). As imagens foram transferidas para um sistema de análise de imagens (Image-Pro Express 6.0, Olympus) e, inicialmente foi realizado a calibração do sistema, considerando o aumento da imagem. Com auxílio do sistema de imagem, uma linha foi traçada da superfície da cápsula adjacente à luz do tubo implantado até o limite com os tecidos adjacentes[3]. Essa linha foi traçada considerando a porção central da cápsula (Figura 9). O valor fornecido pelo programa foi registrado em micrômetros (µm), em cada

corte. Em cada implante, a espessura da cápsula foi calculada a partir da média dos valores obtidos nos três cortes. Em cada grupo, foi calculada a média em cada período. As cápsulas com até 150 µm foram categorizadas como finas, enquanto aquelas com espessura maior que 150 µm foram consideradas espessas[4].

- Estimativa do número de células inflamatórias e de fibroblastos

Em cada implante, o número de células inflamatórias e de fibroblastos foi estimado em três cortes não seriados (com intervalo mínimo entre os cortes de 100 µm) corados com HE. Em cada corte, um campo padronizado (0,09 mm^2) da cápsula adjacente à abertura dos tubos implantados foi capturado com aumento de 695x. Dessa maneira, em cada amostra, o número de células inflamatórias e fibroblastos foi computado em um campo total de 0,27 mm^2.

As imagens foram transferidas para o programa de análise de imagens (Image-Pro Express 6.0, Olympus, Tóquio, Japão) e o número de células inflamatórias (neutrófilos, linfócitos, plasmócitos e macrófagos) bem como o número de fibroblastos foi computado. Características morfológicas como núcleo multilobulado (neutrófilos), célula arredondada com núcleo esférico com cromatina condensada refletindo numa forte coloração pela hematoxilina (linfócitos), células elípticas com núcleo excentricamente localizado no citoplasma (plasmócitos) e células com núcleo irregular (macrófagos) foram usadas para identificar as células inflamatórias[5,6,7]. Com auxílio do sistema de análise de imagens, as células identificadas como células inflamatórias foram computadas pelo operador e o sistema numera sequencial (Figura 10). Os fibroblastos foram diferenciados das células inflamatórias pelo seu formato elíptico/fusiforme. Essas células também foram computadas com o auxílio do sistema de análise de imagem (Figura 11). Assim, o número de células inflamatórias e de fibroblastos por mm^2 foi estimado em cada espécime. Esta análise foi realizada em todos os espécimes de todos os grupos e períodos.

Número de células inflamatórias (CI)

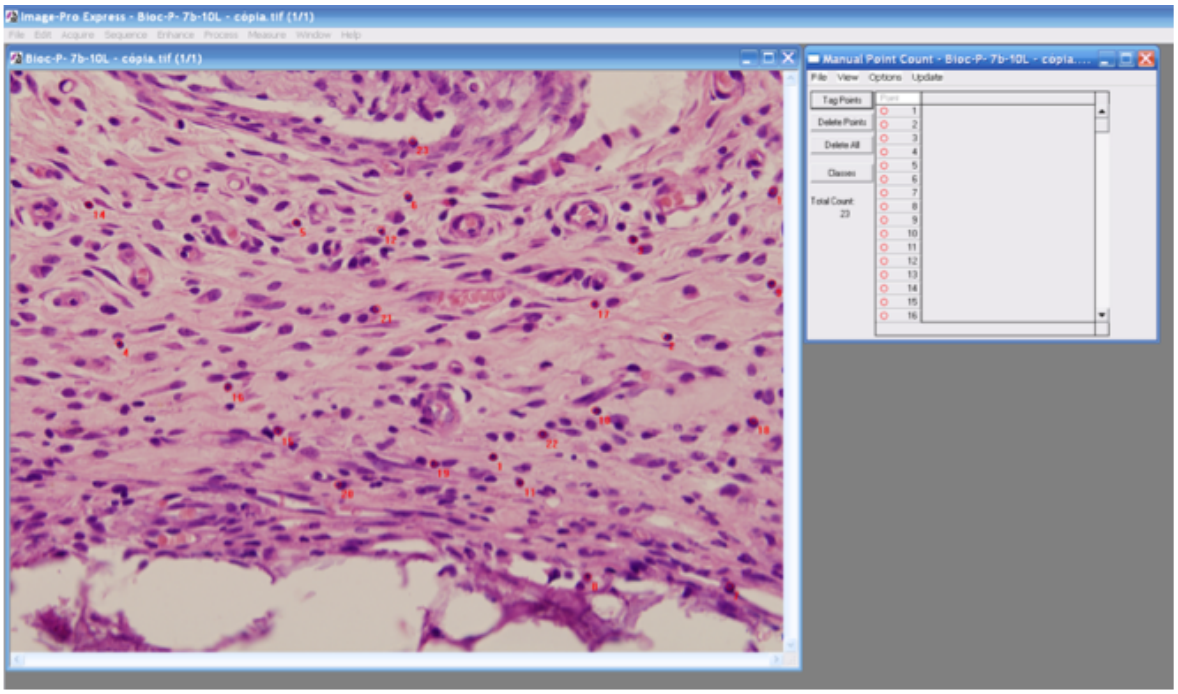

Figura 10- A figura mostra um *print sreen* da imagem capturada com a objetiva de 40x e transferida para o programa de análise de imagem (Image-Pro Express 6,0, Olympus). Após a calibração do sistema, seleciona-se o ícone *Tag Points* para iniciar a contagem de células inflamatórias que aparecem na imagem à esquerda. À medida que o operador clica sobre a célula identificada, o programa registra a mesma com um círculo vermelho junto ao número computado sequencialmente.
Fonte: Própria do autor.

Número de fibroblastos

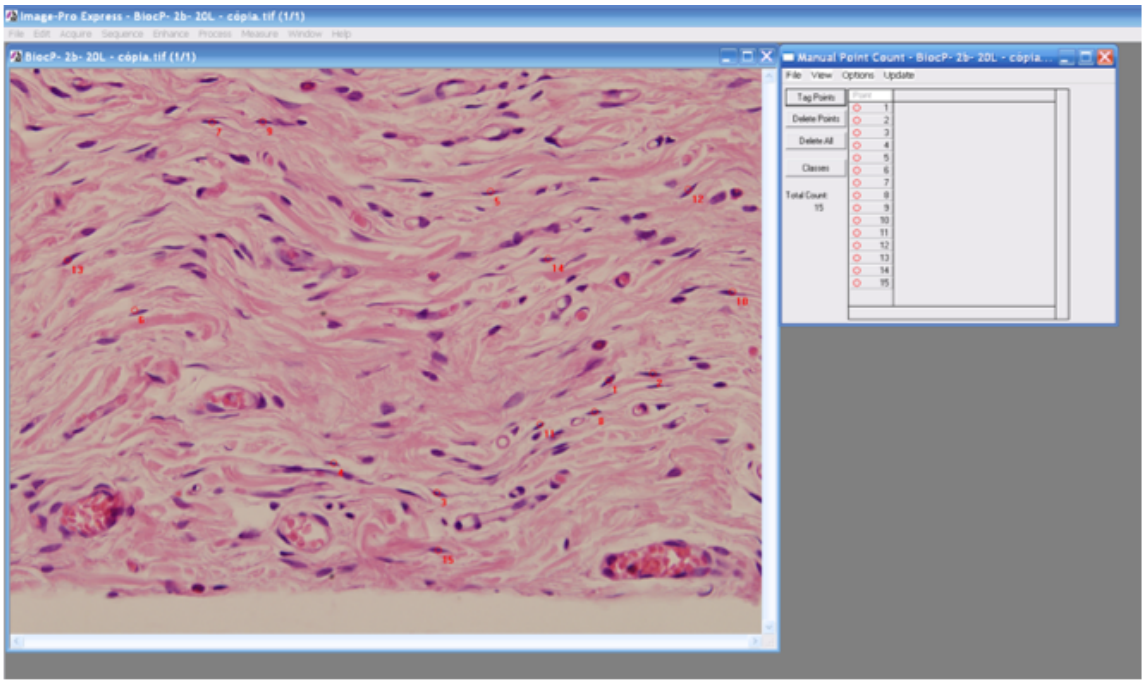

Figura 11- A figura mostra um *print sreen* da imagem capturada com a objetiva de 40x e transferida para o programa de análise de imagem (Image-Pro Express 6,0, Olympus). Após a calibração do sistema, seleciona-se o ícone *Tag Points* para iniciar a contagem de fibroblastos que aparecem na imagem à esquerda. À medida que o operador clica sobre o fibroblasto, o programa registra a célula com um círculo vermelho junto ao número computado sequencialmente.
Fonte: Própria do autor.

- Imuno-histoquímica para detecção de IL-6

Para a detecção de IL-6, foi utilizado o anticorpo monoclonal de camundongo anti-IL-6 (Abcam Inc., Cambridge, MA, EUA; código: ab9324). Após desparafinização e hidratação, as lâminas foram imersas em tampão citrato de sódio 0,001 M com pH 6,0 e submetidas ao aquecimento em micro-ondas por 30 min a 94-98º C para recuperação antigênica. Após o resfriamento, os cortes foram lavados em tampão Tris-HCl 0,05 M com pH 7,4 e, a seguir, imersos em solução aquosa de peróxido de hidrogênio a 5%, protegido da luz, por 20 min para bloqueio da peroxidase endógena. Após as lavagens, os cortes foram incubados em albumina de soro bovino a 2% (BSA, Sigma-Aldrich Co., Saint Louis, Missouri, EUA) por 30 minutos em temperatura ambiente (Figura 12). Em seguida, os cortes foram incubados durante a noite (16 a 18 horas) em uma câmara úmida a 4° C (geladeira) com anticorpo anti-IL-6 na diluição de 1:100. Posteriormente, os cortes passaram por 4 lavagens (5 min cada) em tampão

Tris-HCl por 20 min e, em seguida, os cortes foram incubados por 1 hora à temperatura ambiente com anti-IgG de coelho e camundongo conjugado a polímeros-HRP (EnVision + Dual Link System-HRP, Dako Inc., Carpinteria, CA, EUA; código: K4061). Posteriormente, os cortes foram lavados em tampão TRIS-HCl, e a atividade da peroxidase foi revelada pelo cromógeno 3,3'-diaminobenzidina (DAB, Dako Inc., Carpinteria, Califórnia, EUA; código: K3468) por 3 min. Os cortes foram contracorados com hematoxilina de Carazzi. Como controle negativo, os cortes foram submetidos a todas as etapas exceto a incubação com anticorpo primário, quando os cortes foram incubados com soro não imune.

Para verificar se havia diferenças entre os grupos e períodos, o número de células imunopositivas (em castanho) foi computado nas cápsulas de todos os espécimes. Utilizando uma câmera digital (DP-71, Olympus, Tóquio, Japão) acoplada ao microscópio de luz (BX-51, Olympus, Tóquio, Japão), uma área padrão de 0,09 mm^2 da cápsula adjacente à abertura do tubo implantado foi capturada com a objetiva de 40x (ampliação final de 695x). Usando o programa de análise de imagem (Image Pro-Express 6.0, Olympus), as células imunopositivas à IL-6 foram computadas em cada campo e o número de células imunopositivas por mm^2 de cápsula foi calculado em cada amostra (Figura 13) e, posteriormente, a média por grupo em cada período foi calculada[3,6,7].

Incubação em BSA a 2%

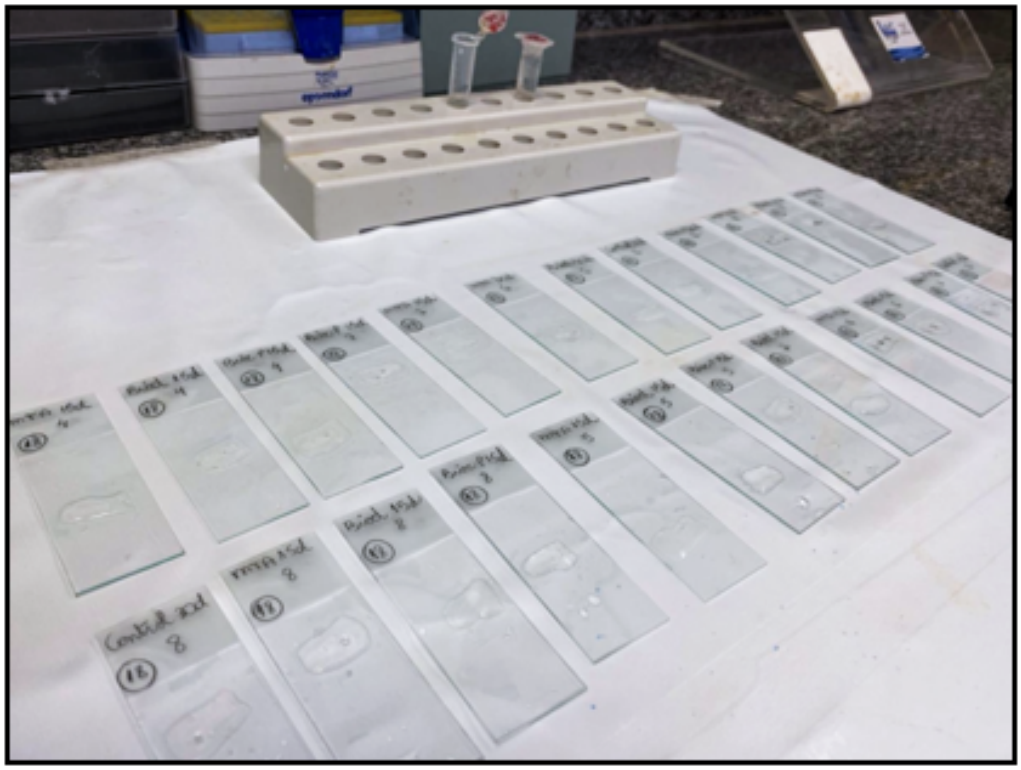

Figura 12- Incubação em albumina de soro bovino 2% (BSA; Sigma-Aldrich Co., Saint Louis, Missouri, EUA) por 30 minutos à temperatura ambiente.
Fonte: Própria do autor.

Quantificação de células IL-6-imunopositivas

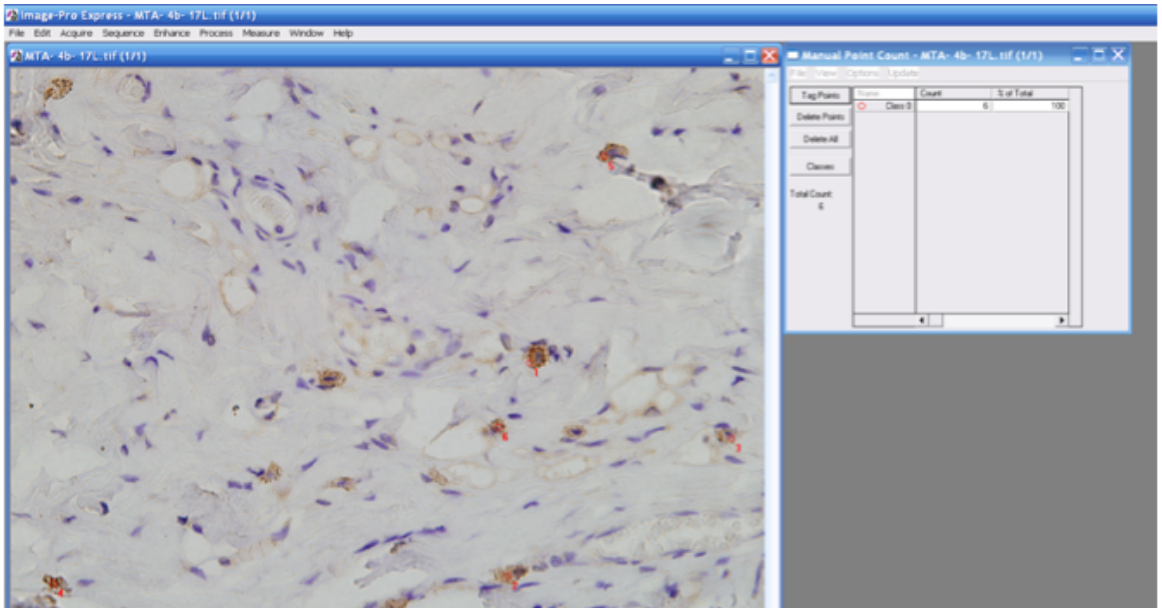

Figura 13- A figura mostra um *print sreen* da imagem capturada com a objetiva de 40x e transferida para o programa de análise de imagem (Image-Pro Express 6,0, Olympus). Após a calibração do sistema, seleciona-se o ícone *Tag Points* para iniciar a contagem do

número de células imunopositivas à IL-6 (em castanho). À medida que o pesquisador identifica a célula imunomarcada, com o *mouse* clica sobre a célula e o sistema registra, marcando a célula com um círculo vermelho e o número correspondente.
Fonte: Própria do autor.

- *Quantidade de colágeno nas cápsulas*

O colágeno nas cápsulas foi quantificado em cortes submetidos à solução de picrosirius-red 0,1% e analisados em microscópio de luz polarizada (BX-51, Olympus). De cada implante foram utilizados três cortes não seriados (distância mínima entre os cortes de 100 µm), totalizando 21 cortes (7 amostras por implante) por grupo em cada período.

Após a desparafinização e hidratação dos cortes, as lâminas foram imersas na solução de picrosírius-red por 1 hora. Subsequentemente à lavagem em água corrente (5 min.), os cortes foram desidratados, tratados com xilol e montados com meio resinoso (Permount®, Fisher Scientific, New Jersey, USA).

Os cortes foram analisados ao microscópio Olympus (modelo BX-51) com os filtros de polarização. Após seleção da região de interesse (superfície da cápsula justaposta à abertura do tubo de polietileno na porção central da cápsula), usando a objetiva de 40x (ampliação final de 695x) e com parâmetros rigorosamente padronizados (intensidade de luz, abertura do diafragma de campo, diafragma do condensador, posição do condensador e tempo de exposição), a imagem polarizada foi obtida com uma câmera digital (DP 72, Olympus).

As imagens foram transferidas para o software de análise de imagem ImageJ® (http://rsbweb.nih.gov/ij) que foi usado para estimar o percentual de área ocupada por colágeno birrefringente nas cápsulas. A definição de matiz considerada na birrefringência foi a seguinte: vermelho/laranja, 2–38 e 230–256; amarelo, 39–51; e verde, 52–128[8,9]. Assim, a quantidade de colágeno foi representada pela porcentagem de área birrefringente ocupada na área total (expressa em pixels) calculada pelo programa de análise de imagens[10].

Potencial bioativo

- Imuno-histoquímica para detecção de osteocalcina (OCN)

Após a desparafinização, a recuperação antigênica foi obtida por imersão dos cortes em tampão citrato de sódio 0,001 M a pH 6,0 aquecido em micro-ondas a 94ºC por 10 min. Após o resfriamento, os cortes foram lavados em tampão fosfato de sódio (PBS 50mM + NaCl 200mM, pH 7,3), a peroxidase endógena foi inativada pela imersão em solução aquosa de peróxido de hidrogênio a 5% durante 30 min, no escuro. Após as lavagens, os cortes foram incubados com BSA 2% por 30min à temperatura ambiente. Os cortes foram então incubados por 18 horas com anticorpo primário anti-osteocalcina produzida em coelho diluído 1: 500 (Sigma-Aldrich Co., Saint Louis, Missouri, EUA; código: SAB 1306277-40TST) a 4° C. No dia seguinte, os cortes foram lavados e incubados por 1 hora com polímero conjugado com HRP (EnVision + Dual Link System-HRP, Dako Inc., Carpinteria, CA, EUA; código: K4061) em temperatura ambiente (Figura 14). Após lavagem em tampão, a reação foi revelada com DAB (Dako Inc., Carpinteria, Califórnia, EUA; código: K3468) e os cortes foram contrastados com hematoxilina de Carazzi. Como controle negativo, cortes foram incubados com soro não imune em substituição à incubação com o anticorpo primário (anti-OCN).

Para verificar se havia diferenças entre os grupos e períodos, o número de células imunopositivas (em castanho) foi computado nas cápsulas de todos os espécimes. Utilizando uma câmera digital (DP-71, Olympus, Tóquio, Japão) acoplada ao microscópio de luz (BX-51, Olympus, Tóquio, Japão), uma área padrão de 0,09 mm^2 da cápsula adjacente à abertura do tubo implantado foi capturada com a objetiva de 40x (ampliação final de 695x). Usando o programa de análise de imagem (Image Pro-Express 6.0, Olympus), as células imunopositivas à OCN (em castanho) foram computadas em cada campo e o número de células imunopositivas por mm^2 de cápsula foi calculado em cada amostra (Figura 15) e, posteriormente, a média por grupo em cada período foi calculada[3,6,7].

Incubação com anticorpo secundário

Figura 14- Incubação com sistema IgG (anti-mouse/rabbit) associado a polímeros (marcado – HRP) por 1 hora (EnVision + Dual Link System – HRP, Dako INC., Carpinteria, CA, EUA; K4061), em temperatura ambiente.
Fonte: Própria do autor.

Número de células imunopositivas à OCN

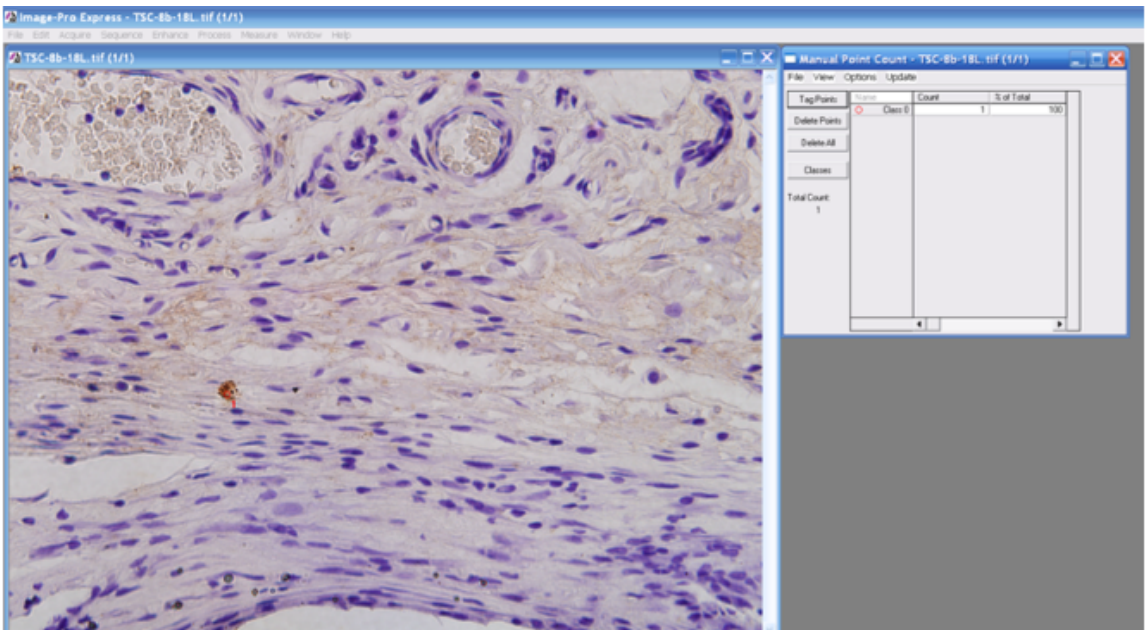

Figura 15- A figura mostra um *print sreen* da imagem capturada com a objetiva de 40x e transferida para o programa de análise de imagem (Image-Pro Express 6,0, Olympus). Após a calibração do sistema, seleciona-se o ícone *Tag Points* para iniciar a contagem de células imunopositivas à OCN. O sistema computa a célula reconhecida pelo pesquisador.
Fonte: Própria do autor.

- Reação de von Kossa e estruturas birrefringentes

Em cada espécime, três cortes não seriados foram submetidos à reação de von Kossa que detecta depósitos de cálcio[11,12], em preto/castanho[11] nas cápsulas. Após a desparafinização e hidratação, os cortes foram imersos em solução resfriada (a 4º C) de nitrato de prata a 5% por 1 hora sob lâmpada incandescente (100 Watts). As lâminas foram rapidamente lavadas em água destilada e, a seguir, imersas em solução de hipossulfito de sódio a 5% por 5 min. Após lavagem em água destilada por 5 min, os cortes foram corados com picrosirius-red[1,7] e montados em meio resinoso (Permount®, Fisher Scientific, New Jersey, EUA). A reação histoquímica de von Kossa foi realizada em todos os implantes de todos os grupos e períodos e analisadas ao microscópio de luz (Figura 16; Olympus, modelo BX-51).

Como controle positivo foi utilizado corte de falange de membro posterior (sem descalcificação) de rato jovem (Figura 17), obtido junto ao arquivo da disciplina de Histologia e Embriologia. No controle negativo, os cortes foram submetidos ao mesmo tratamento, com exceção da incubação em nitrato de prata a 5%.

Cortes desparafinizados (sem coloração) foram montados em meio resinoso e foram analisados sob iluminação polarizada (BX-51, Olympus, Tóquio, Japão) para verificar se as cápsulas continham estruturas birrefringentes, sugestivas de calcita amorfa[13,14,15].

Análise da reação de von Kossa

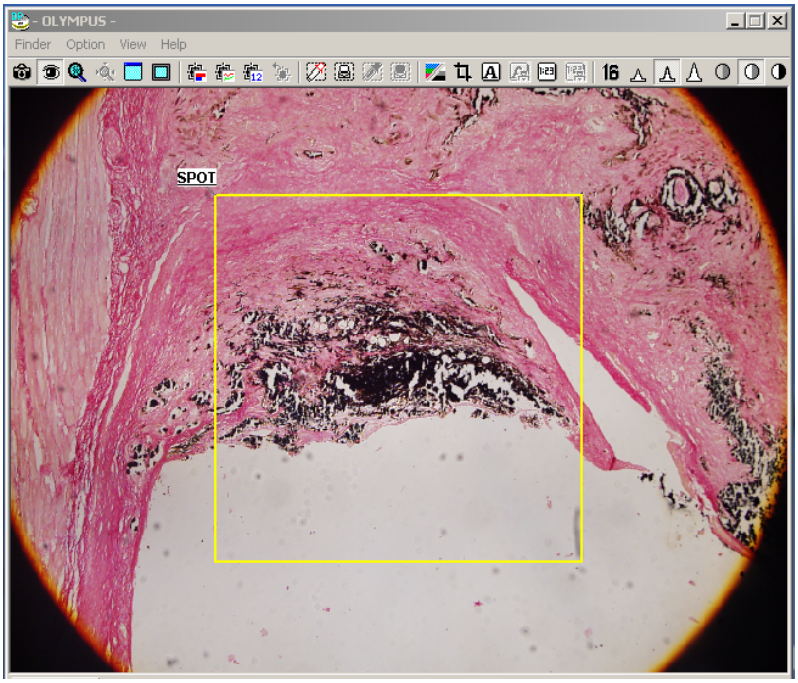

Figura 16- A figura mostra um *print sreen* da imagem com a objetiva de 4x do microscópio (Olympus, modelo BX-51) após reação de von Kossa.
Fonte: Própria do autor.

Reação de von Kossa

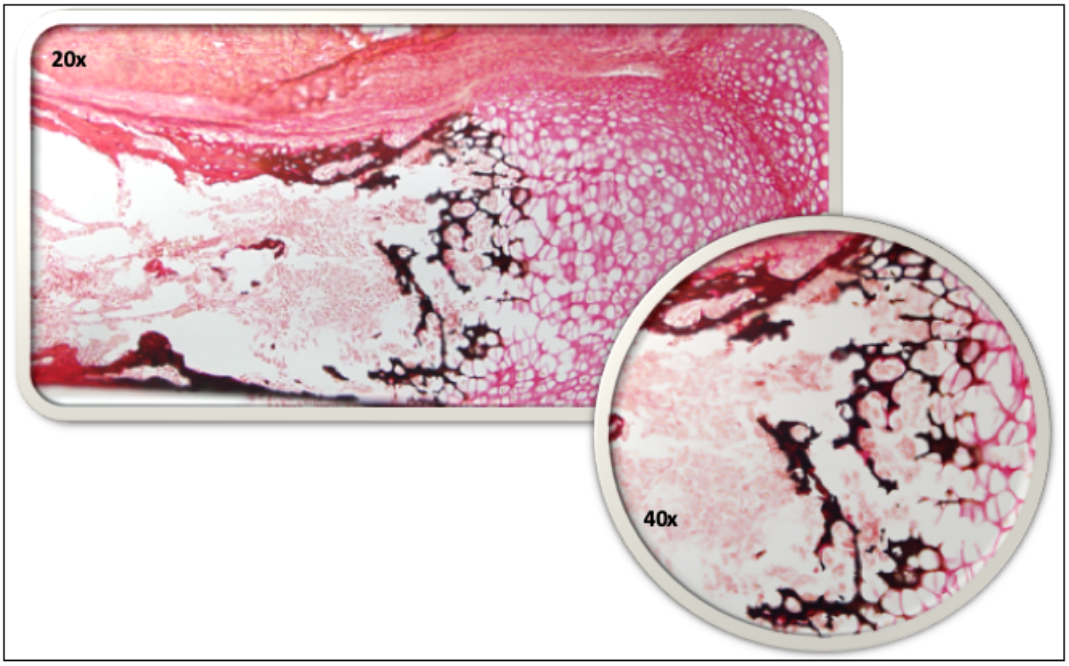

Figura 17- Fotomicrografias de uma porção de corte não descalcificado do membro posterior mostrando a falange média de rato jovem. O corte foi submetido ao von Kossa

e, em seguida, corados pelo picrosirius-red. Note que as trabéculas ósseas em processo de calcificação são observadas em preto/castanho escuro, ou seja, são positivas ao von Kossa.
Fonte: Própria do autor.

Análise estatística

Os dados obtidos nos experimentos foram adicionados ao programa GraphPad Prism 6 (GraphPad Software), no qual foram submetidos os testes estatísticos de ANOVA two-way seguido pelo teste de Tukey (Figura 18) com nível de significância de 5% (p<0,05), no qual foi gerado também um gráfico com os dados da estatística (Figura 18).

Confecção do gráfico da análise estatística

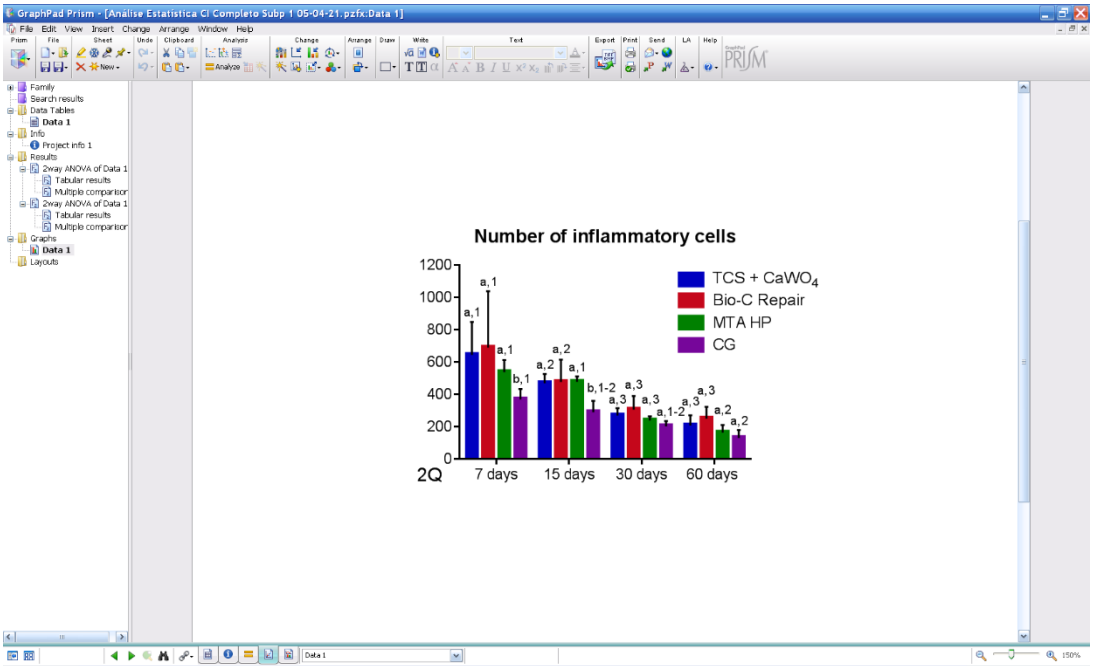

Figura 18- A figura mostra um *print sreen* da imagem gerada após a análise estatística para confecção do gráfico do programa de análise estatística GraphPad Prism 6 (GraphPad Software).
Fonte: Própria do autor.

REFERÊNCIAS - APÊNDICE A

1. Viola NV, Guerreiro-Tanomaru JM, da Silva GF, Sasso-Cerri E, Tanomaru-Filho M, Cerri PS. Biocompatibility of an experimental MTA sealer implanted in the rat subcutaneous: quantitative and immunohistochemical evaluation. J Biomed Mater Res B Appl Biomater. 2012; 100(7):1773-81.
2. Koulaouzidou EA, Economides N, Beltes P, Geromichalos G, Papazisis K. In vitro evaluation of the cytotoxicty of ProRoot MTA and MTA Angelus. J Oral Sci. 2008; 50(4):397-2.
3. Saraiva JA, da Fonseca TS, da Silva GF, Sasso-Cerri E, Guerreiro-Tanomaru JM, Tanomaru-Filho M, et al. Reduced interleukin-6 immunoexpression and birefringent collagen formation indicate that MTA Plus and MTA Fillapex are biocompatible. Biomed Mater. 2018; 20;13(3):035002.
4. Yaltirik M, Ozbas H, Bilgic B, Issever H. Reactions of connective tissue to mineral trioxide aggregate and amalgam. J Endod. 2004; 30(2):95-9.
5. Silva GF, Bosso R, Ferino RV, Tanomaru-Filho M, Bernardi MI, Guerreiro-Tanomaru JM, et al. Microparticulated and nanoparticulated zirconium oxide added to calcium silicate cement: evaluation of physicochemical and biological properties. J Biomed Mater Res A. 2014; 102(12):4336-45.
6. da Fonseca TS, da Silva GF, Tanomaru-Filho M, Sasso-Cerri E, Guerreiro-Tanomaru JM, Cerri PS. In vivo evaluation of the inflammatory response and IL-6 immunoexpression promoted by Biodentine and MTA Angelus. Int Endod J. 2016; 49(2):145-53.
7. Delfino MM, Guerreiro-Tanomaru JM, Tanomaru-Filho M, Sasso-Cerri E, Cerri PS. Immunoinflammatory response and bioactive potential of GuttaFlow bioseal and MTA Fillapex in the rat subcutaneous tissue. Sci Rep. 2020; 28, 10(1):7173.
8. Koshimizu JY, Beltrame FL, de Pizzol JP Jr, Cerri PS, Caneguim BH, Sasso-Cerri E. NF-kB overexpression and decreased immunoexpression of AR in the muscular layer is related to structural damages and apoptosis in cimetidine-treated rat vas deferens. Reprod Biol Endocrinol. 2013; 11:29.

9. de Pizzol Júnior JP, Sasso-Cerri E, Cerri PS. Matrix Metalloproteinase-1 and acid phosphatase in the degradation of the lamina propria of eruptive pathway of rat molars. Cells. 2018; 10, 7(11):206.
10. Silva GF, Guerreiro-Tanomaru JM, da Fonseca TS, Bernardi MIB, Sasso-Cerri E, Tanomaru-Filho M, et al. Zirconium oxide and niobium oxide used as radiopacifiers in a calcium silicate-based material stimulate fibroblast proliferation and collagen formation. Int Endod J. 2017; 50 Suppl 2:e95-e108.
11. Puchtler H, Meloan SN. Demonstration of phosphates in calcium deposits: a modification of von Kossa's reaction. Histochemistry. 1978; 56(4):177-85.
12. Rungby J, Kassem M, Eriksen EF, Danscher G. The von Kossa reaction for calcium deposists: silver lactate staining increases sensitivity and reduces backgroud. Histochem J. 1993; 25(6):446-51.
13. Delfino MM, de Abreu Jampani JL, Lopes CS, Guerreiro-Tanomaru JM, Tanomaru-Filho M, Sasso-Cerri E,et al. Comparison of Bio-C Pulpo and MTA Repair HP with White MTA: effect on liver parameters and evaluation of biocompatibility and bioactivity in rats. Int Endod J. 2021; 54(9):1597-613.
14. Holland R, de Souza V, Nery MJ, Otoboni Filho JA, Bernabé PFE, Dezan Junior E. Reaction of rat connective tissue to implanted dentin tubes filled with mineral trioxide aggregate or calcium hydroxide. J Endod. 1999; 25(3): 161-6.
15. Oliveira LV, de Souza GL, da Silva GR, Magalhães T, Freitas G, Turrioni AP, et al. Biological parameters, discolouration and radiopacity of calcium silicate-based materials in a simulated model of partial pulpotomy. Int Endod J. 2021; 54(11): 2133–44.

ANEXO A – AUTORIZAÇÃO DO COMITÊ DE ÉTICA

unesp UNIVERSIDADE ESTADUAL PAULISTA "JÚLIO DE MESQUITA FILHO"
Câmpus de Araraquara
FACULDADE DE ODONTOLOGIA

CERTIFICADO

Certificamos que a proposta intitulada "*AVALIAÇÃO DA REAÇÃO TECIDUAL E BIOATIVIDADE DE MATERIAIS ENDODÔNTICOS BIOCERÂMICOS REPARADORES EM SUBCUTÂNEO DE RATOS*", registrada com o nº 03/2019, sob a responsabilidade do(a) **Prof(a). Dr(a). Mário Tanomaru Filho** – que envolve a produção, manutenção ou utilização de animais pertencentes ao filo Chordata, subfilo Vertebrata (exceto humanos), para fins de pesquisa científica – encontra-se de acordo com os preceitos da Lei nº 11.794, de 8 de outubro de 2008, do Decreto nº 6.899, de 15 de julho de 2009, e com as normas editadas pelo Conselho Nacional de Controle da Experimentação Animal (CONCEA), e foi aprovado pela **COMISSÃO DE ÉTICA NO USO DE ANIMAIS (CEUA) DA FACULDADE DE ODONTOLOGIA DE ARARAQUARA** em reunião de 26/03/2019.

Finalidade	( ) Ensino (X) Pesquisa Científica
Vigência do Projeto	Março/2021
Espécie/linhagem	Rato – Holtzman (Rattus novergicus albinus)
Nº de animais	160
Peso/Idade	220g – adultos jovens
Sexo	Macho
Origem	Biotério Central da Faculdade de Odontologia de Araraquara – UNESP

Profa. Dra. CARINA APARECIDA FABRÍCIO DE ANDRADE
Coordenadora da CEUA

Comissão de Ética no Uso de Animais - CEUA
Rua Humaitá nº 1.680 - Centro - CEP 14801-903 - Caixa Postal nº 331 - ARARAQUARA – SP
5º andar - fone (16) 3301-6459 / fax (16) 3301-6432 / e-mail: ceua@fcfar.unesp.br - home page: http://www.fcfar.unesp.br

ANEXO B – COMPROVANTE DE SUBMISSÃO E REVISÃO DO ARTIGO 1

unesp

Paulo Sergio Cerri <paulo.cerri@unesp.br>

International Endodontic Journal - Manuscript ID IEJ-21-00758.R1
1 mensagem

International Endodontic Journal <onbehalfof@manuscriptcentral.com> 7 de fevereiro de 2022 19:04
Responder a: iej.office@wiley.com
Para: pcerri@foar.unesp.br

07-Feb-2022

Dear Prof. Cerri

Your manuscript entitled "Biocompatibility and bioactive potential of an experimental tricalcium silicate-based cement in comparison with Bio-C Repair and MTA HP Repair materials" has been successfully submitted online to the International Endodontic Journal.

Your manuscript ID is IEJ-21-00758.R1.

Please mention the above manuscript ID in all future correspondence or when calling the Editorial Office for questions. If there are any changes in your postal or e-mail address, please log in to ScholarOne Manuscripts at https://mc.manuscriptcentral.com/iej and edit your user information as appropriate.

You can also view the status of your manuscript at any time by checking your Author Centre after logging in to https://mc.manuscriptcentral.com/iej.

Thank you for submitting your manuscript to the International Endodontic Journal.

Kind regards

Hal Duncan
Editor, International Endodontic Journal
iej.office@wiley.com

INTERNATIONAL ENDODONTIC JOURNAL
The official journal of the British Endodontic Society and the European Society of Endodontology

Biocompatibility and bioactive potential of an experimental tricalcium silicate-based cement in comparison with Bio-C Repair and MTA HP Repair materials

Journal:	*International Endodontic Journal*
Manuscript ID	IEJ-21-00758.R1
Wiley - Manuscript Type:	Original Scientific Article
Keywords:	tissue reaction, interleukin-6, osteocalcin, bioceramic materials, repair materials, animal model

Accept - Journal of Biomedical Materials Research: Part B - Applied Biomaterials - Manuscript JBMR-B-22-0125.R2

JG

Jeremy Gilbert <onbehalfof@manuscriptcentral.com>
Seg, 02/05/2022 11:34
Para: paulo.cerri@unesp.br
Cc: Você; Rafainada@hotmail.com; milasoares.odonto@gmail.com **+5 pessoas**

Date:02-May-2022
Ref.: JBMR-B-22-0125.R2

Dear Prof. Cerri:

I am pleased to inform you that your manuscript entitled "Bioactive potential of Bio-C Pulpo is evidenced by the presence of birefringent calcite and osteocalcin immunoexpression in the rat subcutaneous tissue" has been accepted for publication in the Journal of Biomedical Materials Research: Part B - Applied Biomaterials.

Your article cannot be published until you have signed the appropriate license agreement. Within the next few days you will receive an email from Wiley's Author Services system which will ask you to log in and will present you with the appropriate license for completion.

This journal offers a number of license options, information about this is available here: https://authorservices.wiley.com/author-resources/Journal-Authors/licensing/index.html. All co-authors are required to confirm that they have the necessary rights to grant in the submission, including in light of each co-author's funder policies. For example, if you or one of your co-authors received funding from a member of Coalition S, you may need to check which licenses you are able to sign.

Your article will be published online via Wiley's EarlyView® service (www.interscience.wiley.com) shortly after receipt of corrections. EarlyView® is Wiley's online publication of individual articles in full-text HTML and/or pdf format before release of the compiled print issue of the journal. Articles posted online in EarlyView® are peer-reviewed, copyedited, author corrected, and fully citable. EarlyView® means you benefit from the best of two worlds—fast online availability as well as traditional, issue-based archiving.

Please feel free to contact the editorial office at jbmrb@wiley.com if you have questions about the process.

Thank you for your support of the Journal of Biomedical Materials Research: Part B - Applied Biomaterials. I look forward to seeing more of your work in the future.

Sincerely,
Jeremy L. Gilbert
Editor in Chief
Journal of Biomedical Materials Research: Part B - Applied Biomaterials

Não autorizo a publicação deste trabalho pelo prazo de 2 anos após a data da minha defesa

Araraquara, 29 de Março de 2022.

Marcela Borsatto Queiroz